



Dipl. Ing. Julia Kruisz, BSc

# **Integration of unit-operation models in a plant wide flowsheet simulation for continuous pharmaceutical manufacturing**

**DOCTORAL THESIS**

to achieve the university degree of  
Doktor der technischen Wissenschaften

submitted to

**Graz University of Technology**

Supervisor

Univ.-Prof. Dipl.-Ing. Dr. techn. Johannes G. Khinast

Institute for Process and Particle Engineering, Graz University of Technology

Research Center Pharmaceutical Engineering GmbH, Graz

Graz, September 2018

*Julia Kruisz*

Integration of unit-operation models in a plant wide flowsheet simulation for continuous pharmaceutical manufacturing

*Dissertation*

*First assessor*

Univ.-Prof. Dipl.-Ing. Dr.techn. Johannes Khinast  
Institute of Process and Particle Engineering, Graz University of Technology  
Research Center Pharmaceutical Engineering GmbH

*Second assessor*

Univ.-Prof. Dr.phil.nat. Andreas Zimmer  
Institute of Pharmaceutical Sciences, University of Graz

Copyright ©2018 by Julia Kruisz

All rights reserved. No part of the material protected by this copyright notice may be reproduced or utilized in any form or by any means, electronically or mechanical, including photocopying, recording or by any information storage and retrieval system without written permission from the author.

## **AFFIDAVIT**

I declare that I have authored this thesis independently, that I have not used other than the declared sources / resources, and that I have explicitly indicated all material, which has been quoted either literally or by content from the used sources. The text document uploaded to TUGRAZonline is identical to the present doctoral thesis.

(Ich erkläre an Eides statt, dass ich die vorliegende Arbeit selbstständig verfasst, andere als die angegebenen Quellen/Hilfsmittel nicht benutzt, und die den benutzten Quellen wörtlich und inhaltlich entnommenen Stellen als solche kenntlich gemacht habe. Das im TUGRAZ hochgeladene Textdokument ist identisch mit der vorliegenden Arbeit.)

September, 2018 .....

Dipl.-Ing. Julia Kruisz, BSc

*Any intelligent fool can make things bigger,  
more complex, and more violent.  
It takes a touch of genius -  
and a lot of courage -  
to move in the opposite direction.*

*EF Schumacher*

## Acknowledgements

I'd like to thank many people for their support during the last years. Without all of you, this thesis would not have been possible. I'd like to name some here.

First of all, I'd like to thank Prof. Johannes Khinast for giving me the opportunity to conduct my PhD thesis at RCPE and giving me the chance to grow into a new field of engineering. Thanks to his patience and valuable inputs, this work is something to be proud of.

Special thanks go to Otto Scheibelhofer and Jakob Rehr for their support solving nearly every problem together. The discussions we had during the last years are something I don't want to miss. I really enjoyed working with you and I loved being challenged by you.

I also want to thank Eva Faulhammer for her guidance and patience. Thank you for introducing me to the world of capsule filling and also to material science.

Furthermore, thanks to Stephan Sacher for his support as Area Leader and also within projects.

I especially want to thank all people who supported the experimental work. In the pilot plant Daniel Kaiser, Mario Unterreiter, Andreas Freidl, the student employees Manuel Zettl, Daniel Wiegele, Vanessa Herndler and many summer interns. Without you, all the data processing and evaluation would not have been possible because I would not have had any data.

There are many more people at RCPE, who I would like to mention here for their support and for being friends not just colleagues:

...Manuel Kreimer, Johannes Poms and Mathias Wolfgang, my "next-door neighbors" for being always here to distract me when I was somewhere lost in code.

...Andreas Witschnigg for his support as project leader.

...People the lab team (Michael Piller, Mario Hainschitz, Paul Rinner, Feroz Ahmed, Wolfgang Sindler etc.) for guiding me through material characterization.

...Michael Martinetz for being open to frequent questions and discussions.

...Many other people, Patrick Wahl, Sarah Zellnitz, Lisa-Maria Schaden, Selma Celikovic (IRT) and Stefan Manz (Bosch) for the interesting conversations and support and also for challenging me and asking the right questions to let me find solutions by myself.

Thank you my friends, the "Hiambara", for being confident when I lost confidence and supporting me through the last years.

I also want to thank Martin Humel for the guitar sessions and introducing me to ukulele. The evenings with you made tough times easier and easy times happier.

Special thanks to my boyfriend Alex, who was on my side through all the ups and downs during the last years. You always asked the right questions to help me choosing my way to finally reach the end of this journey. You have trusted my abilities to navigate around all hindrances even when I could not see a way.

Last but not least, I'd like to thank my family, first my mother, for always supporting me, drinking cocktails to celebrate the little achievements on my way to PhD. Thanks to Lilly for numerous Catan (and other) games.

## **Abstract**

The transition from batch to continuous pharmaceutical manufacturing started about a decade ago and there is still a long way to achieve fully continuous pharmaceutical manufacturing. Thus, the interest in continuous production routes is growing, as there are many benefits. One of these benefits is higher flexibility in order to produce different products with the same equipment and on a smaller scale reducing scale up issues, among others. A key factor in approval of continuously manufactured products is the traceability of materials through the process with simultaneous documentation of process parameters during production. This requires knowledge of the residence time distribution (RTD) of each unit operation as well as a process monitoring system for full process documentation.

This thesis is tackling the part of traceability of materials by RTD measurements and gaining additional benefit by the development of RTD process models for in-silico process development, design, optimization and control. To obtain this goal, three unit operations were characterized and models in the form of transfer functions have been developed. The models can be used in a later stage to be incorporated in larger control strategies by model-based or model-predictive control.

The RTD measurements were conducted either as impulse response experiments (blender and roller compactor) or step response experiments (blender and capsule filling machine) with visible tracer material. In case of impulse response experiments, a fine color pigment was used whereas for the step response experiments, colored bulk powder material served as tracer material. To obtain this bulk tracer material, a coloring procedure was developed. Data acquisition was performed via a consumer camera and a sophisticated video/image processing algorithm was applied to the data to extract the color information. Based on these measured color values, the RTD curves could be determined and used to parametrize the RTD models.

The parametrized models were then connected in-silico to obtain a production line RTD model. This line models enable simulations of feed disruptions and assess the propagation of certain disturbances through the production line. After definition of a certain threshold for out-of-specification material, it is possible to compare the amount of waste material and the discharge times at certain stages in the process, allowing optimized control strategies.

## Kurzfassung

Der Übergang von klassischer Batchproduktion zu kontinuierlichen pharmazeutischen Herstellungsverfahren begann vor ungefähr einer Dekade. Trotzdem ist es noch ein weiter Weg zu komplett automatisierten pharmazeutischen Produktionslinien. Weil es so viele Vorteile gibt ist das Interesse an der Weiterentwicklung von solchen Produktionslinien ungebrochen und die Forschung wird von den vielen Vorteilen, die solche kontinuierlichen Linien mit sich bringen weiter vorangetrieben. Zu den Vorteilen zählen beispielsweise mit kleineren Maschinen verschiedene Produkte herzustellen und die Menge hängt nur mehr von der Produktionszeit und nicht mehr (stark) von der Größe des Equipments ab. Dadurch fallen zeit- und arbeitsintensive Scale-Up Schritte weg. Ein wichtiger Faktor für die Zulassung von kontinuierlich produzierten Produkten ist die Nachverfolgbarkeit über die Prozessbedingungen zurück zum Rohmaterial bis hin zu den Lagerungsbedingungen. Um diese Nachverfolgbarkeit zu erzielen, ist die Kenntnis der Verweilzeitverteilung des Materials in den einzelnen Prozessschritten mit gleichzeitiger Dokumentation der Prozessbedingungen nötig.

Diese Arbeit beschäftigt sich mit dem Teil der Rückverfolgbarkeit der Materialien im Prozess auf Basis von Verweilzeitverteilungen. Zusätzlich werden diese Verweilzeitverteilungen modelliert um Simulationsmodelle zu erhalten, die in Prozessentwicklung, -auslegung, -optimierung und auch Prozessregelung zum Einsatz kommen können. Um diese Prozessmodelle zu erhalten, mussten zuerst Messmethoden entwickelt und getestet werden um die Verweilzeitverteilung der Grundoperationen messen zu können. Die Modelle wurden in Form einer Übertragungsfunktion formuliert um in weiterer Folge im Rahmen von modell-basierter oder modell-prädiktiver Regelung in verschiedene Regelungskonzepte integriert werden zu können.

Die Verweilzeitmessungen wurden entweder als Impuls-Versuche (Mischer und Walzenkompaktierer) oder Sprung-Versuche (Mischer und Kapselfüller) durchgeführt. Als Tracer wurden Farbstoffe im sichtbaren Bereich gewählt. Für die Impuls-Versuche wurde ein feines Pigment mit starker Farbkraft verwendet, und für die Sprung-Versuche das Rohmaterial mit einer Lebensmittelfarbe eingefärbt wurde. Die verschiedenen Ansätze wurden gewählt, um die Messungen möglichst rückwirkungsfrei zu halten. Die Datenaufzeichnung wurde mittels einer Standard Kamera im Video-Modus durchgeführt. Ein Datenauswertungs-Algorithmus wurde entwickelt um aus den Videos/Bildern die Farbinformationen zu extrahieren und damit die Übertragungsfunktions-Modelle zu parametrieren.

Die fertig parametrierten Modelle der einzelnen Grundoperationen wurden im Anschluss mathematisch zu einem Linien-Modell verbunden um verschiedene Dosierer Fehlfunktionen und deren Auswirkungen auf den Prozess simulieren zu können. Es wurden Grenzen definiert, in denen das Endprodukt die Spezifikationen erfüllt. Bei über- oder unterschreiten dieser Grenzen muss Material ausgeschleust, das heißt vom Gutprodukt separiert werden. Diese Simulationen erlauben den Vergleich von verschiedenen



Ausschleusepunkten durch den Prozess auf Basis der ausgeschleusten Materialmenge und erleichtern damit die Auslegung von eventuell benötigten Puffern.

# Table of Contents

<b>Acknowledgements.....</b>	<b>iv</b>
<b>Abstract .....</b>	<b>vi</b>
<b>Kurzfassung.....</b>	<b>vii</b>
<b>Table of Contents.....</b>	<b>ix</b>
<b>Abbreviations.....</b>	<b>xiii</b>
<b>1 Introduction and Motivation .....</b>	<b>1</b>
1.1 Continuous pharmaceutical manufacturing.....	1
1.2 Unit operations.....	3
1.2.1 Feeding.....	3
1.2.2 Blending.....	3
1.2.3 Roller Compaction.....	4
1.2.4 Capsule Filling.....	4
1.3 Residence time distribution.....	5
1.3.1 Measurement methods.....	6
1.3.2 RTD modeling approaches.....	7
1.4 Literature .....	8
<b>2 RTD Modeling of a Continuous Dry Granulation Process for Process Control and Materials Diversion .....</b>	<b>16</b>
2.1 Abstract.....	16
2.2 Introduction .....	17
2.3 Materials and Methods .....	19
2.3.1 Model Development.....	19
2.3.2 Experimental .....	21
2.3.3 Data Processing .....	23
2.3.4 Out-of-Spec Material Handling.....	24

2.4	Results.....	25
2.4.1	Feeder and Blender .....	25
2.4.2	Roller Compactor.....	28
2.4.3	Out-of-Spec Management.....	30
2.5	Discussion .....	35
2.6	Conclusion .....	36
2.7	References .....	38
2.8	Appendix.....	40
2.8.1	Abbreviations .....	40
2.8.2	Variables .....	40
2.8.3	Subscripts .....	41
2.8.4	Supplementary Material.....	42
<b>3</b>	<b>Residence Time Distribution of a Continuously-operated Capsule Filling Machine: Development of a Measurement Technique and Comparison of Three Volume-Reducing Inserts.....</b>	<b>43</b>
3.1	Abstract.....	43
3.2	Introduction .....	44
3.3	Materials and Methods .....	48
3.3.1	Data Processing .....	54
3.4	Results and Discussion.....	56
3.4.1	Material Characterization.....	56
3.4.2	Experimental RTD .....	57
3.5	Conclusion and Outlook.....	63
3.6	Acknowledgements .....	63
3.7	Literature .....	63
3.8	Appendix.....	67

3.8.1 Nomenclature.....	67
3.8.2 Abbreviations .....	68
<b>4 Material tracking in a continuous direct capsule-filling process via residence time distribution measurements .....</b>	<b>69</b>
4.1 Abstract.....	69
4.2 Introduction .....	70
4.3 Materials and Methods .....	72
4.3.1 Material .....	72
4.3.2 Capsule filling machine.....	73
4.3.3 Blender .....	74
4.3.4 Feeders .....	75
4.3.5 Experimental procedures .....	75
4.3.6 Data acquisition and processing.....	76
4.3.7 Modeling.....	76
4.4 Results and Discussion.....	79
4.4.1 Blender .....	80
4.4.2 Capsule Filler .....	83
4.4.3 Direct Continuous Capsule-Filling Line.....	87
4.5 Conclusion and Outlook.....	93
4.6 Acknowledgement.....	93
4.7 References .....	94
4.8 Appendix.....	95
4.8.1 Nomenclature.....	95
4.8.2 Abbreviations .....	95
4.8.3 Subscripts .....	96
4.8.4 Tables.....	97

<b>5</b>	<b>Summary and Conclusion .....</b>	<b>98</b>
<b>6</b>	<b>Outlook .....</b>	<b>100</b>
<b>7</b>	<b>Appendix.....</b>	<b>101</b>
	7.1Curriculum Vitae.....	101
	7.2Publications .....	102
	7.2.1Poster.....	102
	7.2.2Presentation .....	102
	7.2.3Research Articles .....	102
	7.2.4Summer School.....	103

## Abbreviations

AIF	angle of internal friction
AoR	angle of repose
API	active pharmaceutical ingredient
BD	bulk density
C	cohesion
CI	Carr index / compressibility index
CM	continuous manufacturing
cph	capsules per hour
CPL	compressibility
CQA	critical quality attribute
CSTR	continuously stirred tank reactor
DS	design space
EXC	excipient
FBU	Feeding/Blending unit
FDA	Food and Drug Administration
FFC	flow function coefficient
ICH	International Conference on Harmonization
LAB	lightness, a-color value, b-color value
LIF	light induced fluorescence
LIW	loss in weight
NIR	near infrared
OOS	out-of-specification
PAT	Process Analytical Technology
PBH	powder bed height

PFR	plug flow reactor
PSD	particle size distribution
QTPP	quality target product profile
RC	roller compactor
RGB	red-green-blue
RSD	relative standard deviation
RTD	residence time distribution
TD	tapped density
tpm	tamps per min in 1/min
USP	United States Pharmacopeia

*"All things are difficult before they are easy."*

Dr. Thomas Fuller

## **1 Introduction and Motivation**

Flowsheet simulations are a valuable tool in process development and optimization. Such simulations are widely used in various industries and many software tools are available [1–6]. These tools often provide vast libraries with state of the art models, often with the possibility to customize models or develop parts or whole models from scratch [7–10].

Pharmaceutical manufacturing, especially secondary pharmaceutical manufacturing often deals with solids and powder processing steps. For this type of processes, only a few process modeling tools exist. gFormulated Products (Process Systems Enterprise Limited, London, UK) [8] is focusing on modeling of material properties and their change upon processing, e.g. agglomeration and breakage phenomena or drying. Such phenomenological models cannot be applied for material tracking, as nearly all currently available models are based on first-in-first-out principle. This means, no backmixing inside the unit operations can be modeled. However, in continuous pharmaceutical manufacturing, material tracking is crucial as the tracability of the final product back to the raw materials is important for quality assurance [11–20]. In case of process disruptions, it is highly important, to know, which part of the final product stream is affected. This information can easily be obtained in-silico by connection of the residence time distribution (RTD) models of single unit operations allowing integration of unit-operation models in a plant wide flowsheet simulation for continuous pharmaceutical manufacturing [11–13,20,21].

This work aims for the RTD model development and their integration into various modeling tools and combined with the phenomenological models leading to improved process models.

### **1.1 Continuous pharmaceutical manufacturing**

In the past, batch production processes were well established whereas, during the last 15 years, a shift to continuous manufacturing takes place. In 2004, the FDA launched their PAT initiative [22], which marked a significant point in the history of continuous pharmaceutical manufacturing and hence driving more and more pharmaceutical companies to invest into continuous manufacturing research. Together with the ICH guidelines for pharmaceutical development (Q8) [23], quality risk management (Q9) [24], pharmaceutical quality system (Q10) [25], development and manufacture of drug substances (Q11) [26] and the technical and regulatory considerations for pharmaceutical product lifecycle management (Q12) [27], the regulatory framework for continuous manufacturing has been provided. The industry's interest is also amplified by



many benefits a continuous production line can have. First of all, continuous production equipment can be built smaller as the production volume is only governed by production time and not by equipment capacity anymore. Smaller equipment size reduces the overall footprint of the production facility. There are whole tableting lines available, which fit into one single portable container, requiring external power and water supply. Such small production lines offer a very high flexibility. On the one hand, small amounts of certain drugs can be effectively produced resulting in rentability of product development for rare diseases. On the other hand, a “production on demand” concept is easier to realize. Furthermore, as in CM there are commonly direct interfaces between the unit operations, the need for intermediate material storage is significantly reduced. This direct interface also allows the exchange of single unit operations and hence build a modular production line depending on product requirements. This flexibility can then be exploited further by scheduling production in a way, that during equipment revision certain other products can be produced [17,28–33].

In contrast to batch processing, process monitoring and control in CM is more challenging. In batch processing, each batch undergoes certain (offline) testing steps, starting with raw material inspection, to in-process sampling for endpoint determination in a fluidized bed granulation device to the (final) product testing. It has to be shown, that each batch has been produced under certain specified conditions allowing limited flexibility in reacting to disturbances. In continuous manufacturing, sensors and sensor systems have been established under the umbrella of Process Analytical Technology (PAT) enabling continuous monitoring of many process parameters and material attributes [22,29,34–38]. Data records and eventually additional analysis of the acquired data can be used as process documentation. Furthermore, these data can be applied for process control [6,12,20,21,38–56]. Control actions as response to certain process disruptions can be made to keep the process in certain limits and hence reduce waste material. In cases, where control actions cannot keep the process within specified limits, discharge points can be implemented at each interface, separating the out-of-specification (OOS) material from well processed material. Nevertheless, such discharge points might introduce the need for buffers as during discharge, the powder flow to the next unit operation is interrupted and it might run empty. Again, starting to fill material into an emptied unit operation might lead again to OOS material. Hence, a buffer will be required. Depending on the complexity of the production line, a sophisticated control concept is necessary. The above described chain in development of continuous processes can be supported very well by modeling of the unit operations as well as their interfaces. Many scientific articles on modeling of (continuous) pharmaceutical processes have been published, dealing with a vast variety of relevant aspects of CM. The most relevant aspect for this thesis is the residence time distribution (RTD) [4,11,13,18–20,57–68]. Combination of RTD models for each unit operation is composing the RTD of a production line. In the following subsection, common unit operations are described, followed by a subsection about measurements and modeling approaches of RTD.

## 1.2 Unit operations

The unit operations (production steps) for powder materials in CM sometimes differ from those used in batch processing. In this chapter, commonly used unit operations in CM are described.

### 1.2.1 Feeding

In batch processing, an actual feeding step is not necessary as the powder is weighted and loaded into the subsequent unit operation, usually a batch blender. Continuous feeding is usually the first unit operation in a continuous processing line, as it introduces raw material to subsequent unit operations. A second feeding step, where additional substances are introduced to the process before tableting is frequently included in a continuous production. Most commonly, a lubricant is added to either a preblend or granulate material. Commonly used are screw feeders. There are two feeding modes possible; first, the volumetric mode, where a constant volume of material over time is fed to the next downstream unit operation. With this mode, bulk density changes influence the mass flow rate. Second, the gravimetric mode, requires a scale, on which the feeder is mounted. Based on the loss-in-weight (LIW) principle, the mass flow is adjusted. If the feeders are operated in this mode, the mass flow rate is kept constant whereas the volumetric flow rate can vary.

Other types of feeders are also used but not frequently in pharmaceutical manufacturing. Examples include vibratory feeders or rotary valve feeders.

Depending on the flow properties of raw materials or preblends and the hopper and screw geometry of the feeder, various negative effects can occur, such as bridging/arching, ratholing, clogging of the screws and electrostatic bearding. For additional information on feeder types, feeding mechanisms and effects on the process, the reader is referred to [69,70].

### 1.2.2 Blending

Batch blenders, such as V-blenders or rotary drum blenders cannot be used continuously as material cannot be fed and removed continuously from the mixing volume (container). Typical continuous blenders consist of a cylindrical tube with a rotating impeller inside. They can have one or more inlets and have one single outlet, which is the interface to the subsequent unit operation. There are two major types of continuous blenders: plough shear blenders, where the paddles are passing through a powder bed at the bottom of the cylinder whereas a fluidizing blender agitates the powder bed building a gas-like powder

distribution inside the cylinder. The number of paddles, their shape, their arrangement/orientation as well as the paddle speed influence the mixing behavior and hence the blend uniformity [70].

### 1.2.3 Roller Compaction

A roller compactor is inherently a continuous unit operation, meaning that the same equipment can be used for batch as well as for continuous processing. The powder is fed to two counter rotating rolls with a certain roller gap. Between those rolls, the powder is compressed to a solid ribbon which is afterwards broken by a mill. The detailed arrangement of the feeding screws and sometimes pre compacting screws can differ among manufacturers but the principle is the always the same. Granule properties are influenced by the roll gap, the compression force, the roll speed and the mill speed. Additionally, the grid size of the mill's sieve can be changed affecting the granule size [70].

### 1.2.4 Capsule Filling

Capsule filling is a wide term, describing the manufacturing of capsules, ranging from hard capsules to soft capsules. Capsules can contain either liquid or solid material. Solid material can consist of other capsules, or tablets, pellets, granules, powders and all combinations thereof. This variety of shells and its content requires various manufacturing processes. In this work, dry powder filled (two piece) hard capsules are investigated.

There are four major types of automated capsule filling machines for filling of dry powder into hard capsules. All of them are inherently capable of continuous operation [71].

- 1) Auger capsule filling
- 2) Drum capsule filling
- 3) Dosator capsule filling
- 4) Tamping pin capsule filling

A tamping pin capsule filling machine is based on the tamping of pins in a powder bed, compressing the powder plug inside a dosing disc. To compress this plug, powder needs to flow into the dosing disc bores. The downward movement of the pins is responsible for compression. The extent of this compression is determined by the compression force. Additionally, the immersion depth can be adjusted. The tamping speed also influences the capsule and plug properties. A more detailed process description can be found in chapters 2 and 3.

### 1.3 Residence time distribution

Residence time theory was first reported by Dankwerts in 1953 in a publication called “Continuous flow systems” [72]. The flow systems he investigated were all fluid systems. The equations are even older and date back to the work of Langmuir [73] published in 1908. This was the reason for a review paper published in 2008 for the 100<sup>th</sup> anniversary of residence time theory [74].

Dankwerts showed and explained four types of flow, (i) piston flow or plug flow, (ii) piston flow or plug flow with some longitudinal mixing and (iii) complete mixing, equal to CSTR (see Figure 1). He published diagrams, explaining the mixing behavior of the systems, showing the F-curve, equal to a step response of the considered systems. The F-curve by definition has its steady state value at 1. The inverse (1-F-curve) is resulting in the wash-out function W, which was measured for the blender and the capsule filling machine in this work.

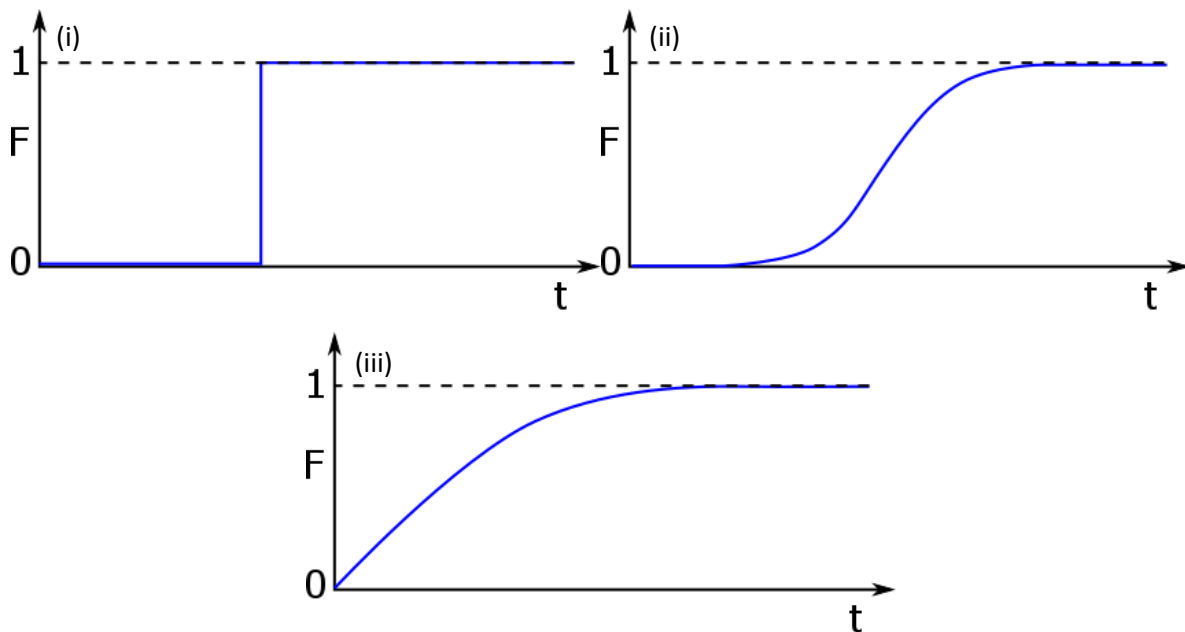


Figure 1: F-Curves for (i) plug flow, (ii) plug flow with longitudinal mixing and (iii) complete mixing.

Similar to the F- and W- curves, the E-curve or exit-age distribution can be derived (see Figure 2). It can be calculated by derivation of the F-curve or measured by applying a tracer impulse which needs to be normalized to the area under the curve equal to 1. The normalization is necessary as the E-curve is representing a probability density distribution and the integral need to be 1. All these curves contain the same information and can be translated into each other. From a practical point of view, this means, that

either impulse response or step response experiments will give the same information about the mixing behavior of the system under investigation.

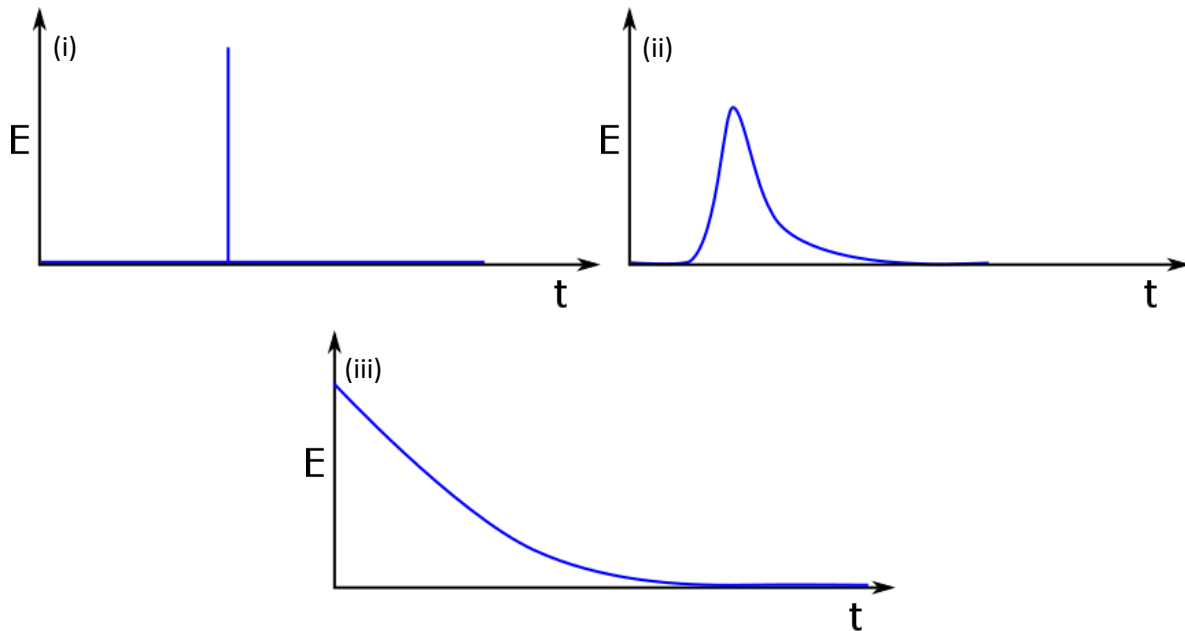


Figure 2: E-Curves for (i) plug flow, (ii) plug flow with longitudinal mixing and (iii) complete mixing.

The broader the E-curve, the better will the system's capability of attenuating disturbances but in contrast to this, the system will have a longer batch transition time. On the other hand, when the E-curve is narrow and hence high (as the area under the E-curve always needs to be 1), disturbances will pass the unit operation slightly dampened but the batch transition time will be short. Therefore, knowledge of the RTD curve allows optimization of batch sizes as it is known, how long a batch transition lasts and how much material will consist of two raw material batches and so needs to be separated from the processing stream.

The in-silico connection of the E-curves of each used unit operation by convolution of the E-curves leads to a RTD model for the whole production line [20].

### 1.3.1 Measurement methods

Residence time distribution measurements are always based on the measurement of a concentration of either an API or some other detectable material as tracer and a suitable (sensitive) sensor to measure the tracer concentration. Moreover, the tracer material or change in API concentration must not (strongly) affect the flow behavior of the material/mixture/granulate.

The tracer addition (system's excitation) can be performed either by application of a tracer impulse (additionally to the material flow into the unit) [11] or by a step change in e.g. API concentration (10 wt% → 20 wt%) or the transition of colored to uncolored material or vice versa [13].

The application of a tracer impulse is leading directly to the measurement of a scaled exit age distribution whereas a step response experiment can be translated to a scaled positive or negative wash-out function [12].

There are many aspects when designing a RTD measurement strategy. Dependent on the unit operation, accessibility of the powder inlet and the mixing behavior, an adequate tracer addition method needs to be chosen. Furthermore, the sensitivity, time and spatial resolution, measurement range and mechanical/chemical stability of the detection device need to be taken into account. Furthermore, adequate sample representation to the measurement device can be challenging.

Usually, step response experiments are preferred because the signal intensity is higher and the range can be chosen arbitrarily e.g. for a step in API concentration. Nevertheless, it has to be kept in mind, that a large change in composition of the mixture might lead to different mixing behavior in the system and hence leading to incorrect results. The tradeoff between signal intensity and influence of mixing behavior needs to be carefully considered. In case of impulse response experiments, the mass flow into the system changes for a short period of time which can also influence the mixing behavior in the system but as the tracer (in our case a fine color pigment) is well distributed among the bulk powder particles due to mixing and hence the local concentration of the tracer will be fairly low, the effects influencing the system's response are considered insignificant.

The step response experiments in this work were selected because the nature of the process did not allow to perform well defined impulse response experiments as the volume of the powder bowl is so large that the amount of tracer needed to obtain a valid color signal at the output was high and an impact on mixing was likely. Therefore, a method was developed to color the bulk powder material minimizing the influence of tracer material on the measurement and simultaneously obtaining high signal intensities.

### 1.3.2 RTD modeling approaches

There are many different RTD modeling approaches reported in literature ranging from simple equations to highly complex particle based models. A tradeoff between computational effort and model complexity, which has to be carefully evaluated dependent on the application. In this work, connected RTD models are required to predict the effect of feed disruption on the processing line. Furthermore, this production line model can be used for control purposes in model-based control, where the models are used for controller design or even suitability for model-predictive control (MPC) is desired. The applicability of MPC requires

models, which can be solved extremely fast, as for each time step, an optimization problem needs to be solved to optimize the control actions based on actual, previous and predicted future data.

There are simple equations as in the tanks-in-series models [11–13,20,21,51], where the equations for a single CSTR are cascaded leading to an intermediate mixing behavior between plug flow and CSTR. If the number of cascaded CSTRs approaches zero, the system shows plug flow behavior whereas when an infinite number of CSTRs is cascaded, perfect mixing is obtained.

Taylor dispersion model [74–78] is based on a convection-diffusion equation to describe the evolution of the tracer concentration over time. The shape of the curve is determined by the Peclet number.

Similar to the tanks-in-series models are transfer functions [11–13,21]. The multiplication of first order low pass terms is equivalent to cascaded CSTRs. Additionally, high pass terms can be added to model more complex shapes of the RTD curves. The benefit of modeling the RTD with transfer functions is, that there are a large variety of tools for controller design which can be applied straight forward to this model structure [79].

A more complex modeling approach which allows deeper insight into process dynamics are population balance models (PBM) [3,52,53,80–89]. These models describe the evolution of certain attributes over time. This can be in one dimension e.g. the particle size where breakage and agglomeration kernels govern the dynamics to multi-dimensional PBMs, where more attributes are models. These PBMs allow to predict the evolution of the population of a single material species and hence model the concentrations of substances at the system outlet. PBM models represent models with intermediate to high complexity, dependent on the dimensionality. Thus, the simpler one-dimensional PBMs are suitable for controller design but limited for MPC, dependent on the controller speed required for the application.

The most complex models with highest computational costs are discrete element models (DEM) [60,90–92] where force balances are calculated for each single particle. Coupling of DEM with continuous fluid dynamics (CFD) [93–97] or PBM [80,87,89,98–103] is also possible. The computational effort to solve a model is dependent on the complexity.

## 1.4 Literature

- [1] E.U. Hartge, M. Pogodda, C. Reimers, D. Schwier, G. Gruhn, J. Werther, Flowsheet Simulation of Solids Processes, *Kona*. 24 (2006) 146–158. doi:10.14356/kona.2006017.
- [2] F. Boukouvala, V. Niotis, R. Ramachandran, F.J. Muzzio, M.G. Ierapetritou, An integrated approach for dynamic flowsheet modeling and sensitivity analysis of a continuous tablet manufacturing process, *Comput. Chem. Eng.* 42 (2012) 30–47. doi:10.1016/j.compchemeng.2012.02.015.
- [3] F. Boukouvala, A. Chaudhury, M. Sen, R. Zhou, L. Mioduszewski, M.G. Ierapetritou, R.

- Ramachandran, Computer-Aided Flowsheet Simulation of a Pharmaceutical Tablet Manufacturing Process Incorporating Wet Granulation, *J. Pharm. Innov.* 8 (2013) 11–27. doi:10.1007/s12247-012-9143-9.
- [4] S. García-Munoz, A. Butterbaugh, I. Leavesley, L.F. Manley, A flowsheet model for the development of a continuous process for pharmaceutical tablets – an industrial perspective, 00 (2017) 1–15. doi:10.1002/aic.
- [5] M. Sen, A. Chaudhury, R. Singh, J. John, R. Ramachandran, Multi-scale flowsheet simulation of an integrated continuous purification-downstream pharmaceutical manufacturing process., *Int. J. Pharm.* 445 (2013) 29–38. doi:10.1016/j.ijpharm.2013.01.054.
- [6] C. Reimers, J. Werther, G. Gruhn, Design specifications in the flowsheet simulation of complex solids processes, *Powder Technol.* 191 (2009) 260–271. doi:10.1016/j.powtec.2008.10.012.
- [7] G.M. Troup, C. Georgakis, Process systems engineering tools in the pharmaceutical industry, *Comput. Chem. Eng.* 51 (2013) 157–171. doi:10.1016/j.compchemeng.2012.06.014.
- [8] PSE: Home, (n.d.). <https://www.psenterprise.com/home> (accessed September 3, 2018).
- [9] Aspen HYSYS, (n.d.). <https://www.aspentech.com/products/engineering/aspen-hysys> (accessed September 3, 2018).
- [10] ProSimPlus software - Steady-state simulation and optimization of chemical processes - process engineering software that performs rigorous mass and energy balance calculations for a wide range of ind, (n.d.). <http://www.prosim.net/en/software-prosimplus-steadystate-simulation-and-optimization-of-processes-1.php> (accessed September 3, 2018).
- [11] J. Kruisz, J. Rehr, S. Sacher, I. Aigner, M. Horn, J.G. Khinast, RTD Modeling of a Continuous Dry Granulation Process for Process Control and Materials Diversion, *Int. J. Pharm.* 528 (2017) 334–344. doi:10.1016/j.ijpharm.2017.06.001.
- [12] J. Kruisz, E. Faulhammer, J. Rehr, O. Scheibelhofer, A. Witschnigg, J.G. Khinast, Residence Time Distribution of a Continuously-operated Capsule Filling Machine: Development of a Measurement Technique and Comparison of Three Volume-Reducing Inserts, *Int. J. Pharm.* (2018). doi:10.1016/J.IJPHARM.2018.08.017.
- [13] M.C. Martinetz, A.-P. Karttunen, S. Sacher, P. Wahl, J. Ketolainen, J.G. Khinast, O. Korhonen, RTD-based Material Tracking in a Fully-Continuous Dry Granulation Tableting Line, *Int. J. Pharm.* 547 (2018) 469–479. doi:10.1016/J.IJPHARM.2018.06.011.
- [14] G. Allison, Y.T. Cain, C. Cooney, T. Garcia, T. Goonen, O. Holt, B. Komasa, E. Korakianiti, D. Kourti, R. Madurawe, E. Morefield, M. Nasr, W. Randolph, J. Robert, D. Rudd, D. Zezza, Regulatory and Quality Considerations for Continuous Manufacturing, Symposium. (n.d.).
- [15] EDQM, European Pharmacopoeia, 2011.
- [16] R. Meier, M. Thommes, N. Rasenack, K.-P.P. Moll, M. Krumme, P. Kleinebudde, Granule size distributions after twin-screw granulation ??? Do not forget the feeding systems, *Eur. J. Pharm. Biopharm.* 106 (2016) 59–69. doi:10.1016/j.ejpb.2016.05.011.
- [17] J. Rantanen, J. Khinast, The Future of Pharmaceutical Manufacturing Sciences, *J. Pharm. Sci.* 104 (2015) 3612–3638. doi:10.1002/jps.24594.



- [18] J. Rehr, A.-P. Karttunen, N. Nicolai, T. Hörmann, M. Horn, O. Korhonen, I. Nopens, T. De Beer, J.G. Khinast, Control of three different continuous pharmaceutical manufacturing processes: Use of soft sensors, *Int. J. Pharm.* 543 (2018) 60–72. doi:10.1016/J.IJPHARM.2018.03.027.
- [19] B. Van Snick, J. Holman, C. Cunningham, A. Kumar, J. Vercruyse, T. De Beer, J.P. Remon, C. Vervaet, Continuous direct compression as manufacturing platform for sustained release tablets, Elsevier B.V., 2017. doi:10.1016/j.ijpharm.2017.01.010.
- [20] W. Engisch, F. Muzzio, Using Residence Time Distributions (RTDs) to Address the Traceability of Raw Materials in Continuous Pharmaceutical Manufacturing, *J. Pharm. Innov.* 11 (2016) 64–81. doi:10.1007/s12247-015-9238-1.
- [21] J. Rehr, J. Krusz, S. Sacher, J. Khinast, M. Horn, Optimized continuous pharmaceutical manufacturing via model-predictive control, *Int. J. Pharm.* 510 (2016) 100–115. doi:10.1016/j.ijpharm.2016.06.024.
- [22] FDA, Guidance for Industry Guidance for Industry PAT — A Framework for Innovative Pharmaceutical, (2004) 19.
- [23] I.C. on Harmonisation, Pharmaceutical Development Q8(R2), 2009. [https://www.ich.org/fileadmin/Public\\_Web\\_Site/ICH\\_Products/Guidelines/Quality/Q8\\_R1/Step4/Q8\\_R2\\_Guideline.pdf](https://www.ich.org/fileadmin/Public_Web_Site/ICH_Products/Guidelines/Quality/Q8_R1/Step4/Q8_R2_Guideline.pdf) (accessed September 3, 2018).
- [24] I.C. on Harmonisation, Quality Risk Management Q9, 2005. [https://www.ich.org/fileadmin/Public\\_Web\\_Site/ICH\\_Products/Guidelines/Quality/Q9/Step4/Q9\\_Guideline.pdf](https://www.ich.org/fileadmin/Public_Web_Site/ICH_Products/Guidelines/Quality/Q9/Step4/Q9_Guideline.pdf) (accessed September 3, 2018).
- [25] International Conference on Harmonisation, Pharmaceutical Quality System Q10, 2008. [https://www.ich.org/fileadmin/Public\\_Web\\_Site/ICH\\_Products/Guidelines/Quality/Q10/Step4/Q10\\_Guideline.pdf](https://www.ich.org/fileadmin/Public_Web_Site/ICH_Products/Guidelines/Quality/Q10/Step4/Q10_Guideline.pdf) (accessed September 3, 2018).
- [26] International Conference on Harmonisation, Development and Manufacture of Drug Substances Q11, 2012. <https://www.fda.gov/downloads/Drugs/GuidanceComplianceRegulatoryInformation/Guidances/UCM542176.pdf> (accessed September 3, 2018).
- [27] International Conference on Harmonisation, Technical and Regulatory Considerations for Pharmaceutical Product Lifecycle Management Q12, 2017. [http://www.ich.org/fileadmin/Public\\_Web\\_Site/ICH\\_Products/Guidelines/Quality/Q12/Q12\\_DraftGuideline\\_Step2\\_2017\\_1116.pdf](http://www.ich.org/fileadmin/Public_Web_Site/ICH_Products/Guidelines/Quality/Q12/Q12_DraftGuideline_Step2_2017_1116.pdf) (accessed September 3, 2018).
- [28] J.S. Srai, C. Badman, M. Krumme, M. Futran, C. Johnston, Future supply chains enabled by continuous processing-opportunities and challenges May 20-21, 2014 continuous manufacturing symposium, *J. Pharm. Sci.* 104 (2015) 840–849. doi:10.1002/jps.24343.
- [29] S. Chatterjee (FDA), FDA Perspective on Continuous Manufacturing, in: IFPAC Annu. Meet., 2012.
- [30] M. Ierapetritou, F. Muzzio, G. Reklaitis, Perspectives on the continuous manufacturing of powder-based pharmaceutical processes, *AIChE J.* 62 (2016) 1846–1862. doi:10.1002/aic.15210.
- [31] S. Stegemann, The future of pharmaceutical manufacturing in the context of the scientific, social, technological and economic evolution, *Eur. J. Pharm. Sci.* (2015). doi:10.1016/j.ejps.2015.11.003.

- [32] J. Woodcock, The concept of pharmaceutical quality, *Am. Pharm. Rev.* 7 (2004) 10–15. <http://www.scopus.com/inward/record.url?eid=2-s2.0-57349152279&partnerID=tZOtx3y1>.
- [33] P.D. Sarantopoulos, T. Altiok, E.A. Elsayed, Manufacturing in the pharmaceutical industry, *J. Manuf. Syst.* 14 (1995) 452–467. doi:10.1016/0278-6125(95)99917-3.
- [34] H. Wu, M. White, M.A. Khan, Quality-by-Design (QbD): An integrated process analytical technology (PAT) approach for a dynamic pharmaceutical co-precipitation process characterization and process design space development., *Int. J. Pharm.* 405 (2011) 63–78. doi:10.1016/j.ijpharm.2010.11.045.
- [35] A.S. Rathore, QbD/PAT for bioprocessing: moving from theory to implementation, *Curr. Opin. Chem. Eng.* 6 (2014) 1–8. doi:10.1016/j.coche.2014.05.006.
- [36] S. Adam, D. Suzzi, C. Radeke, J.G. Khinast, An integrated Quality by Design (QbD) approach towards design space definition of a blending unit operation by Discrete Element Method (DEM) simulation., *Eur. J. Pharm. Sci.* 42 (2011) 106–15. doi:10.1016/j.ejps.2010.10.013.
- [37] E. Stocker, G. Toschkoff, S. Sacher, J.G. Khinast, Use of Mechanistic Simulations as a Quantitative Risk-Ranking Tool within the Quality by Design Framework, *Int. J. Pharm.* 475 (2014) 245–255. doi:10.1016/j.ijpharm.2014.08.055.
- [38] Z. Shi, K.C. McGhehey, I.M. Leavesley, L.F. Manley, On-line Monitoring of Blend Uniformity in Continuous Drug Product Manufacturing Process – the Impact of Powder Flow Rate and the Choice of Spectrometer: Dispersive vs FT, *J. Pharm. Biomed. Anal.* (2015). doi:10.1016/j.jpba.2015.11.005.
- [39] R. Singh, K. V. Gernaey, R. Gani, Model-based computer-aided framework for design of process monitoring and analysis systems, *Comput. Chem. Eng.* 33 (2009) 22–42. doi:10.1016/j.compchemeng.2008.06.002.
- [40] S. Heinrich, J. Blumschein, M. Henneberg, M. Ihlow, M. Peglow, L. Mörl, Study of dynamic multi-dimensional temperature and concentration distributions in liquid-sprayed fluidized beds, *Chem. Eng. Sci.* 58 (2003) 5135–5160. doi:10.1016/j.ces.2003.08.010.
- [41] R.T. Dec, A. Zavaliangos, J.C. Cunningham, Comparison of various modeling methods for analysis of powder compaction in roller press, *Powder Technol.* 130 (2003) 265–271. doi:10.1016/S0032-5910(02)00203-6.
- [42] H. Liu, S.C. Galbraith, B. Ricart, C. Stanton, B. Smith-Goettler, L. Verdi, T. O’Connor, S. Lee, S. Yoon, Optimization of critical quality attributes in continuous twin-screw wet granulation via design space validated with pilot scale experimental data, *Int. J. Pharm.* 525 (2017) 249–263. doi:10.1016/j.ijpharm.2017.04.055.
- [43] M. Andersson, O. Svensson, S. Folestad, M. Josefson, K. Wahlund, NIR spectroscopy on moving solids using a scanning grating spectrometer — impact on multivariate process analysis, *75* (2003) 1–11. doi:10.1016/j.chemolab.2003.10.007.
- [44] M. de Matas, T. De Beer, S. Folestad, J. Ketolainen, H. Lindén, J.A. Lopes, W. Oostra, M. Weimer, P. Ohrngren, J. Rantanen, Strategic framework for education and training in quality by design (QbD) and process analytical technology (PAT)., *Eur. J. Pharm. Sci.* (2016). doi:10.1016/j.ejps.2016.04.024.
- [45] R. Ramachandran, C.D. Immanuel, F. Stepanek, J.D. Litster, F.J. Doyle, A mechanistic model for breakage in population balances of granulation: Theoretical kernel development and experimental

- validation, *Chem. Eng. Res. Des.* 87 (2009) 598–614. doi:10.1016/j.cherd.2008.11.007.
- [46] C. Srinivasakannan, A. Al Shoaibi, N. Balasubramanian, Continuous Fluidized Bed Drying With and Without Internals : Kinetic Model, 26 (2012) 97–104.
- [47] J.G. Osorio, F.J. Muzzio, Effects of processing parameters and blade patterns on continuous pharmaceutical powder mixing, *Chem. Eng. Process. Process Intensif.* 109 (2016) 59–67. doi:10.1016/j.cep.2016.07.012.
- [48] I. Banerjee, S. Pal, S. Maiti, Computationally efficient black-box modeling for feasibility analysis, *Comput. Chem. Eng.* 34 (2010) 1515–1521. doi:10.1016/j.compchemeng.2010.02.016.
- [49] W.R. Ketterhagen, J.S. Curtis, C.R. Wassgren, B.C. Hancock, Modeling granular segregation in flow from quasi-three-dimensional, wedge-shaped hoppers, *Powder Technol.* 179 (2008) 126–143. doi:10.1016/j.powtec.2007.06.023.
- [50] K. V. Gernaey, A.E. Cervera-Padrell, J.M. Woodley, A perspective on PSE in pharmaceutical process development and innovation, *Comput. Chem. Eng.* 42 (2012) 15–29. doi:10.1016/j.compchemeng.2012.02.022.
- [51] B. Wagner, T. Brinz, S. Otterbach, J. Khinast, Rapid automated process development of a continuous capsule-filling process, *Int. J. Pharm.* 546 (2018) 154–165. doi:10.1016/J.IJPHARM.2018.05.009.
- [52] A. Rogers, M. Ierapetritou, Challenges and Opportunities in Modeling Pharmaceutical Manufacturing Processes, *Comput. Chem. Eng.* (2015). doi:10.1016/j.compchemeng.2015.03.018.
- [53] F. Boukouvala, R. Ramachandran, A. Vanarase, J. Fernando, M.G. Ierapetritou, *Computer Aided Design and Analysis of Continuous Pharmaceutical Manufacturing Processes*, Elsevier B.V., 2011. doi:10.1016/B978-0-444-53711-9.50044-4.
- [54] T. Kamiya, H. Kondo, H. Hiroma, K. Yamashita, T. Hakomori, K. Sako, Y. Iwao, S. Noguchi, S. Itai, Impact of process parameters on Mg–St content and tablet surface wettability in the external lubrication method for a rotary tablet press, *Adv. Powder Technol.* 27 (2016) 193–198. doi:10.1016/J.APT.2015.11.012.
- [55] S. Yu, M. Adams, B. Gururajan, G. Reynolds, R. Roberts, C.-Y. Wu, The effects of lubrication on roll compaction, ribbon milling and tableting, *Chem. Eng. Sci.* 86 (2013) 9–18. doi:10.1016/j.ces.2012.02.026.
- [56] C. Vervaet, J.P. Remon, Continuous granulation in the pharmaceutical industry, *Chem. Eng. Sci.* 60 (2005) 3949–3957. doi:10.1016/j.ces.2005.02.028.
- [57] A. Rogers, A. Hashemi, M. Ierapetritou, Modeling of Particulate Processes for the Continuous Manufacture of Solid-Based Pharmaceutical Dosage Forms, *Processes.* 1 (2013) 67–127. doi:10.3390/pr1020067.
- [58] A.U. Vanarase, F.J. Muzzio, Effect of operating conditions and design parameters in a continuous powder mixer, *Powder Technol.* 208 (2011) 26–36. doi:10.1016/j.powtec.2010.11.038.
- [59] L. Pernenkil, *Continuous Blending of Dry Pharmaceutical Powders*, IIT Madras, 2003.
- [60] A. Dubey, A. Sarkar, M. Ierapetritou, C.R. Wassgren, F.J. Muzzio, Computational Approaches for Studying the Granular Dynamics of Continuous Blending Processes, 1 - DEM Based Methods, *Macromol. Mater. Eng.* 296 (2011) 290–307. doi:10.1002/mame.201000389.

- [61] Z. Wang, M.S. Escotet-Espinoza, M. Ierapetritou, Process analysis and optimization of continuous pharmaceutical manufacturing using flowsheet models, *Comput. Chem. Eng.* (2017). doi:10.1016/j.compchemeng.2017.02.030.
- [62] A. Companies, M. Continuous, R. Guidat, S. Bioscience, F. Systems, E. Summary, Equipment and Analytical Companies Meeting Continuous Challenges, (n.d.) 1–18.
- [63] Stephen Byrn, M. Futran, H. Thomas, E. Jayjock, N. Maron, R.F. Meyer, A.S. Myerson, M.P. Thien, B.L. Trout, Achieving Continuous Manufacturing for Final Dosage Formation: Challenges and How to Meet Them, *Int. Symp. Contin. Manuf. Pharm.* (2014) White Paper 2. doi:10.1002/jps.24247.
- [64] S.L. Lee, T.F. O'Connor, X. Yang, C.N. Cruz, S. Chatterjee, R.D. Madurawe, C.M. V. Moore, L.X. Yu, J. Woodcock, Modernizing Pharmaceutical Manufacturing: from Batch to Continuous Production, *J. Pharm. Innov.* 10 (2015) 191–199. doi:10.1007/s12247-015-9215-8.
- [65] E. Reitz, H. Podhaisky, D. Ely, M. Thommes, Residence time modeling of hot melt extrusion processes, *Eur. J. Pharm. Biopharm.* 85 (2013) 1200–1205. doi:10.1016/j.ejpb.2013.07.019.
- [66] Y. Gao, F.J. Muzzio, M.G. Ierapetritou, A review of the Residence Time Distribution (RTD) applications in solid unit operations, *Powder Technol.* 228 (2012) 416–423. doi:10.1016/j.powtec.2012.05.060.
- [67] R.D. B. Allan S. Myerson, Markus Krumme, Moheb Nasr, Hayden Thomas, A.S. Myerson, M. Krumme, M. Nasr, H. Thomas, R.D. Braatz, Control Systems Engineering in Continuous Pharmaceutical Manufacturing - White Paper 6, *Int. Symp. Contin. Manuf. Pharm.* (2014) 1–13. <https://iscmp.mit.edu/white-papers/white-paper-6>.
- [68] S.-P. Simonaho, J. Ketolainen, T. Ervasti, M. Toiviainen, O. Korhonen, Continuous manufacturing of tablets with PROMIS-line – Introduction and case studies from continuous feeding, blending and tableting, *Eur. J. Pharm. Sci.* (2016). doi:10.1016/j.ejps.2016.02.006.
- [69] G. Vetter, *Handbuch Dosieren*, Vulkan-Verl, 2002. [https://books.google.at/books/about/Handbuch\\_Dosieren.html?id=CBTdYGhyPecC&redir\\_esc=y](https://books.google.at/books/about/Handbuch_Dosieren.html?id=CBTdYGhyPecC&redir_esc=y) (accessed September 3, 2018).
- [70] J. Khinast, J. Rantanen, *Continuous Manufacturing of Pharmaceuticals*, John Wiley & Sons, Ltd, Chichester, UK, 2017. doi:10.1002/9781119001348.
- [71] F. Podczeczek, B.E. Jones, Dry filling of hard capsules, *Pharm. Capsul.* (2004) 119–138. [www.pharmpress.com](http://www.pharmpress.com).
- [72] P.V. Danckwerts, Continuous flow systems, *Chem. Eng. Sci.* 2 (1953) 1–13. doi:10.1016/0009-2509(53)80001-1.
- [73] I. Langmuir, The Velocity of Reactions in Gases Moving through Heated Vessels and the Effect of Convection and Diffusion., *J. Am. Chem. Soc.* 30 (1908) 1742–1754. doi:10.1021/ja01953a011.
- [74] E.B. Nauman, Residence Time Theory, *Ind. Eng. Chem. Res.* 47 (2008) 3752–3766. doi:10.1021/ie071635a.
- [75] T.D. Theory, Taylor Dispersion Theory Chapter 3, in: 1950: pp. 25–42.
- [76] Taylor, Dispersion of soluble matter in solvent flowing slowly through a tube, (1953).

- [77] G.I. Taylor, Diffusion and Mass Transport in Tubes, Proc. Phys. Soc. Sect. B. 67 (1954) 857–869. doi:10.1088/0370-1301/67/12/301.
- [78] M.R. Thompson, B. Mu, P.J. Sheskey, Aspects of foam stability influencing foam granulation in a twin screw extruder, Powder Technol. 228 (2012) 339–348. doi:10.1016/j.powtec.2012.05.050.
- [79] C.-T. Chen, Signals and Systems, 3rd ed., 2004.
- [80] A.-I. Yeh, Y. Jaw, Modeling Residence Time Distributions for Single Screw Extrusion Process, J. Food Eng. 35 (1997) 211–232. doi:10.1016/j.crci.2006.07.006.
- [81] T. Glaser, C.F.W. Sanders, F.Y. Wang, I.T. Cameron, J.D. Litster, J.M.-H. Poon, R. Ramachandran, C.D. Immanuel, F.J. Doyle, Model predictive control of continuous drum granulation, J. Process Control. 19 (2009) 615–622. doi:10.1016/j.jprocont.2008.09.001.
- [82] R. Gupta, Fluid bed granulation and drying, Elsevier Ltd, 2016. doi:10.1016/B978-0-08-100154-7.00006-5.
- [83] M. Hussain, J. Kumar, E. Tsotsas, A new framework for population balance modeling of spray fluidized bed agglomeration, Particuology. 19 (2015) 141–154. doi:10.1016/j.partic.2014.06.005.
- [84] R. Ramachandran, A. Chaudhury, Model-based design and control of a continuous drum granulation process, Chem. Eng. Res. Des. 90 (2012) 1063–1073. doi:10.1016/j.cherd.2011.10.022.
- [85] D. Barrasso, S. Walia, R. Ramachandran, Multi-component population balance modeling of continuous granulation processes: A parametric study and comparison with experimental trends, Powder Technol. 241 (2013) 85–97. doi:10.1016/j.powtec.2013.03.001.
- [86] E. Bilgili, J. Yepes, B. Scarlett, Formulation of a non-linear framework for population balance modeling of batch grinding: Beyond first-order kinetics, Chem. Eng. Sci. 61 (2006) 33–44. doi:10.1016/j.ces.2004.11.060.
- [87] A. Chaudhury, A. Niziolek, R. Ramachandran, Multi-dimensional mechanistic modeling of fluid bed granulation processes: An integrated approach, Adv. Powder Technol. 24 (2013) 113–131. doi:10.1016/j.appt.2012.03.005.
- [88] F.Y. Wang, I.T. Cameron, A multi-form modelling approach to the dynamics and control of drum granulation processes, Powder Technol. 179 (2007) 2–11. doi:10.1016/j.powtec.2006.11.003.
- [89] T.C. Seem, N. a. Rowson, A. Ingram, Z. Huang, S. Yu, M. de Matas, I. Gabbott, G.K. Reynolds, T. Chan Seem, N. a. Rowson, I. Gabbott, M. de Matas, G.K. Reynolds, A. Ingram, T.C. Seem, N. a. Rowson, A. Ingram, Z. Huang, S. Yu, M. de Matas, I. Gabbott, G.K. Reynolds, Twin screw granulation - A literature review, Powder Technol. 276 (2015) 89–102. doi:10.1016/j.powtec.2015.01.075.
- [90] P.A. Cundall, O.D.L. Strack, A discrete numerical model for granular assemblies, Géotechnique. 29 (1979) 47–65.
- [91] A. Sarkar, C.R. Wassgren, Comparison of flow microdynamics for a continuous granular mixer with predictions from periodic slice DEM simulations, Powder Technol. 221 (2012) 325–336. doi:10.1016/j.powtec.2012.01.021.
- [92] P. Boehling, G. Toschkoff, S. Just, K. Knop, P. Kleinebudde, A. Funke, H. Rehbaum, P. Rajniak, J.G. Khinast, Simulation of a tablet coating process at different scales using DEM, (2016). doi:10.1016/j.ejps.2016.08.018.

- [93] L. Li, J. Remmelgas, B.G.M. van Wachem, C. von Corswant, M. Johansson, S. Folestad, A. Rasmuson, Residence time distributions of different size particles in the spray zone of a Wurster fluid bed studied using DEM-CFD, *Powder Technol.* 280 (2015) 124–134. doi:10.1016/j.powtec.2015.04.031.
- [94] M. Ebrahimi, E. Siegmann, D. Prieling, B.J. Glasser, J.G. Khinast, An investigation of the hydrodynamic similarity of single-spout fluidized beds using CFD-DEM simulations, (2017). doi:10.1016/j.appt.2017.05.009.
- [95] D. Jajcevic, E. Siegmann, C. Radeke, J.G. Khinast, Large-scale CFD–DEM simulations of fluidized granular systems, *Chem. Eng. Sci.* 98 (2013) 298–310. doi:10.1016/j.ces.2013.05.014.
- [96] J. Jang, H. Arastoopour, CFD simulation of a pharmaceutical bubbling bed drying process at three different scales, *Powder Technol.* 263 (2014) 14–25. doi:10.1016/j.powtec.2014.04.054.
- [97] L. Fries, S. Antonyuk, S. Heinrich, S. Palzer, DEM–CFD modeling of a fluidized bed spray granulator, *Chem. Eng. Sci.* 66 (2011) 2340–2355. doi:10.1016/j.ces.2011.02.038.
- [98] T. Kulju, Modeling Continuous High-Shear Wet Granulation with DEM-PB, (n.d.).
- [99] A. Chaudhury, A. Niziolek, R. Ramachandran, Multi-dimensional mechanistic modeling of fluid bed granulation processes: An integrated approach, *Adv. Powder Technol.* 24 (2013) 113–131. doi:10.1016/j.appt.2012.03.005.
- [100] M. Sen, A. Dubey, R. Singh, R. Ramachandran, Mathematical Development and Comparison of a Hybrid PBM-DEM Description of a Continuous Powder Mixing Process, *J. Powder Technol.* 2013 (2013) 1–11. doi:10.1155/2013/843784.
- [101] D. Barrasso, R. Ramachandran, Qualitative Assessment of a Multi-Scale, Compartmental PBM-DEM Model of a Continuous Twin-Screw Wet Granulation Process, *J. Pharm. Innov.* 11 (2016) 231–249. doi:10.1007/s12247-015-9240-7.
- [102] D. Barrasso, A. Tamrakar, R. Ramachandran, Model Order Reduction of a Multi-scale PBM-DEM Description of a Wet Granulation Process via ANN, *Procedia Eng.* 102 (2015) 1295–1304. doi:10.1016/j.proeng.2015.01.260.
- [103] D. Barrasso, T. Eppinger, F.E. Pereira, R. Aglave, K. Debus, S. Bermingham, R. Ramachandran, A multi-scale, mechanistic model of a wet granulation process using a novel bi-directional PBM-DEM coupling algorithm, *Chem. Eng. Sci.* (2014). doi:10.1016/j.ces.2014.11.011.

---

*"Know how to solve every problem that has ever been solved."*

*Richard Feynman."*

## 2 RTD Modeling of a Continuous Dry Granulation Process for Process Control and Materials Diversion

Julia Krusisz<sup>1</sup>, Jakob Rehr<sup>1,2</sup>, Stephan Sacher<sup>1</sup>, Isabella Aigner<sup>1</sup>, Martin Horn<sup>2</sup>, Johannes G. Khinast<sup>1,3</sup>

<sup>1</sup>Research Center Pharmaceutical Engineering GmbH, Graz, Austria

<sup>2</sup>Institute of Automation and Control, Graz University of Technology, Graz, Austria

<sup>3</sup>Institute for Process and Particle Engineering, Graz University of Technology, Graz, Austria

### 2.1 Abstract

Disturbance propagation during continuous manufacturing processes can be predicted by evaluating the residence time distribution (RTD) of the specific unit operations. In this work, a dry granulation process was modelled and four scenarios of feeding events were simulated. We performed characterization of the feeders and developed RTD models for the blender and the roller compactor based on impulse-response measurements via color tracers. Out-of-specification material was defined based on the active pharmaceutical ingredient (API) concentration. We calculated the amount of waste material at various diversion points, considering four feeder-related process-upset scenarios and formulated considerations for the development of a control concept. The developed RTD models allow material tracking of materials that may be used for following the spread contaminants within the process and for batch definition. The results show that RTD modeling is a valuable tool for process development and design, as well as for process monitoring and material tracking.

**Keywords:** Continuous Manufacturing, RTD Modelling, Out-of-Spec Handling, Dry Granulation, Process Control

## 2.2 Introduction

In the pharmaceutical industry, a transition from batch processing to continuous manufacturing (CM) is taking place [1], [2] due to the advantages of CM, such as smaller production equipment, higher flexibility and elimination of scale-up issues. By applying CM, the amount of product is determined by the production time rather than by equipment size. Thus, the same equipment can be used for development and industrial production [3]. Furthermore, through CM the amount of material in stock can be reduced via supply chain management. In addition, CM approaches are more flexible and agile and speed up the development process (e.g., during the transition from small-scale clinical trials to industrial-scale batches). This reduces time-to-market and provides extended patent life time [4].

Process understanding is a critical prerequisite for CM. To facilitate process understanding, the Food and Drug Administration (FDA) launched guidelines for the development of Process Analytical Technologies (PAT) in 2004 [5]. Moreover, the International Conference on Harmonization (ICH) guidelines (Q8 [6] and Q10 [7]) were released. These guidelines created a new mindset in terms of quality, incorporating process monitoring of the intermediates and not only of the end product.

For assuring a constant product quality within a CM framework, real-time process monitoring of intermediate quality attributes is a prerequisite. Handling out-of-spec (OOS) material is a significant challenge in this context. In general, production disturbances may lead to faulty intermediate products, resulting in an OOS end product. In batch processing, an entire batch must be destroyed due to OOS material, which can be costly since a whole batch is lost and the disposal can be expensive. In CM, it is possible to reject only the OOS material at some point during the process, as well as counteract process disturbances and keep the final product in-spec. Due to interconnection of all unit operations, reacting adequately requires deep process knowledge and a sophisticated control concept.

The decision whether to divert material (material diversion or segregation) can be based on monitoring the process parameters or in-line measurement of critical quality attributes (CQAs). In this work, a general concept of concentration measurements using NIR and other PAT tools is presented for a *continuous dry granulation line*. NIR is a commonly used technique to measure the API concentration. A model is applied which predicts the concentration based on calibration measurements. The prediction is not instantaneous since data acquisition (integration time) and solving the model require time, which has to be taken into account when developing diversion strategies. Hence, the diversion points have to be chosen such that the OOS material can be detected before the diversion points are reached. To determine if the locations of the measurement- and diversion-points are chosen in a suitable manner, the RTD of the process must be analyzed. Furthermore, with regard to regulatory approval of a continuously-manufactured pharmaceutical product, material tracking is crucial, i.e., for establishing a “bill of materials (BOM)”.



Knowing the RTD allows calculation of the position of material introduced into the process at any given time [8]. Process simulation is a valuable tool in this context [9], [10].

Dry granulation is an important unit operation in pharmaceutical manufacturing, making it possible to process poorly flowing and highly cohesive materials by enhancing their flowability via particle size enlargement [11], [12]. Moreover, segregation and dusting during subsequent processing steps can be decreased. Furthermore, this type of particle size enlargement requires no liquid addition, allowing to process moisture-sensitive or easily dissolving materials. In this work, a dry granulation step via roller compaction (RC) was combined with a feeding/blending unit (FBU) and a tablet press to create a continuous pharmaceutical process for tablet manufacturing (similarly to the dry granulation presented in [13]) shown in Figure 3.

In the line considered, the tablet press is the last in a sequence of continuously operated units. It typically has a hopper, which may be used as buffer in case of diversion OOS material before it reaches the tablet press. Accurate diversion of OOS material can be achieved via PAT (e.g., near infrared spectroscopy) [14], [15], [16], better process understanding and sophisticated predictions of the concentrations based on the internal control/monitoring systems of the unit operations (e.g., loss-in-weight (LIW) feeder signal).

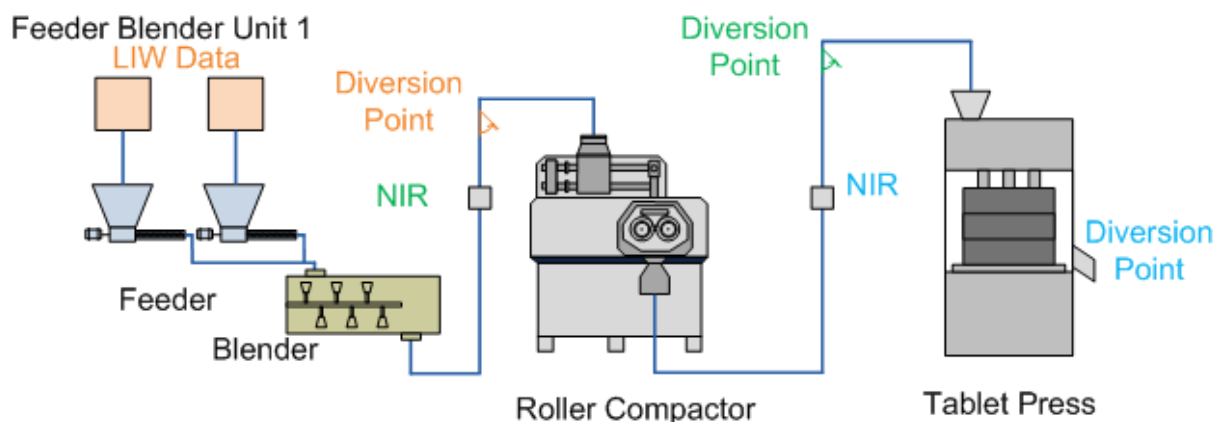


Figure 3: Schematic of the modeled dry granulation process line. The three possible measurement/diversion point pairs are marked in the same color. The first in orange using LIW measurement data for the detection of OOS material and diversion happens after the blender. The second pair is marked in green, with NIR measurement of concentration after the blender and diversion after the roller compactor (RC) and the last, marked in blue with NIR measurement after the RC and diversion after the tablet press.

Our work focused on the development of a concept for OOS detection based on deviations in concentrations. The proposed models, presented in Section 2.3.1, Sections 2.3.2 and 2.3.3 provide an experimental description and highlight the data-processing approach. Simulations of disturbance scenarios are discussed in Section 2.3.4, with a comparison of diversion times and waste material. Finally, simulations are presented for a continuous dry granulation line, with the evaluation of various

measurement- and diversion point-combinations and prediction of the amount of waste material in Section 2.4. Specifically, material diversion after the blender and the RC unit was considered and the impact of process disruptions by the feeder on the amount of OOS material was studied.

## 2.3 Materials and Methods

### 2.3.1 Model Development

Based on the RTD of each unit operation, concentrations after each processing step can be predicted and used for the development of a control concept. Moreover, studies of different material diversion scenarios can be carried out and hopper design (i.e., optimized storage capacity) can be based on rational science. In this work, we focused on the material diversion strategies in combination with PAT measurement positions to address fluctuations of the API concentrations.

The feeder model was developed under the assumption that the feeder has a constant feed rate with some additional noise and a periodic disturbance caused by the feed screw. A start-up phase with higher mass-flow deviations due to internal signal processing/calibrations of the feeder was not considered. The mass flow rate of the feeders is given by Eq. 1, where  $\dot{m}_0$  is the nominal mass flow rate (set-point),  $\omega_{feeder}$  is the screw speed in revolutions per minute and  $\mathcal{N}(0, \sigma)$  is normally distributed white noise with a certain standard deviation  $\sigma$  that depends on the equipment and material used and can be characterized via measurements.  $k$  is a scaling constant. Both  $\omega$  and  $\sigma$  are functions of the nominal mass flow rate  $\dot{m}_0$ .

$$\dot{m}_{feed} = \dot{m}_0 + k \sin(\omega t) + \mathcal{N}(0, \sigma) \quad (1)$$

Concentrations at the inlet of the blender are given by Eq. 2 based on the mass flow rates of the API and excipient feeders.

$$C_{API}(t) = \frac{\dot{m}_{API}(t)}{\dot{m}_{API}(t) + \dot{m}_{EXC}(t)}; \quad C_{EXC}(t) = \frac{\dot{m}_{EXC}(t)}{\dot{m}_{API}(t) + \dot{m}_{EXC}(t)} \quad (2)$$

The exit-age distribution  $E(t)$  used for determining the RTD is provided in Eq. 3, where  $C(t)$  is the time-dependent concentration of a tracer at the outlet of the unit operation. Normalization according to Eq. 3 is required since the RTD is per definition a probability density function and the condition  $\int_0^\infty E(t) dt = 1$  has to be satisfied. Experimentally, this RTD can be determined via impulse response tests, as described below and as proposed by Engisch et.al [8]. Operating conditions are known to have an influence on the RTD curve [17]–[23], meaning that  $E(t)$  is a function of the rotational speed  $\omega_{bl}$  and the mass flow  $\dot{m}$ . Although other parameters (i.e., the blade's angle and weir options) may also affect RTD, they were not investigated in this work since adjustment of these parameters during operation was not possible. Characteristic parameters of the exit-age distribution were also determined ( $\tau, t_5, t_{50}, t_{95}$ ).  $\tau$  is the mean residence time (calculated using Eq. 4) and  $t_x$  is the time until either 5%, 50% or 95% of the tracer material are removed from the system after the impulse injection (Eq. 5).

$$E(t) = \frac{c(t)}{\int_0^{\infty} c(t) dt} \quad (3)$$

$$\tau = \int_0^{\infty} t E(t) dt \quad (4)$$

$$\int_0^{t_x} E(t) dt = \frac{x}{100} \quad (5)$$

RTD models based on solving the Fokker-Plank Equation have been reported in the literature [19], [24]–[26]. This approach to describing the mixing behavior of components based on dimensionless convection-diffusion equations dates back to 1950s [27]. We propose another type of model, applying a transfer function  $P(s)$  (Eq. 6) to estimate the RTD. In Eq. 6,  $C_{in}(s)$  and  $C_{out}(s)$  are the Laplace-transformed [28] concentrations at the inlet and outlet of a unit operation, respectively. Note that we used the same variable names in the Laplace and time domains, i.e.,  $C_{in}(s) = \mathcal{L}\{C_{in}(t)\}$ , where  $\mathcal{L}$  is the Laplace transform [28]. The time constants  $T_1, T_2, T_3$ , the dead-time  $T_t$  (time delay from application of tracer until the tracer appears at the outlet) and the scaling factor  $K$  were identified using the experimental data generated via impulse response tests, as described in Section 2.3.2. These parameters are also a function of the rotational speed  $\omega_{bl}$  and the mass flow  $\dot{m}$ . The resulting concentration curve was normalized according to Eq. 3. The blender transfer function is then given by:

$$P_{bl}(s) = \frac{C_{out,bl}(s)}{C_{in,bl}(s)} = K \cdot \frac{(1+sT_1)}{(1+sT_2)} \cdot \frac{1}{(1+sT_3)} \cdot e^{-sT_t} \quad (6)$$

The roller compactor (RC) was modelled in a similar way. A transfer function was used to describe the mixing behavior of powder in the RC equipped with a co-mill to break the ribbon into granules. The equation for the blender was slightly modified. This modification was necessary to reduce the model error. The transfer function for the roller compaction process is shown in Eq. 7. The operating parameters that affected the RTD were the throughput, which depends on the roll speed and the roll gap, and the co-mill speed [11].

$$P_{RC}(s) = \frac{C_{out,RC}(s)}{C_{in,RC}(s)} = K \cdot \frac{1}{(1+sT_1)} \cdot \frac{1}{(1+sT_2)} \cdot e^{-sT_t} \quad (7)$$

An optimization problem (Eq. 8) was solved to estimate the parameters for both unit operations. It was implemented in Matlab® (Mathworks Inc., Natick, USA) with the integrated function `fmincon`. The optimization variables were collected in the vector  $\mathbf{x} = [T_1, T_2, T_3, T_t, K]$ .  $y_i$  is the measured intensity/concentration and  $\hat{y}$  is the concentration predicted by the model with transfer function  $P(s)$ . The constraints were set to allow only positive time constants, dead time and scaling constants.

$$\mathbf{x}_{opt} = \arg \min \sum_i (y_i - \hat{y}_i(\mathbf{x}))^2 \quad (8)$$

The model output was computed via the impulse response of the transfer function, where  $T_s$  is the sampling time. In our case,  $T_s = 1$  s was chosen.

$$\hat{y}_i(\mathbf{x}) = \text{impulse}\{P(s)|_{\mathbf{x}=[T_1, T_2, T_3, T_t]}\}|_{t=i T_s} \quad (9)$$

The models of the unit operations connected in series were combined to predict the RTD of total dry granulation process by multiplying the individual transfer functions [29].

### 2.3.2 Experimental

Experiments were performed with a total integral mass flow of 5 kg/h. Feeding and blending experiments were conducted using Avicel PH-112 (a microcrystalline cellulose, MCC, from FMC Corporation, PA, USA) with  $d_{50} = 120 \mu\text{m}$  as a single excipient and ASS 3020 (GL Pharma, Lannach, Austria) with  $d_{50} = 445 \mu\text{m}$  as the API with a mass fraction of 5%. For the roller compactor experiments a similar blend was used, containing 85% Avicel PH-101 (another MCC from FMC H&N, Philadelphia, USA) with a  $d_{50} = 50 \mu\text{m}$  with 10% Paracetamol (Mallinckrodt Pharmaceuticals, Dublin, Ireland) having a  $d_{50} = 200 \mu\text{m}$  and 5% Kollidon CL (BASF, Ludwigshafen am Rhein, Germany) with  $d_{50} = 50 \mu\text{m}$ . This was done to highlight the large range of applicability of the developed method, using different formulations

A K-tron KT20 gravimetric feeder (Coperion K-Tron, NJ, USA) was used for the excipient (EXC) and a Brabender MT-S Hyg gravimetric feeder (Brabender Technologie GmbH & Co.KG, Duisburg, Germany) for the API. The RTD of the Modulo Mix (Hosokawa, Doetinchem, Netherlands), a continuous blender, was determined via yellow tracer (see below) experiments at rotational speeds of 500 rpm, 1000 rpm and 1500 rpm. The influence of rotational speed  $\omega_{bl}$  on the RTD was evaluated. From the blender's outlet, the material fell onto a belt conveyor, equipped with a camera on top. To reduce dusting, an acrylic glass housing was installed at the blender's outlet to allow the powder to settle on the belt. A combination of a rotating brush with a vacuum cleaner was used to remove the powder from the belt, eliminating artifacts from powder that adhered to the belt during previous rotations.

For the roller compaction experiments the pre-blend was mixed in a batch blender (Typ VMA 70). Two 20 kg batches were prepared, each in a container with a volume of 70 l placed on top of the BRC 25 (LB Bohle, Ennigerloh, Germany) RC. Yellow tracer was also used for the RC experiments.

Tracer experiments were performed separately for each unit. By separating measurements for the individual units, RTD models of single units were developed and a simple exchange/addition of unit operations during the simulation was made possible. Yellow pigments (color: "Sonnengelb", azo compounds) were used as a tracer material for the blender and roller compaction experiments. This coloring method was chosen due to an excellent coloring potency of the fine pigments ( $d_{50} \sim 3.5 \mu\text{m}$ ) at low concentrations and due to the easy handling. A digital SLR camera (Nikon D5200) was used for data acquisition. A video sequence with 50 frames/s was recorded after performing manually a white balance (e.g., capturing a white sheet of paper under measurement conditions). It was essential to provide a bright and homogeneous illumination. These arrangements were necessary to prevent undesired effects in the

video sequence, (e.g., a change in the lightness due to a changing ambient light) and to assure reproducible measurements.

### 2.3.2.1 Feeder/Blender

Feeder characterization was performed by feeding the material (either EXC or API) onto a catch scale and simultaneously logging the feeder- and catch-scale data. Before starting the experiments, the feeder-hoppers were filled with enough material to complete the run without refilling. When performing the blender RTD experiments, the feeders were placed on top of the blender to benefit from the gravitational transport of powder via a funnel into the continuous blender. A schematic of the experimental setup is shown in Figure 4.

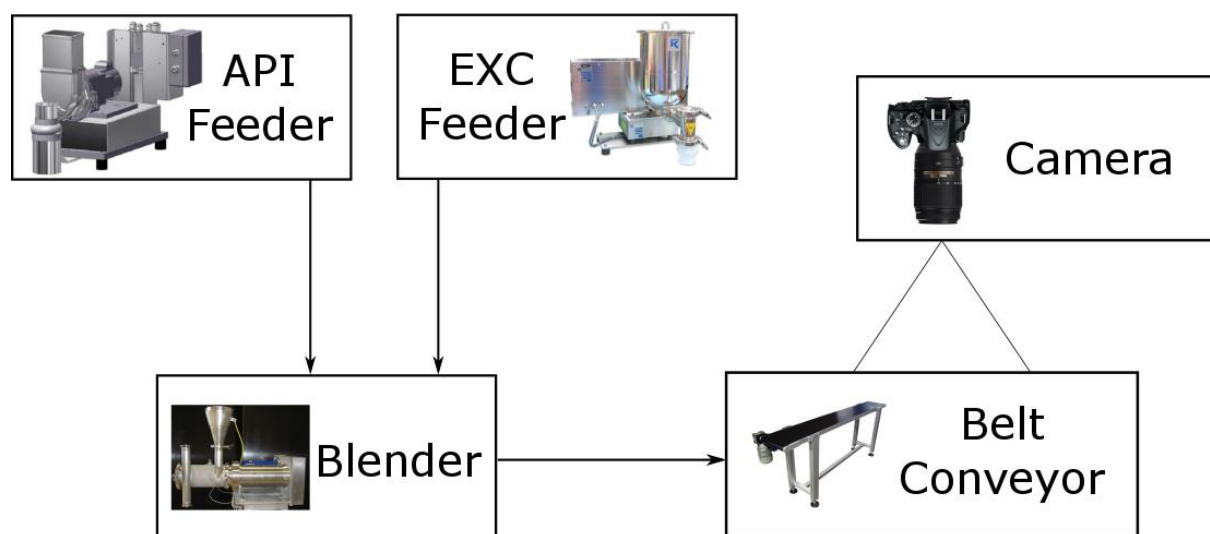


Figure 4: Experimental setup of the feeder-blender experiments.

### 2.3.2.2 Roller Compactor

Tracer experiments were performed using rolls with a diameter of 250 mm and a width of 25 mm. The roller speed can be varied between 1 and 30 rpm and the gap width between 0.5 mm and 6 mm to achieve a maximum mass flow rates of 100 kg/h (depending on raw material). The roller speed and gap width for the experiments in this work were selected in order to obtain the desired mass flow rate of 5 kg/h (Table 1). The co-mill speed could be adjusted between 0 and 900 rpm. For the presented experiments, 200 rpm was chosen (see Table 1).

Table 1: Process parameters for the dry granulation experiments.

Mass Flow	Roll Speed	Roll Gap	Co-mill Speed
5 kg/h	2 rpm	1.5 mm	200 rpm

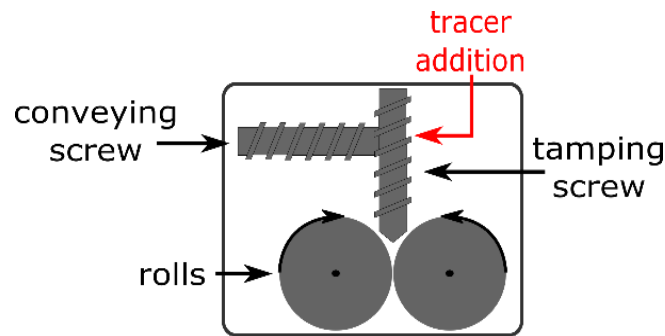


Figure 5: Schematic of the compaction unit of the roller compactor with a conveying screw and a tamping screw [30].

Figure 5 shows a schematic of the compaction unit of the roller compactor. The position at which the tracer was introduced into the process, at the junction between conveying screw and tamping screw, is marked as well in Figure 3 in red. The camera that recorded the evolution of the tracer concentration was positioned at the outlet of the co-mill, which is located beneath the compaction roll of the BRC 25.

### 2.3.3 Data Processing

Data processing for the feeder characterization was performed using Matlab®. The catch scale data acquired with a high sampling frequency of  $F_s = 1613 \text{ Hz}$  were low-pass filtered to remove noise (attenuation of high frequencies, for detailed information please refer to [31]). A zero-phase moving average over 2 s was used. Afterwards, the mass flow was computed via discrete forward differentiation of the weight. This mass flow was again filtered through the same zero-phase moving average filter to suppress the noise introduced by numerical differentiation. This approach to data processing allows the comparison of the (internally filtered) mass flow signal from the feeder with the catch-scale data in order to check the feeding accuracy and reliability of the recorded signals from the feeder.

For RTD experiments, the image processing was performed using Matlab®. A region of interest was selected in the center of the main powder stream on the conveying belt. The selected pixels originally provided in the red-green-blue (RGB) color space by the camera were transformed into LAB space to reduce the effects of variation in the brightness of material due to the tracer content and separate the lightness from the color values [32]. The yellow color is represented by the b-value in LAB space. The b-value was used for further data processing. The influence of a non-linear relationship between color value and concentration, as discussed in Peng et al. [33], was neglected since the measured tracer concentration only vary within a small range, with an approximately linear relationship.

### 2.3.4 Out-of-Spec Material Handling

In a continuous pharmaceutical manufacturing plant, OOS material cannot be used for the final product, and thus, must be removed from the process via diversion (segregation) measures. Two types of information are available to support the decision, if a specific part of the material stream is OOS and needs to be diverted: PAT data and model predictions (soft sensors) that are based on the simulation of the continuous manufacturing line. While PAT data are critical for monitoring quality, simulations provide detailed estimates of the effects of disturbance propagation during processes *in-silico*. Moreover, knowledge of the dampening characteristics of the unit operations makes it possible to predict the magnitude and duration of a disturbance before it results in any OOS material. The RTD provides information about the dampening characteristics of the unit operation. The broader the RTD is, the better the mixing and the dampening are (yet, too broad RTDs are not beneficial either). Hence, not every disturbance leads to an OOS material. However, if the amplitude and/or duration of the disturbance are too large, the material has to be diverted at some point in the process. It is well known that blenders and roller compactors have a low-pass behavior with additional dead time, which results in damping of high frequency oscillations [29]. Thus, small-scale fluctuations will not yield OOS products.

Different types of process disturbances (process upsets) can be introduced via various unit. Common sources for disturbances are feeder units, e.g., cohesive/compressible material that is fed in chunks or material that was adhering to a surface and suddenly breaks off (bearding). In this work, only deviations in the concentration are considered, which are mainly introduced by the feeders or are due to segregation during the process.

In general, the time delay required for the measurement device to detect a disturbance and the powder flow during this time has to be taken into account when planning a robust diversion strategy, as this has impact on the location of PAT tool and diversion point. In this work, the following measurement/diversion point pairs are possible in the considered dry granulation line:

- measurement of mass flow from LIW feeders / blender outlet
- NIR measurement at blender outlet / roller compactor outlet
- NIR measurement at roller compactor outlet / tablet press outlet

NIR measurement and diversion after the same unit operation is not feasible in this case because during data acquisition, the OOS material has already entered the next unit operation before being diverted.

In this work, the emphasis is on theoretical considerations and simulations. Various disturbance scenarios and their effect on the material composition throughout the process are investigated. Based on these simulations, measurement and diversion strategies are developed and compared. Our simulations are considering four disturbance scenarios. First, the API feeder has an impulse-like disturbance, which can be

interpreted as an instantaneous increase of some accumulated material from the feeder's outlet. Second, the API feeder's mass flow rate decreases over time, which is likely to occur when the feeding screws are clogged with material and the maximum screw speed is reached. The third scenario is when the API feeder stops working immediately and no API is fed into the unit. In the fourth scenario, various time spans for interruptions in the API feed are investigated.

## 2.4 Results

### 2.4.1 Feeder and Blender

Figure 6 (left) presents a step response experiment of the feed rate set-point performed with the EXC feeder. The red and blue lines show the set-point and data, respectively, obtained at a high sampling frequency of 1613 Hz on the catch scale. The blue line is the catch-scale signal. The green line represents the hopper weight data. Clearly, the feeder tracks the set-point well and reaches the steady state quickly. The Fourier analysis of the catch-scale data indicated a periodic signal at  $f_{screw} = 0.9$  Hz (Figure 6, right), which is in good agreement with the screw speed of the feeder. The set-point for feeder characterization was set to 5 kg/h, because experiments were carried out in the range of 4.75 kg/h to 5.25 kg/h under the assumption, that a change of  $\pm 10\%$  from the nominal feed rate does not affect feeding accuracy. Based on these characterization experiments, a start-up time of 2 minutes to assure stable feeding was chosen before the RTD experiments were performed.

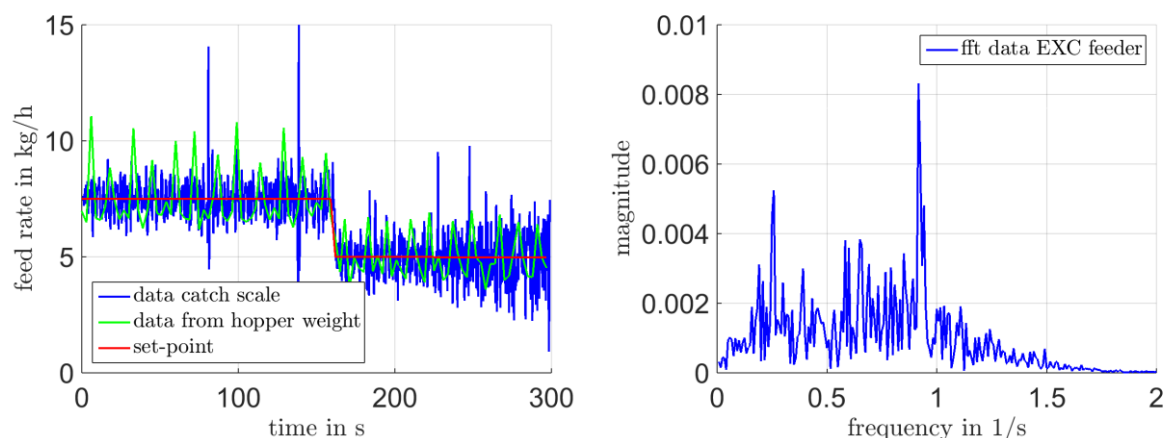


Figure 6: Step response experiment for the characterization of EXC feeder (left) and Fourier spectrum of 5 kg/h from 170-290 s (right).

A feeder signal can be described via the mean and standard deviation. This is provided in Table 2, which also shows the relative standard deviation (RSD) from the set-points based on the actual set-point recorded by the LIW feeder. The low deviations can be attributed to internal data processing during the relatively long sampling interval of 3 s. The high deviations from the set-point in Figure 6 are caused by measurement noise due to the extremely high sampling frequency of the catch scale. The API feeder offers



a much more stable feed than the EXC feeder, which can be attributed to the feeder equipment itself (represented by a lower RSD). Thus, even for low feed rates stable feeding can be obtained.

Table 2: Overview of feeder stability during RTD experiments.

	Feed rates			
	Set-point in kg/h	Mean in kg/h	Standard deviation in kg/h	RSD
API	0.25	0.24998	0.00017	0.07%
EXC	4.75	4.73393	0.01436	0.30%

Figure 7 shows the results for the blender from the tracer step-function experiments performed for a throughput of 5 kg/h at 1000 rpm, which had excellent reproducibility. With an acquisition time of 20 min, the long tail of the RTD was captured. As can be seen the RTD is closer to an ideally stirred tank, compared to a plug-flow reactor, indicating that significant back-mixing occurs. In addition, there is a strong secondary peak at 300-400 s, indicating powder accumulation and a dead zone. Smaller periodic peaks suggest powder build-up (small dead zones) and/or periodic detachment of material from the wall or the rotating blades of the blender.

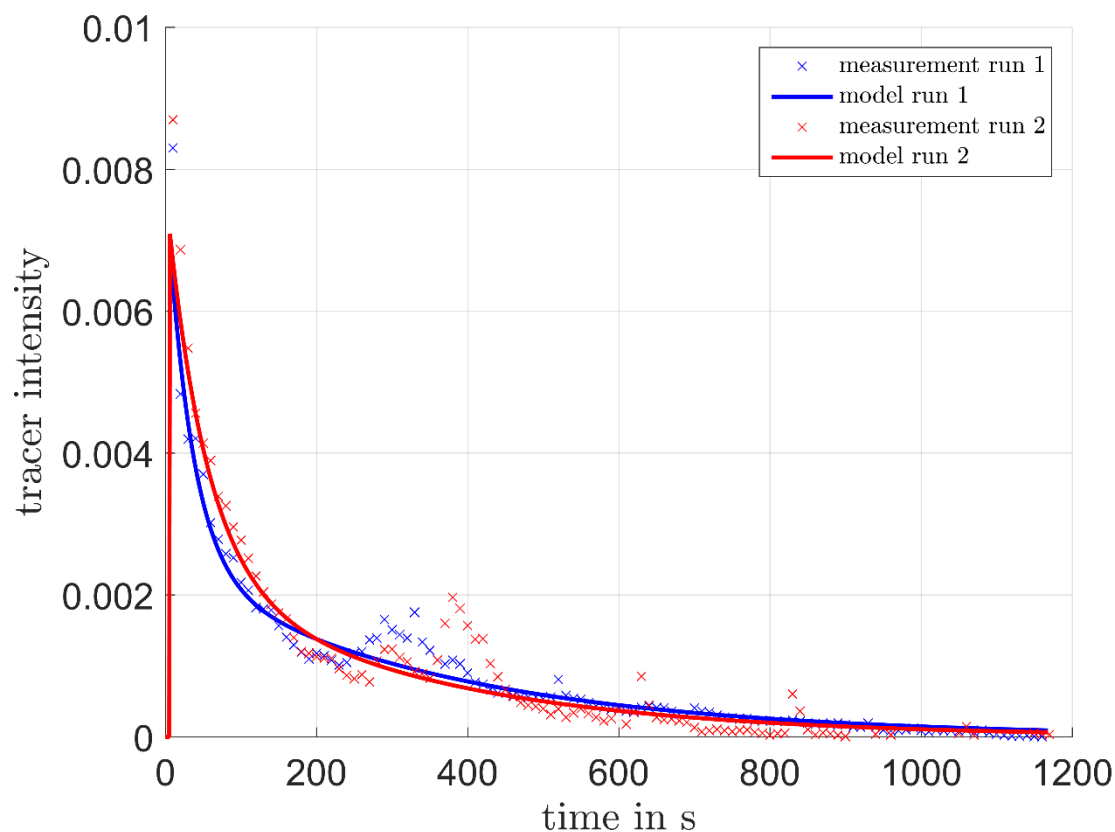


Figure 7: RTD curve of the blender for 5 kg/h and at 1000 rpm. The different colors represent different runs. The measured data and the corresponding fitted curve are shown.

An overview of the characteristic parameters of the blender's RTD curves is provided in Table 3. The dependence of the mean residence time  $\tau_{bl}$  on the rotational speed  $\omega_{bl}$  of the blender is small since the blender operated at low throughputs in comparison to the possible maximum throughput. The high mean residence time for the second run at 1000 rpm can be attributed to a larger amount of accumulated material, which was ejected later in the process at approximately 400 s (see Figure 7). In general, the mean residence time increases at higher rotational speeds (in contrast to other systems, such as double-screw extruders) due to more vigorous mixing leading to higher radial velocities and thus higher hold-ups [17].

Table 3: Characteristic parameters of RTD curves for the continuous blender. All experiments were conducted twice using the same settings, indicated by run 1 and run 2.

No	Speed in rpm	$\dot{m}$ in kg/h	$\tau_{bl}$ Run 1 in s	$\tau_{bl}$ Run 2 in s	$t_5$ Run 1 in s	$t_5$ Run 2 in s	$t_{50}$ Run 1 in s	$t_{50}$ Run 2 in s	$t_{95}$ Run 1 in s	$t_{95}$ Run 2 in s
1	500	5	201.70	195.29	13.32	15.00	85.48	97.26	734.04	699.36
2	1000	5	204.71	254.92	13.10	11.66	130.52	177.60	601.02	763.46
3	1500	5	234.73	237.67	9.76	10.70	135.24	159.44	800.80	743.08

Table 4: Time constants to model the continuous blender.

Run	$T_1$	$T_2$	$T_3$	$T_t$
500 rpm (Run 1)	326.86	589.66	57.92	7.62
1000 rpm (Run 1)	155.27	329.38	81.62	6.54
1500 rpm (Run 1)	106.73	332.92	29.24	3.82
500 rpm (Run 2)	348.32	523.82	93.71	5.26
1000 rpm (Run 2)	125.15	381.74	62.92	4.23
1500 rpm (Run 2)	128.82	389.55	45.30	4.06

The results of parameter estimation of the time constants for the transfer function of continuous blender are shown in Table 4. The parameters for 1000 rpm (Run1) were used for the OOS simulations, presented below.

## 2.4.2 Roller Compactor

The RTD for a mass flow of 5 kg/h was investigated, and an overview is provided in Table 5. Performing the RTD measurements for the roller compactor were more challenging than for the blender. For the blender experiments (see above) the powder on the conveyor belt could be easily analyzed via the camera. In contrast, the roller compaction setup did not allow the use of a conveyor belt due to limited space available. An alternative strategy was developed, where the color of a free falling powder inside a funnel was captured by the camera.

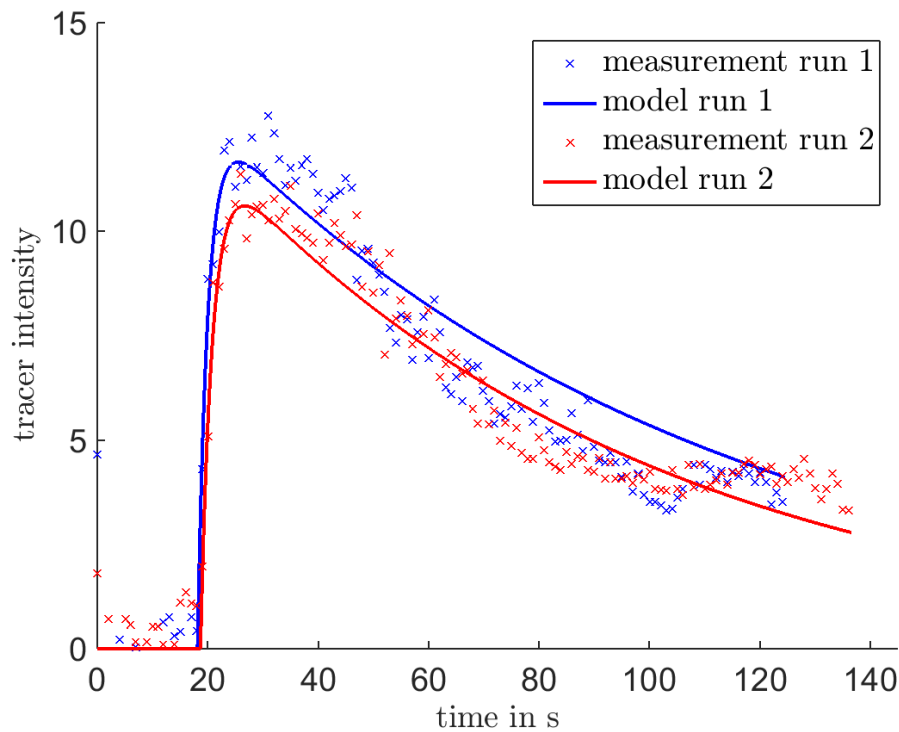


Figure 8: RTD of the roller compactor at 5 kg/h, reproducibility experiments.

Tracer was added at the junction between conveying screw and tamping screw (see Figure 3 above). This junction acted as a dead zone, accumulating a portion of the tracer material at the walls. Thus, for a long time tracer was observed in the product and no perfect pulse of tracer could be achieved. This might be the reason for the plateau apparent after 90 s in the measurement data shown in Figure 8.

The RTD model was fit to the data without taking into account the dead zone (and the plateau) and to demonstrate the conceptual framework for development of a control strategy. Eq. 7 was used to extrapolate the tail of RTD calculate the impulse response on a larger time scale. This is essential when normalizing the data to obtain the RTD (Eq.3).

Table 5: Fitted time constants and mean residence time for the roller compaction experiments.

Run	$T_1$	$T_2$	$T_t$	$\tau_{RC}$
5kg/h (Run 1)	1.85	93.21	18.15	113.18
5kg/h (Run 2)	2.15	80.47	18.69	101.30

The overall process RTD is the result of a convolution of both RTD curves from blender and roller compactor, i.e.

$$E_{overall}(t) = \int_0^t E_{bl}(t - \tilde{t}) \cdot E_{RC}(\tilde{t}) d\tilde{t}. \quad (10)$$

$E_{overall}$  represents the impulse response of the overall process model  $P_{overall}$ .  $P_{overall}$  can be computed via multiplying the transfer functions of the individual unit operations:

$$P_{overall}(s) = P_{bl}(s) \cdot P_{RC}(s) \quad (11)$$

The convolution of the two RTDs is shown in Figure 9.

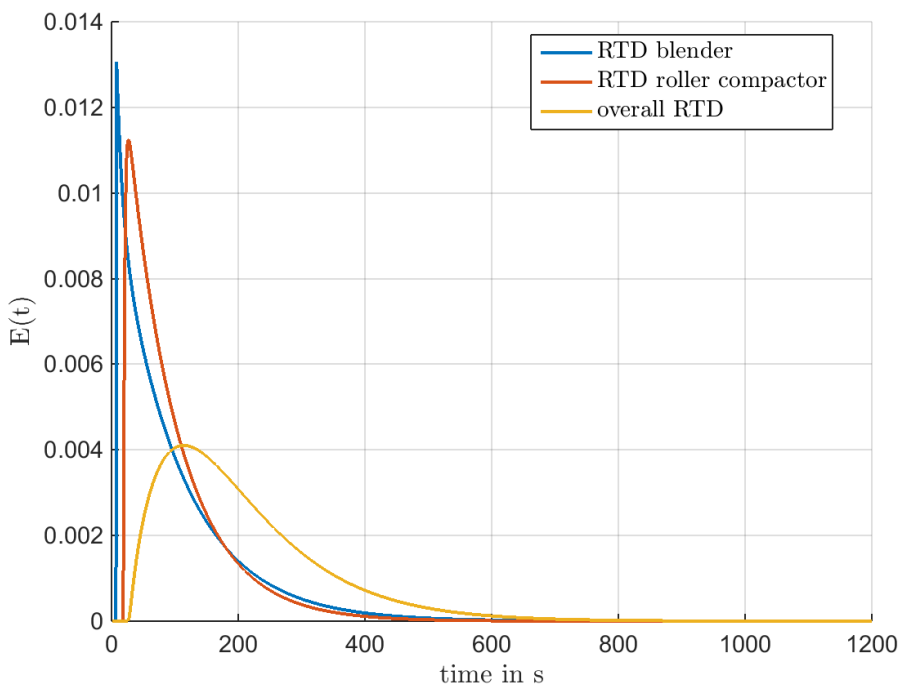


Figure 9: RTD of single unit operations (blender in blue and roller compactor in orange) and overall process RTD in yellow.

### 2.4.3 Out-of-Spec Management

Simulations analyzing different scenarios for out-of-spec handling were performed with the feed rate determined from the hopper weight by time differentiation. It was decided to perform the time differentiation in order to avoid using the “reported” feed rate of the feeder, which is strongly filtered. Due to the differentiation, high frequency measurement noise is amplified. However, this represents a “worst case” estimation of the feed rate variability and is therefore used for the further analysis, as shown in Figure 10.

The simulation results for concentrations at the outlets of the blender and the roller compactor are shown as well in Figure 10. The feeder fluctuations were strongly dampened, and the concentration at the blender outlet is smooth. In addition, after the roller compactor, the concentration is constant with an additional time delay due to  $T_{t_{RC}}$  and additional mixing due to the low pass character of the roller compaction process. The threshold defining the OOS material was chosen to be  $\pm 5\%$ . For specific applications, this threshold has to be adapted according to regulatory requirements. The selected threshold ( $\pm 5\%$ ) is marked with a red line in Figure 10 to Figure 14.

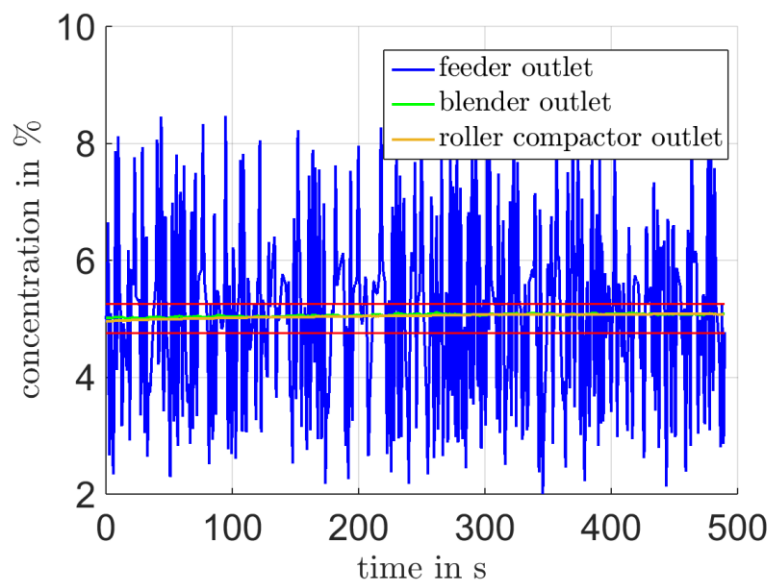


Figure 10: API outlet concentrations for the blender and the roller compactor. The input signal, feed rate, was calculated from the time-differentiation of the recorded hopper weight. The red lines are denoting the  $\pm 5\%$  limit around the nominal API concentration.

Simulation results for different process upset scenarios were carried out. For all these simulations, the assumption was made, that a (small) change in throughput does not affect the RTD. This is valid as the changes are applied to the API feeder, which contributes to only 5% of the total throughput.

For both feeders used in this work, the characterization showed that the actual feed rate is very close to the set-point (Table 2). In the simulated scenarios we assumed that the feeders reach a new set-point (upon a set point change) instantaneously.

In the first scenario we assumed an impulse-like disturbance. Figure 11 indicates that despite a high impulse (twice the nominal feed rate for 1 second corresponding to additional 70 mg of API) the API concentration remains within the acceptable limit. As such, although the magnitude of the disturbance is high, no diversion of material is required. The resulting concentration never exceeds the  $\pm 5\%$  boundaries. The maximum possible fluctuation is 350 mg of material without obtaining OOS product.

In case of an impurity entering the production line in the same manner, it is crucial to divert all the intermediate material containing this impurities. These impurities first appear after 7 s at the outlet of the blender, and all impurities are washed out after 650 s. After the RC operation, due to the dead-time, this material appears after 24 s and passes this point after 800 s. These diversion times correspond to 893 g and 1078 g of waste material at a nominal feed rate of 5 kg/h.

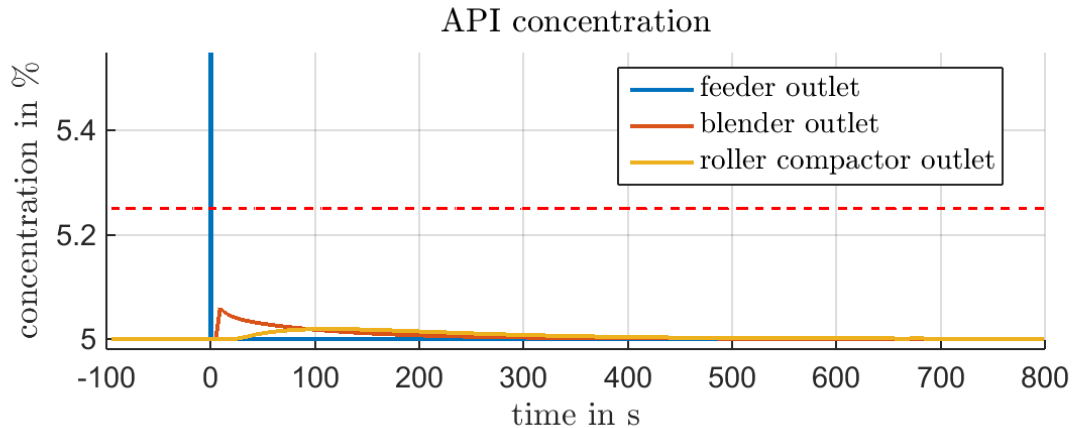


Figure 11: Impulse disturbance propagation in the API concentration during the dry granulation process.

Gradual clogging of the feeding screws might cause a ramp-like decrease in the feed rate until no more material is fed. The corresponding disturbance and the responses are shown in Figure 12. The decrease rate was assumed to be 0.025 g/h/s. In this case, OOS material leaves the blending and RC unit after 95 s and 160 s, respectively. Shut-down can occur later and compared to an immediate shut-down, this corresponds to 132 g or 222 g of waste reduction, respectively.

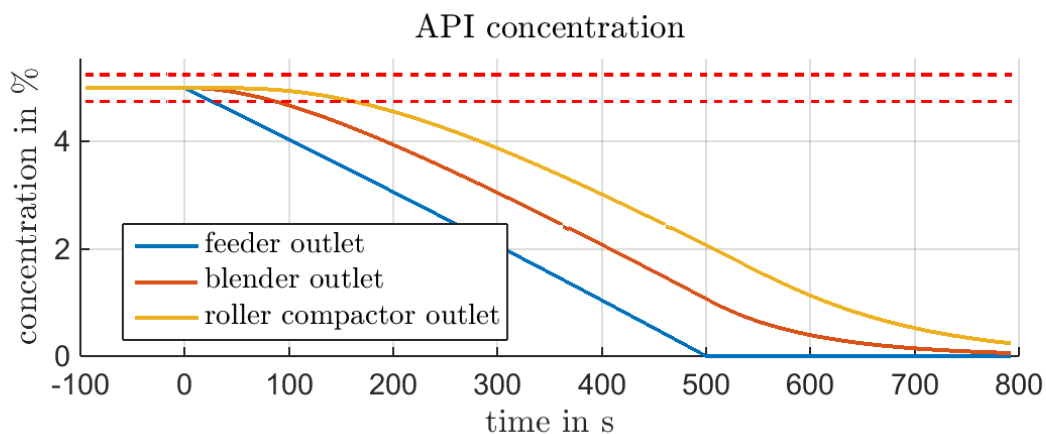


Figure 12: Ramp-like disturbance propagation in the API concentration during the dry granulation process.

In the case of complete disruption of the mass flow of one feeder, simulations can help to estimate the maximum time before shut-down to maximize the amount of final product. Figure 13 shows a scenario under which the feeder immediately stops feeding but the material at the outlet is in-spec for 10 s thereafter due to the dead-time and mixing of the blender. At the roller compactor outlet, in-spec product is obtained for 50 s. This corresponds to a decrease of 70 g, compared to the immediate shut-down with a nominal mass flow of 5 kg/h.

This simulation can also be used to investigate a change in the raw material batch. In this case, an immediate switch from batch 1 to batch 2 is assumed. The results show that after 800 s the concentration in batch 1 is nearly zero (Figure 13). A washout of 95% after the blender takes 500 s whereas after the RC it takes 800 s. To achieve a washout of 99%, the time it takes increases to 760 s after the blender and >800 s after the RC. As such, for this configuration, the batch change can be performed within this time, with about 1 kg material produced during the transition containing material from both batches. This is an important information for the bill of materials, i.e., for traceability reasons.

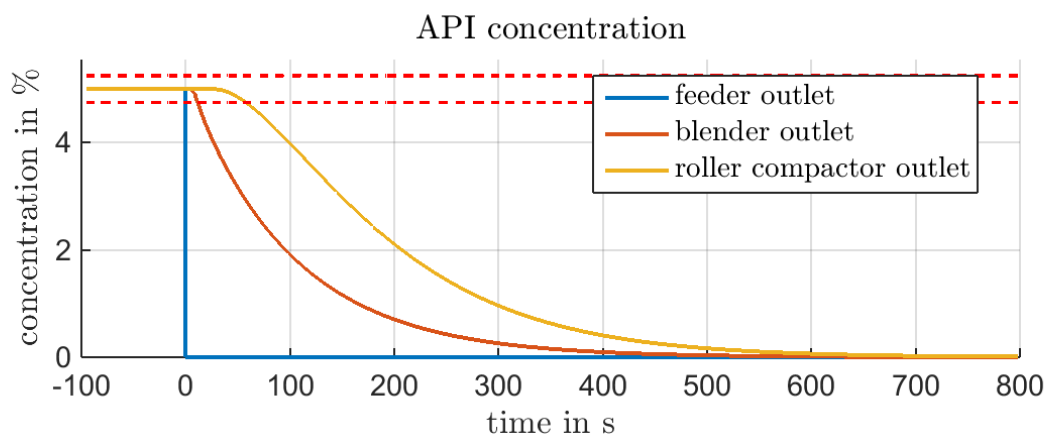


Figure 13: Total shutdown of the API feeder and propagation in the API concentration during the dry granulation process.

An immediate and permanent shut-down of one feeder always leads to a shut-down of the entire processing line. If a disruption in the API mass flow is of a shorter duration, it might be possible to buffer the disruption by material inherently stored inside the hoppers of unit operations (e.g., included in a roller compactor, tablet press). If the time is short enough, the final product might even remain in-spec. Various (short) shut-down times of the API feeder were considered in the simulations. The time during which the material is OOS determines the required buffer capacity of the down-stream unit operations (i.e., tableting machine) to continue production undisrupted.



For example, the concentrations after blending and RC for a 2-minute shut-down are shown in Figure 14 (top). A 2-minute disruption in the API feed leads to 370 s of OOS material after blending and 460 s after RC, corresponding to a loss in the material of 515 g and 640 g, respectively.

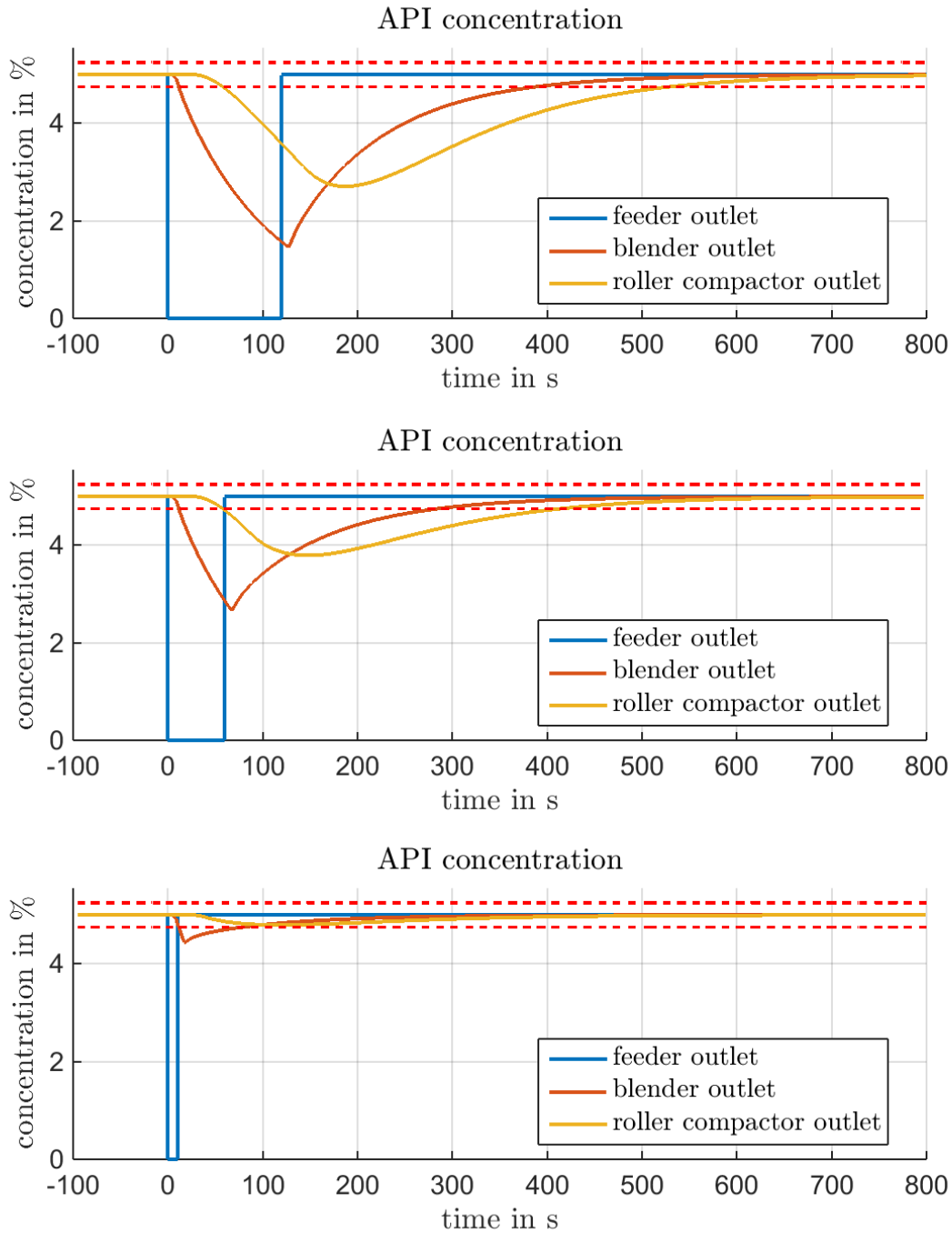


Figure 14: API concentration for various shut-down times of the API feeder.

The effect of reducing the shut-down time of the API feeder to 60s is shown in Figure 14 (middle). The OOS time is decreased to 270 s and 350 s for blender and RC, respectively, corresponding to a loss of material of 375 g or 486 g, depending on the diversion point used. A 10 s API feed interruption does not lead to OOS material at all, as shown in Figure 14 (bottom). The concentration of API after blending is OOS for 75 s leading to diversion of 105 g whereas the concentration after RC remains within the limit of  $\pm 5\%$ , meaning that the final product is expected to be in-spec.

According to [34], a feeder refill typically takes 8-10 s. During this period of time, the weight signal of the integrated scale is lost, and volumetric feeding is achieved. Thus, the exact feed rate is unknown during this period of time. However, neither a complete stop of the feed stream nor a doubling of the mass flow during this period would lead to OOS material (under the assumption that no other disturbances occur at the time when the material composition is near 5% limit). Thus, for the specific setup considered, feeder refill is not critical in terms of achieving quality product. Diversion times and material loss for different shut-down times is summarized in Table 6.

Table 6: Summary of diversion times and corresponding material loss for different shut-down times.

Shut-down time	Diversion after blender		Diversion after roller compactor	
	Diversion time	Diverted material	Diversion time	Diverted material
120 s	370 s	514 g	460 s	639 g
60 s	270 s	375 g	350 s	486 g
10 s	75 s	104 g	-	-

## 2.5 Discussion

Feeder characterization is crucial for assessing the reliability and accuracy of the mass flow introduced into the manufacturing line. It should be the starting point with regard to the selection of unit operations since feed fluctuations determine the necessary dampening capacity of the subsequent unit operations. Simulations can show the effect of such scenarios on the process and serve as a valuable risk assessment tool, e.g., for estimation of the severity of a failure mode.

The dampening characteristic of unit operations can be determined by RTD measurements. Such measurements were performed for a continuous blender and a roller compactor by the application of a tracer impulse. A data processing algorithm based on color intensity recorded by camera was written in Matlab® to obtain the RTD curve. Models in the form of a transfer function were developed for blender and roller compactor. The experimentally obtained RTD curve was used for parameter identification.

Simulations of the four scenarios and disturbance propagation were performed using this parameterized RTD models.

On the one hand, such simulations can help to characterize unit operations and gain process knowledge that can be applied to designing the production line within specific process interruption limits (e.g., it gives information about the buffer sizes if it is desired to bridge a certain time of material diversion).

On the other hand, predicting diversion times due to certain events/disturbances aids in selecting measurement and diversion points. Shorter diversion times lead to less waste material and require smaller buffers. In the studied cases, where there is no permanent feed failure, it was beneficial to divert material after the blender to keep diversion times as short as possible. In contrast to the roller compactor, the tablet press has a rather large buffer by design, which can be used. This might save constructional effort to build a large enough buffer between blender and roller compactor, when diverting material at the blender outlet. This highlights the trade-off between additional constructional effort and longer diversion times. Dependent on material costs, an optimal decision can be made.

Based on Table 6, an estimation of the needed hopper size can be made. To be able to produce tablets without disruption of material flow into the tablet press, the hopper after the blender (before the roller compactor) needs to be capable of storing about 550 g in case of a 2 min shut-down of the API feeder and about 400 g in case of a 1 min shut-down.

When diverting material after the roller compactor, the hopper of the tablet press need to be capable of storing 700 g for buffering a 2 min shut-down of the API feeder or 500 g in case of a 1 min shut-down scenario. These hopper sizes are taking only one of the describe disturbance events into account and need to be filled completely during start-up to be capable of exerting their full capacity. For realistic application, the hopper size should be increased to have the ability to compensate for more than one failure event and/or longer duration of a failure.

Using RTD simulations, material tracking, especially relevant for removal of impurities, showed that the clearance (wash out) of impurities introduced during 1 second (70 mg) corresponds to roughly 1 kg of waste material. This calculation highlights the importance of careful operation and advanced control concepts.

## 2.6 Conclusion

Disturbances in the feed rate that occur in continuous manufacturing lines can be dampened via mixing behavior of various unit operations. Information about the residence time distribution, which describes the mixing behavior, allows to develop models for prediction of concentrations throughout the process. This facilitates optimized process design (e.g., buffer size), out-of-spec handling and material tracking (e.g., measurement/diversion point pairs). Material tracking is crucial for traceability of material, which is

important with regard to meeting the regulatory body requirements. Process knowledge and models are efficient tools for saving costs and time through the entire life cycle of the process, from design and development to process control and monitoring.

### *Acknowledgement*

This work was funded through the Austrian COMET Program by the Austrian Federal Ministry of Transport, Innovation and Technology (BMVIT), the Austrian Federal Ministry of Economy, Family and Youth (BMWFI) and by the State of Styria (Styrian Funding Agency SFG). We thank our colleagues at the Research Center Pharmaceutical Engineering, Daniel Wiegele, Manuel Zettl, Mario Unterreiter and Daniel Kaiser for their help conducting the experiments in our pilot plant as well as Arlin Gruber for participating in model development.

## 2.7 References

- [1] K. Plumb, "Continuous Processing in the Pharmaceutical Industry: Changing the Mind Set," *Chem. Eng. Res. Des.*, vol. 83, no. 6, pp. 730–738, Jun. 2005.
- [2] S. L. Lee *et al.*, "Modernizing Pharmaceutical Manufacturing: from Batch to Continuous Production," *J. Pharm. Innov.*, vol. 10, no. 3, pp. 191–199, 2015.
- [3] J. S. Srai, C. Badman, M. Krumme, M. Futran, and C. Johnston, "Future supply chains enabled by continuous processing-opportunities and challenges May 20-21, 2014 continuous manufacturing symposium," *J. Pharm. Sci.*, vol. 104, no. 3, pp. 840–849, 2015.
- [4] S. D. Schaber, D. I. Gerogiorgis, R. Ramachandran, J. M. B. Evans, P. I. Barton, and B. L. Trout, "Economic Analysis of Integrated Continuous and Batch Pharmaceutical Manufacturing: A Case Study," *Ind. Eng. Chem. Res.*, vol. 50, no. 17, pp. 10083–10092, Sep. 2011.
- [5] FDA, "Guidance for Industry Guidance for Industry PAT — A Framework for Innovative Pharmaceutical," no. September, p. 19, 2004.
- [6] ICH, "ICH Q8(R2), Pharmaceutical Development, Part I: Pharmaceutical development, and Part II: Annex to pharmaceutical development," 2009.
- [7] ICH, "ICH Q10, Pharmaceutical Quality System," 2008.
- [8] W. Engisch and F. Muzzio, "Using Residence Time Distributions (RTDs) to Address the Traceability of Raw Materials in Continuous Pharmaceutical Manufacturing," *J. Pharm. Innov.*, 2015.
- [9] F. Boukouvala, V. Niotis, R. Ramachandran, F. J. Muzzio, and M. G. Ierapetritou, "An integrated approach for dynamic flowsheet modeling and sensitivity analysis of a continuous tablet manufacturing process," *Comput. Chem. Eng.*, vol. 42, pp. 30–47, Jul. 2012.
- [10] F. Boukouvala *et al.*, "Computer-Aided Flowsheet Simulation of a Pharmaceutical Tablet Manufacturing Process Incorporating Wet Granulation," *J. Pharm. Innov.*, vol. 8, no. 1, pp. 11–27, Jan. 2013.
- [11] G. Reynolds, R. Ingale, R. Roberts, S. Kothari, and B. Gururajan, "Practical application of roller compaction process modeling," *Comput. Chem. Eng.*, vol. 34, no. 7, pp. 1049–1057, Jul. 2010.
- [12] G. Bindhumadhavan, J. P. K. Seville, M. J. Adams, R. W. Greenwood, and S. Fitzpatrick, "Roll compaction of a pharmaceutical excipient: Experimental validation of rolling theory for granular solids," *Chem. Eng. Sci.*, vol. 60, no. 14, pp. 3891–3897, Jul. 2005.
- [13] S.-P. Simonaho, J. Ketolainen, T. Ervasti, M. Toiviainen, and O. Korhonen, "Continuous manufacturing of tablets with PROMIS-line – Introduction and case studies from continuous feeding, blending and tableting," *Eur. J. Pharm. Sci.*, Feb. 2016.
- [14] E. Skibsted and S. B. Engelsen, "Spectroscopy for Process Analytical Technology (PAT)," in *Encyclopedia of Spectroscopy and Spectrometry*, 2017, pp. 188–197.
- [15] O. Scheibelhofer, D. M. Koller, P. Kerschhaggl, and J. G. Khinast, "Continuous powder flow monitoring via near-infrared hyperspectral imaging," in *2012 IEEE International Instrumentation and Measurement Technology Conference Proceedings*, 2012, pp. 748–753.
- [16] P. R. Wahl, G. Fruhmann, S. Sacher, G. Straka, S. Sowinski, and J. G. Khinast, "PAT for tableting:

- inline monitoring of API and excipients via NIR spectroscopy.," *Eur. J. Pharm. Biopharm.*, vol. 87, no. 2, pp. 271–8, Jul. 2014.
- [17] E. L. Paul, *Handbook of Industrial Mixing*. Wiley, 2004.
- [18] Y. Gao, F. J. Muzzio, and M. G. Ierapetritou, "A review of the Residence Time Distribution (RTD) applications in solid unit operations," *Powder Technol.*, vol. 228, pp. 416–423, Sep. 2012.
- [19] Y. Gao, A. Vanarase, F. Muzzio, and M. Ierapetritou, "Characterizing continuous powder mixing using residence time distribution," *Chem. Eng. Sci.*, vol. 66, no. 3, pp. 417–425, Feb. 2011.
- [20] F. J. Muzzio, M. Llusa, C. L. Goodridge, N.-H. Duong, and E. Shen, "Evaluating the mixing performance of a ribbon blender," *Powder Technol.*, vol. 186, no. 3, pp. 247–254, Sep. 2008.
- [21] P. M. Portillo, M. G. Ierapetritou, and F. J. Muzzio, "Effects of rotation rate, mixing angle, and cohesion in two continuous powder mixers—A statistical approach," *Powder Technol.*, vol. 194, no. 3, pp. 217–227, Sep. 2009.
- [22] P. M. Portillo, M. G. Ierapetritou, and F. J. Muzzio, "Characterization of continuous convective powder mixing processes," *Powder Technol.*, vol. 182, no. 3, pp. 368–378, Mar. 2008.
- [23] A. U. Vanarase and F. J. Muzzio, "Effect of operating conditions and design parameters in a continuous powder mixer," *Powder Technol.*, vol. 208, no. 1, pp. 26–36, Mar. 2011.
- [24] T. D. Theory, "Taylor Dispersion Theory Chapter 3," 1950, pp. 25–42.
- [25] P. V. Danckwerts, "Continuous flow systems," *Chem. Eng. Sci.*, vol. 2, no. 1, pp. 1–13, Feb. 1953.
- [26] O. Levenspiel and W. K. Smith, "Notes on the diffusion-type model for the longitudinal mixing of fluids in flow," *Chem. Eng. Sci.*, vol. 6, no. 4–5, pp. 227–235, Apr. 1957.
- [27] P. V. Danckwerts, "Continuous flow systems: Distribution of residence times," *Chem. Eng. Sci.*, vol. 2, no. 1, pp. 1–13, 1953.
- [28] J. Schiff, *The Laplace transform: theory and applications*. Springer, 1999.
- [29] W. S. Levine, "The Control Handbook," *Control Handb.*, p. 1566, 1996.
- [30] "Dry Granulation Technology by Bohle - L.B. Bohle Maschinen + Verfahren - PDF Katalog | technische Unterlagen | Prospekt." [Online]. Available: <http://pdf.medicaexpo.de/pdf-en/lb-bohle-maschinen-verfahren/dry-granulation-technology-bohle/115137-165667.html#open>. [Accessed: 03-Nov-2016].
- [31] A. V. Oppenheim, R. W. Schaffer, and J. R. Buck, *Discrete-time signal processing*. Prentice Hall, 1999.
- [32] X. Wang, R. Hänsch, L. Ma, and O. Hellwich, "Comparison of Different Color Spaces for Image Segmentation using Graph-cut."
- [33] J. Peng, H. E. Huff, and F. Hsieh, "An RTD Determination Method for Extrusion Cooking," *J. Food Process. Preserv.*, vol. 18, no. 11997, pp. 263–277, 1994.
- [34] S. Nowak, "Improving Feeder Performance in Continuous Pharmaceutical Operations," *Pharm. Technol.*, vol. 40, no. 10, pp. 68–73, 2016.

## 2.8 Appendix

### 2.8.1 Abbreviations

RTD	Residence time distribution
API	Active pharmaceutical ingredient
CM	Continuous manufacturing
OOS	Out-of-Spec
FDA	Food and Drug Administration
ICH	International Conference on Harmonization
PAT	Process analytical technology
NIR	Near infrared spectroscopy
LIW	Loss-in-weight
CQA	Critical quality attribute
FBU	Feeding/Blending unit
RC	Roller compactor
EXC	Excipient
RSD	Relative standard deviation
RGB	Red-Green-Blue
LAB	Lightness, a color value, b color value

### 2.8.2 Variables

$\dot{m}$	Mass flow
$\sigma$	Standard deviation
$\mathcal{N}(0, \sigma)$	Normal distribution with zero mean and $\sigma$ as standard deviation
$t$	Time
$C$	Concentration

$E$	Residence time distribution
$t_x$	Time until x% tracer removed from the system
$\tau$	Mean residence time
$P$	Transfer function
$\mathcal{L}$	Indicating Laplace transform
$T$	Time constants
$k, K$	Scaling constants
$y$	Measured concentration/intensity
$\hat{y}$	Predicted concentration
$T_s$	Sampling time
$F_s$	Sampling frequency
$d_{50}$	Mean particle size
$f$	Frequency
$\omega$	Rotational speed

### 2.8.3 Subscripts

0	Nominal
$bl$	Blender
$RC$	Roller compactor
$feeder$	Feeder
$API$	Related to API
$EXC$	Related to EXC
$in$	Inlet
$out$	Outlet
$i$	Variable for iteration over samples



*screw* Feeder screw

## 2.8.4 Supplementary Material

To analyze the image coverage, a snapshot of the region used for data processing was transformed into a grayscale image to be able to evaluate the histogram. Nonetheless, data processing was performed in LAB color space. Figure S1 shows a snapshot of the region of interest in the blender and the roller compactor and the corresponding histograms. The data processing algorithm is set to suppress dark background pixels and remove those pixels from RTD evaluation because the background does not carry any tracer information. The more homogeneous the image, the better is the powder coverage in front of the camera, resulting in a better signal-to-noise ratio. The coverage for the blender experiments is very homogeneous, whereas in the roller compactor setup, more grey background can be seen in the image. These pixels are suppressed by the data processing algorithm, which reduces the number of pixels for calculation of the average color value.

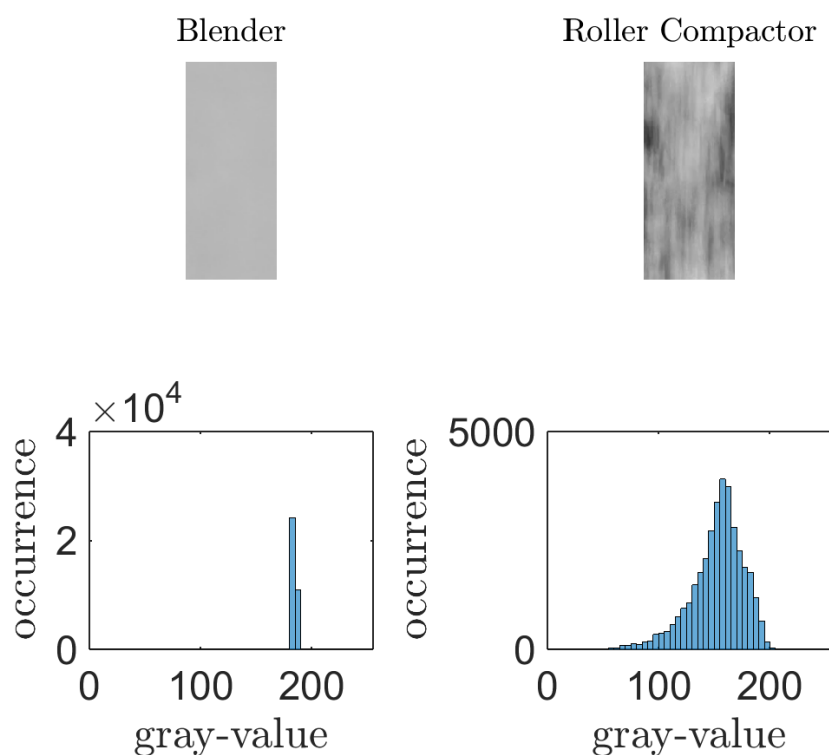


Figure S1: Powder coverage in front of the camera on the conveying belt for the blender (left) and the free falling powder from the roller compactor (right) via a gray-scale picture. The picture above shows the region of interest chosen to evaluate the histogram within the corresponding region.

*You've achieved success in your field  
when you don't know whether  
what you're doing is work or play.*

Warren Beatty

### **3 Residence Time Distribution of a Continuously-operated Capsule Filling Machine: Development of a Measurement Technique and Comparison of Three Volume-Reducing Inserts**

Julia Krusz<sup>1</sup>, Eva Faulhammer<sup>1</sup>, Jakob Rehr<sup>1</sup>, Otto Scheibelhofer<sup>1</sup>, Andreas Witschnigg<sup>1</sup>, Johannes G. Khinast<sup>1,2</sup>

<sup>1</sup>Research Center Pharmaceutical Engineering GmbH, Graz, Austria

<sup>2</sup>Institute for Process and Particle Engineering, Graz University of Technology, Graz, Austria

#### **3.1 Abstract**

This paper presents the measurement and analysis of the residence time distribution (RTD) of a tamping-pin capsule filling machine. The tamping speed and the amount of material inside the powder bowl proved to have a significant effect on the RTD. Various inserts into the powder bowl that reduce the volume and alter mixing and transport in the bowl were experimentally investigated. To obtain the RTD, a tracer-based measurement method was applied and a sophisticated data processing strategy was developed. The tracer-based method also allowed investigations of stagnant zones in the powder bowl, another important aspect in continuous manufacturing (CM). The suitability of tracer material was assessed based on a detailed characterization of bulk and tracer material. Characteristic parameters of the RTD were extracted and compared, proposing a systematic strategy for selection of a suitable insert.

**Keywords:** continuous manufacturing, capsule filling, residence time distribution

## 3.2 Introduction

Continuous manufacturing (CM) is increasingly gaining interest in the pharmaceutical industry for many reasons. For example, there are fewer scale-up issues and higher flexibility can be achieved in terms of production volume. Moreover, since storage capacities can be optimized, an effective supply chain management can lead to a reduction of the footprint of a plant [1–3]. Process knowledge, sophisticated process monitoring and control strategies result in waste reduction by keeping the process within the limits of a defined design space (DS).

With regard to the development of control strategies, the residence time distribution (RTD) of material in every process unit (unit operation) must be known. The RTD can be used, for example, to predict the impact of concentration changes (e.g., due to variations in the feed rate due to feeder disturbances, such as feeder bearding) on the intermediate material processed in subsequent unit operations. Due to mixing of material during each unit operation, the amplitude of these disturbances is reduced. This property is called the “damping capability”, which can be described by means of RTD. The time until the material is out-of- or in-spec can be calculated based on information about disturbance propagation throughout the process based on RTD models. Additionally, knowing the RTD is beneficial for batch definition, making it possible to change raw material batches without interrupting the process [4], while exactly knowing which material(s) ended up in which product (i.e., required for the bill of materials). An illustration of the concept of batch transition is shown in Figure 15. The circles in each column correspond to the dosage forms made at one instant in time, i.e., filled capsules in this specific investigation.

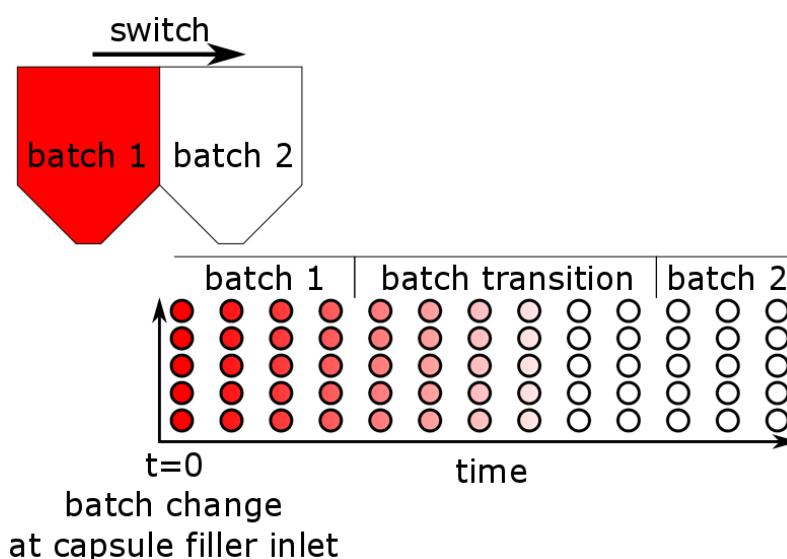


Figure 15: Batch definition - transition between raw material batches. The red circles are indicating the production volume from single raw material batch 1, whereas the white circles are indicating the batch 2. In the batch transition period the color changes gradually from red to white. During this time, the final product contains material from two raw material batches.

As shown in Figure 15, there is a gradual transition from the raw material batch 1, indicated in red, to raw material batch 2, shown in white. The length of the batch transition period depends on the RTD and on the acceptable amount of a material from batch 1 ending up in the product of the next batch 2 (e.g., 1% or 5%). In continuous manufacturing, short mean residence times and a narrow RTD are beneficial in terms of batch transition, since less in-process material contains material originating from different raw-material batches (short batch transition period). A shorter mean residence time corresponds to less material inside the system and a narrow RTD can be correlated with less mixing. However, when mixing is necessary, to dampen potential feeder fluctuations, a broader RTD is beneficial. Thus, there is an optimum RTD for each process, which can be estimated by assuming expected feeder fluctuations or feeder shut down.

In the past, many RTD studies of various unit operations have been performed. The most widely investigated unit operations are blenders [5–14] and twin-screw granulators [5],[15–22]. Recently, RTD experiments in a roller compactor were reported in [23]. Using the combination of all RTDs of unit operations (called a convolution), the propagation of process disturbances throughout the entire process line can be investigated. Recently, the RTD of a direct compaction process was discussed in Engisch et al. [24] and García-Muñoz et al. [25] and a dry granulation process in Kruisz et al. [23].

To the best of our knowledge, all continuous pharmaceutical production processes described in the literature to date focus on tableting [24,26–37]. Yet, RTD measurements for a capsule filling machine have not been reported. However, capsules have many benefits [38]. For example, powders, granules, pellets, tablets and their combinations can easily be filled into capsules in a flexible way, which is advantageous during clinical studies and for individualized drug doses. Modified release formulations can be achieved either by modifying the capsule shell or by coating the pellets inside the capsules. Additionally, materials and mixtures, which are hard to compact, can be filled into capsules [38]. Furthermore, capsule shells inherently provide taste masking.

The capsule filler considered in our work is shown in Figure 16 and consists of a powder bowl with 5 tamping stations (stations 1-5) and 1 transfer station (station 6).

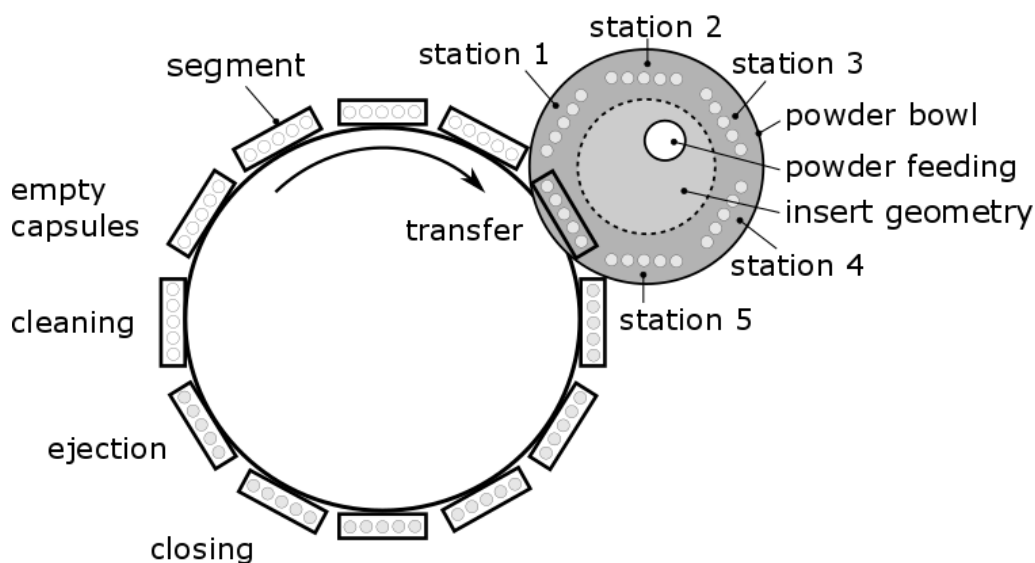


Figure 16: Sketch of the machine setup, depicting the empty capsule insertion, powder bowl with insert geometry, the tamping stations 1-5, the transfer station as well as closing and ejection step with subsequent segment cleaning.

The tamping stations are located in the powder bowl and work in parallel (see sketch in Figure 17). The fill weight of the capsules can roughly be adjusted based on the thickness of the dosing disc. Fine-tuning can be performed by altering the immersion depth of tamping pins at each station and the powder bed height. The pin immersion depth correlates to the compression of powder plugs inside the dosing disc bores. The powder plugs are moving via the rotation of the dosing disc and the bowl through all 5 stations and are tamped five times. At the 6<sup>th</sup> (transfer) station, the powder plug is transferred into the capsule body after removal of additional powder via a so-called “ship”, sealing the powder plug from the powder bed. As mentioned, the dosing disc is rotating, whereas the ship is fixed at the transfer station. The powder inside the bowl is moving in the direction of rotation. The ship is representing a resistance to this movement, and hence, in front of the ship, there is powder piling up, leading to an uneven powder bed height.

The powder bed height is maintained close to the desired level using an on/off control mechanism. Refilling of the bowl with powder from the hopper is initiated by an inductive fill level sensor. When the powder bed height reaches a lower threshold, the feeding system is activated for a fixed time to refill the powder bowl. After this time, powder flow stops until the lower threshold is reached again. The time for one such feeding cycle is also called feeding interval. The speed of the hopper’s dosing screw can be selected manually. Newer systems, however, provide a PID control of the powder level, which allows a tight control of this important CPP [39].

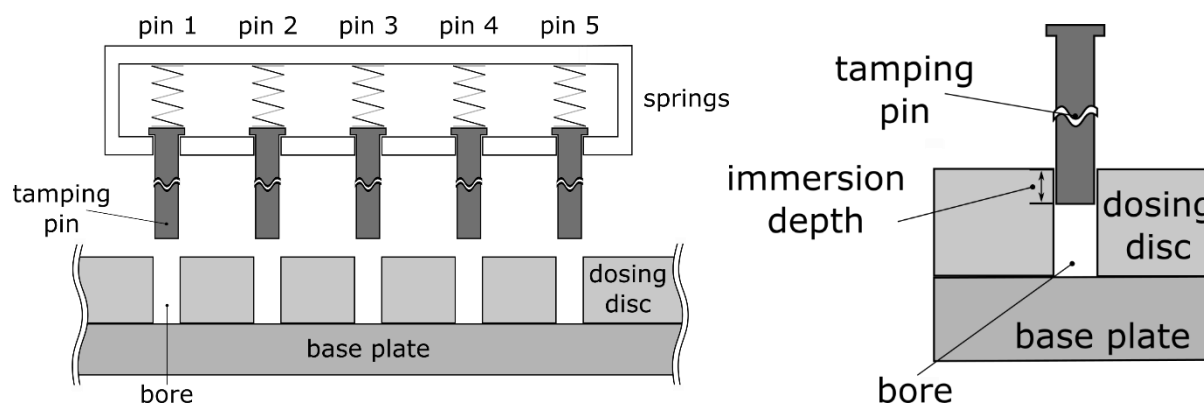


Figure 17: Schematic of a tamping pin capsule filling process. Each tamping station has 5 pins (left). A tamping pin at full immersion as set at the station (right).

An evenly distributed powder bed inside the bowl is beneficial in terms of reaching a constant fill weight. Clearly, the dynamics of the powder bed are closely linked to the powder flowability. Another important aspect is the content uniformity of filled capsules [40]. Significant differences in the particle properties of different materials in the powder mixtures are likely to result in segregation inside the powder bowl and in the filled capsules, especially if the materials are relatively free-flowing.

The machine's speed can be set between 50 and 140 tamps per minute (tpm), corresponding to an output of 15,000–42,000 capsules per hour (cph). The start-stop movement of the powder bowl leads to mixing and redistribution of the powder due to acceleration, depending on the tamping speed. Hence, the tamping speed influences the powder bed homogeneity and the capsule filling performance.

The average RTD and the shape of the distribution provide important information about the mixing in the powder bowl [9]. The RTD is affected by the mixing in the powder bowl and the amount of material inside the bowl. The powder volume inside the bowl mainly determines the mean residence time. The more material there is in the bowl, the longer the mean residence time is. Moreover, a compromise between a narrow residence time distribution (good for material tracking / batch changes) and a broad residence time distribution (good for mixing) must be found. In general, both the average residence time and the width of the RTD determine the batch transition time. The wider the RTD and the longer the mean RT, the longer the batch transition time is.

In order to reduce the powder volume and the mean residence time, the powder bed height and the volume of the bowl can be reduced. The powder bed height is a CPP, which affects CQAs of the final product, as reported in [41,42]. Typically, the PBH should have a minimum value to achieve consistent filling behavior. Therefore, the best way to reduce the powder volume inside the bowl, is the selection of an appropriate insert that reduces the free volume. The main focus of this paper is to present a nondestructive online RTD characterization method which can be applied to various inserts, enabling the comparison of the obtained RTDs. Nevertheless, an insert also may influence the filling performance of



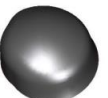
the capsule filling machine. The filling performance will be investigated in a separate study. Note that the RTD is not the only important process parameter. The fill weight, fill weight variation and content uniformity have to be considered as well. However, they are beyond the scope of this work.

The paper is structured as follows. The next section contains a detailed description of material characterization and the experimental setup. The main section presents the results, with subsections dealing with material characterization and RTD results. Conclusions and an outlook to future work are provided in the last section.

### 3.3 Materials and Methods

This section describes the methods we used to experimentally obtain RTDs for three selected inserts shown in Table 7. These inserts are placed inside the powder bowl, to reduce the volume of the powder bed and alter the flow behavior of powder inside the bowl. The RTD is related to the flow structure of powder inside the bowl. However, a complete determination of the RTD with arbitrary insert geometries is out of the scope of this work.

*Table 7: Overview of the inserts used for RTD experiments. The bowl volume gives the free volume of the bowl filled with powder to reach the desired powder bed heights (PBH) of 35 mm or 20 mm.*

tag	reference	geometry 1	geometry 2
shape			
bowl volume – 35 mm PBH	720 cm <sup>3</sup>	817 cm <sup>3</sup>	*607 cm <sup>3</sup>
bowl volume – 20 mm PBH	*283 cm <sup>3</sup>	*361 cm <sup>3</sup>	265 cm <sup>3</sup>

\* not used in this work

The reference geometry is a simple conical insert made of stainless steel, which is flattened at the top. Geometry 1 and geometry 2 were 3D printed and are made of plastic. The reference geometry and the geometry 1 insert are co-rotating with the same speed as the powder bowl. The geometry 2 insert is standing still. The position of the insert inside the powder bowl can be seen in Figure 18 (a). The dark element inside the powder bowl is the so-called “ship” at the transfer station (station 6).

As pointed out, geometry 1 is like the reference shape a rotating geometry. Its turbine-like shape is designed to facilitate powder transport in the direction of the rotation, and hence, reduce the powder pile-up in front of the ship. A detailed view of the powder bowl with geometry 1 is depicted in Figure 18 (b). In contrast geometry 2 is fixed and does not rotate with the bowl. Its asymmetric shape is due to the

ship (transfer station) on the one side. The purpose of this insert is to minimize the powder bed volume in the bowl. The maximum dimensions of geometry 2 were selected as trade-off between minimum powder volume and acceptable powder pile-up of powder in front of the ship. The shape and position of geometry 2 can be seen in Figure 18 (c).

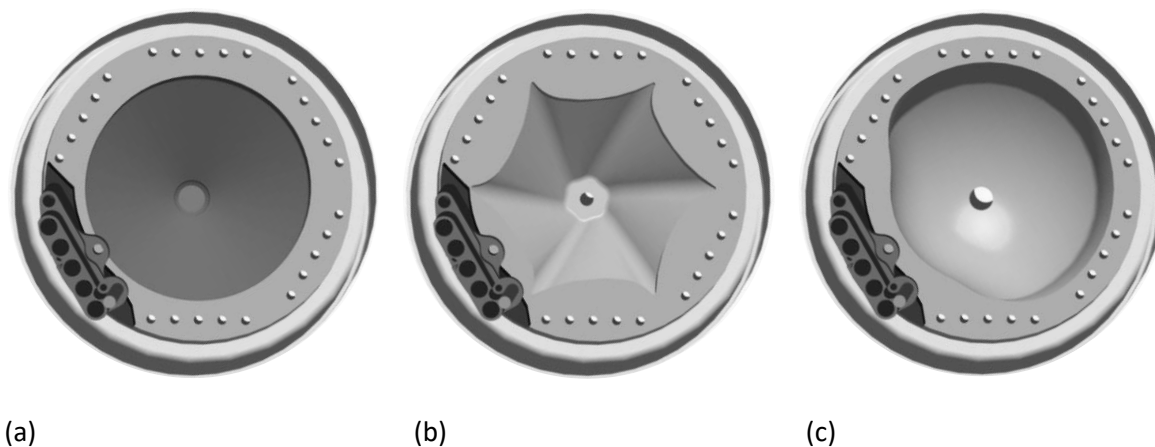


Figure 18: Powder bowl with ship and (a) reference geometry, (b) geometry 1 and (c) geometry 2.

To compare the three inserts concerning their effect on RTD, a methodology for the determination of the RTD of a tamping pin capsule filling machine was developed. This methodology includes experimental setup, tracer application and sophisticated data processing. Previous studies presented RTD measurements either via colored tracer material, e.g., as reported in [17,22,23,43] or via defined changes in API concentration as shown in e.g., [44–46]. An API pulse was not found to be feasible, as non-hazardous material was preferred at this development stage. Therefore, two different color-based methodologies were investigated: First, a food-dye coloring of bulk powder material, and second, light-induced fluorescence (LIF) were employed. The food dye coloring procedure was shown to give the most accurate RTD measurements.

Sugar pellets (Pharm-a-Spheres, Hanns G. Werner GmbH + Co.KG, Tornesch, Germany) were selected due to their spherical shape, good flowability and low health/environmental risks. Furthermore, the sugar pellets are poorly compressible which is eliminating the pin immersion depth as an influential process parameter. The natural color of sugar pellets is white. A 4-step coloring procedure was developed to produce colored (red) sugar pellets as a tracer. First, the pellets and food dye were placed into a rotary drum blender (JEM RRM, Engelsmann Mischtechnik, Germany) and mixed with isopropanol for 30 min at 28 rpm. Then, the tracer material was placed under a fume hood for drying. Next, the agglomerates formed during drying were deagglomerated by applying manual shear. Finally, a sieving step was performed to remove any remaining agglomerates. Material characterization was carried out for white and colored



sugar pellets to evaluate the effect of the coloring procedure, which should be small. The particle size distribution (PSD), the bulk and tapped density and other relevant powder bulk properties were investigated and compared.

Particle size measurements were performed using a dynamic image analysis system QICPIC (OASIS/L wet and dry dispersing system, Sympatec GmbH, Clausthal-Zellerfeld, Germany). The dispersion pressure was set to 0.5 bar. Windox 5.6.0.0 was used for automated image analysis of pictures taken by a QICPIC camera. The measurements were performed in triplicates to obtain the average PSD data. Mass-based particle size indicators ( $x_{50}$ ,  $x_{10}$  and  $x_{90}$ ) were determined.

The Pharmatester (PT-TD200, Pharma Test Apparatebau AG, Germany) was used to establish bulk and tapped densities (BD/TD) according to the standard method described by the United States Pharmacopeia (USP) [47]. Based on the known volume before and after tapping, the Carr index / compressibility index (CI) that correlates to flowability can be calculated. Powder with CI <10 is considered to have excellent flowability [48].

Rheometry measurements were performed with the FT4 powder rheometer (Freeman Technology, Tewkesbury, United Kingdom), which allows determining powder flow properties, such as the flow function coefficient (ffc), cohesion (C), angle of internal friction (AIF) and compressibility (CPL). The ffc index is defined by the ratio between consolidated stress and unconfined yield strength. It was measured with a 25 mm shear-cell module at a maximum pressure of 9 kPa. The higher the ffc is, the better the flowability. Generally, a value of >10 corresponds to a free-flowing material.

Cohesion is a measure for inter-particle interactions, which is mainly affected by the particle size and surface area and by the moisture content. High inter-particle forces make the powder more cohesive. The AIFd describes the effect of yield locus, i.e., the point of failure for various normal stress states. CPL is defined as the volume reduction in a material when normal pressure is applied. We determined it at a pressure of 15 kPa. A detailed description of the methods, as realized in the FT4, can be found in [49].

The AoR is another index for classifying powders. It relates to the density, surface roughness and shape of particles. To determine the AoR, the powder is poured from a defined height to a horizontal base plate through an orifice. The angle of the resulting cone is the AoR. Generally, a lower AoR indicates better flowability [50].

Prior to the RTD measurements, a calibration curve (Figure 19) for the image analysis was created for 0%, 5%, 10%, 15%, 20%, 25%, 50%, 75% and 100% of colored pellets. The chosen fitting curve is a third-order polynomial

$$c(a) = k_3 a^3 + k_2 a^2 + k_1 a + k_0 \quad (1)$$

fitting the measurement data. The error bars are determined via the definition of error propagation as

$$\Delta c = \frac{dc}{da} \Delta a = (3k_3 a^2 + 2k_2 a + k_1) \Delta a \quad (2)$$

where  $c$  is the concentration,  $a$  is the measured a-value (color value in LAB color space [51]),  $k_i$  are the polynomial coefficients,  $\Delta c$  is the corresponding standard deviation of concentration and  $\Delta a$  is the standard deviation of the measured a-value calculated based on 10 measurements. As can be seen, the standard deviations are rather small, especially at lower concentrations.

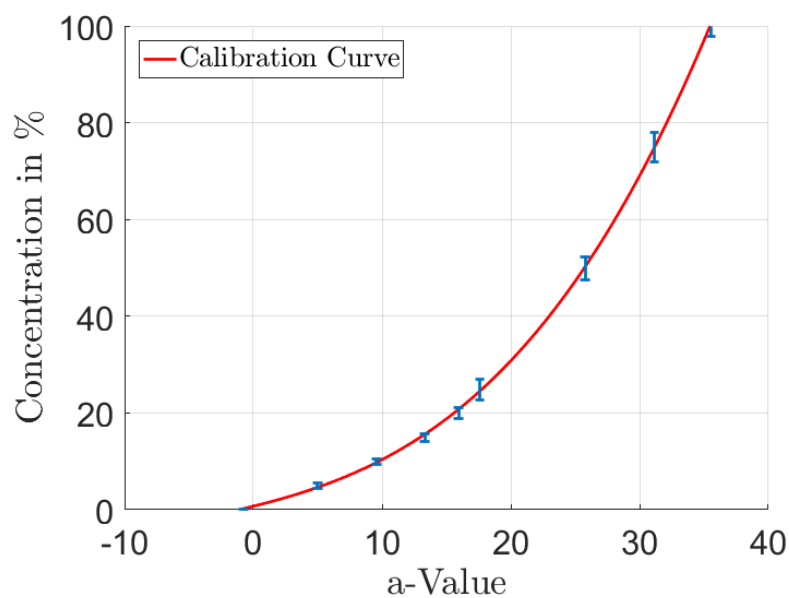
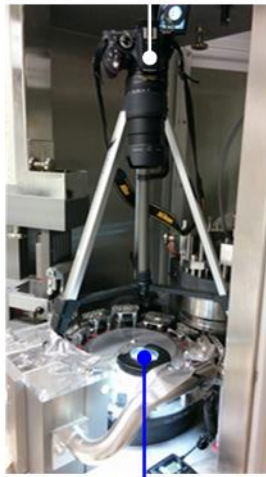


Figure 19: Calibration curve for colored sugar pellets. Error bars indicate the standard deviation between 10 capsules.

The experimental setup is depicted in Figure 20 and a schematic of the setup is shown in Figure 21.

camera  
on tripod



ring light

lamp



segment



lamp

(a)

(b)

(c)

Figure 20: (a) Camera setup and (b) lamp illuminating the tamping station segment. (c) One frame of the video taken from experiment.

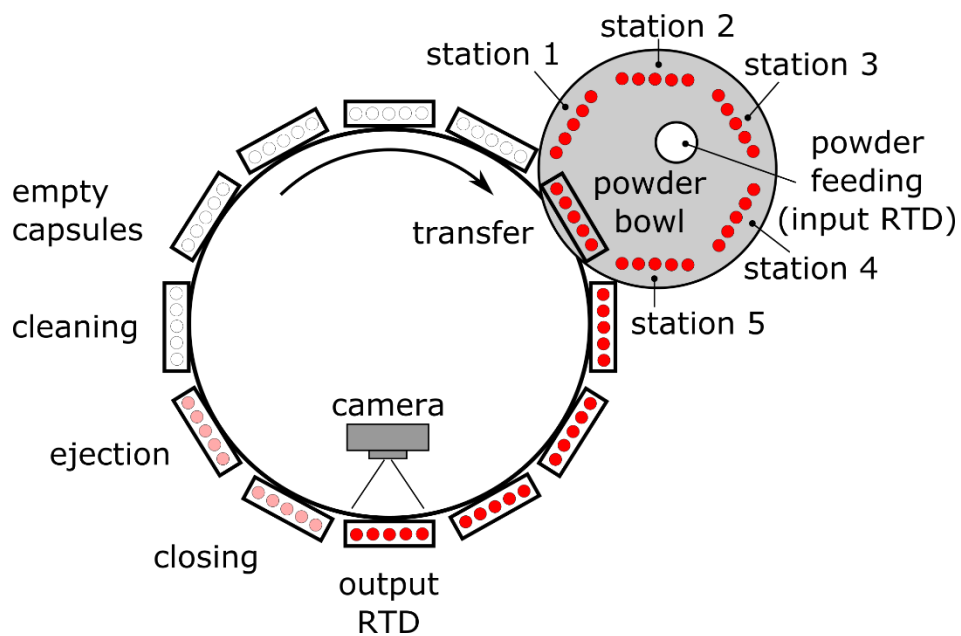


Figure 21: Experimental setup (schematic) for RTD measurements, including the system input and output.

A video camera was used to estimate the fraction of colored powder in the capsules. A customer camera (Nikon D5200), which was placed on top of the station just before the capsules were sealed. Figure 20a

shows the measurement setup including the camera on a tripod inside the capsule filling machine. Above the measurement site, a ring light is located. This ring light was later replaced by a lamp which was installed on top of the machine's housing (Figure 20b) which provided a more homogeneous illumination of the measurement area. With this setup, all measurements presented in this work were acquired. Figure 20c is showing one exemplary frame, i.e., the screenshot of a video. A detailed description of the video data processing can be found in the section below. The decay of color intensity was measured for 30 min to completely capture the tail of the RTD, which is important for predicting wash-out of a raw-material batch and for completely removing the out-of-spec material. The RTD was determined by measuring the concentration of red material (delivered at the inlet of the powder bowl via a step response) to the measurement point at the segment immediately before closing the capsules (see "input RTD" and "output RTD" in Figure 21). With this measurement method, only the surface of the powder plug in the open capsule shell can be assessed and not the total content of the capsule. However, this is the only non-destructive online measurement technique available.

Furthermore, such tracer experiments can also be used to identify stagnant zones inside the process (i.e., in the powder bowl). Such stagnant zones get apparent during careful vacuum cleaning of the powder bowl, when layer by layer of powder was removed ensuring to keep the powder bed structure unaffected. With this procedure the location of tracer accumulation (stagnant zones) was revealed.

The powder bowl was initially filled with red tracer material to a PBH of 35 mm (reference geometry and geometry 1). When operating the capsule filler with geometry 2 at a PBH of 35 mm, the powder bowl was overfilled after the first dosing was initiated due to the large volume of geometry 2. Material was pushed through the cover plate and resulted in material loss. To overcome this problem, the PBH was reduced to 20 mm. The attempt was made, to reduce the PBH for the reference geometry and geometry 1 to 20 mm but due to the rotation of those two inserts, the first two tamping stations run empty. This means, that the powder is all concentrated at the last three tamping stations and no homogeneous PBH could be obtained, thus, processing at a PBH of 20 mm using ref. geometry or geometry 1 is not feasible.

The initial fill weight of the bowl was calculated based on its free volume and the bulk density of sugar pellets. The bulk material was placed into the hopper of the capsule filling machine and dosing was initiated when the fill level sensor was not in contact with powder anymore. While the dosing strategy was not altered, the speed of the dosing screw was set as slow as possible to mimic continuous feeding and to reduce artifacts due to intermittent feeding. An overview over the conducted RTD experiments with the machine settings is given in Table 8.

Table 8: Experimental overview for RTD.

Run number	Tamping speed in tpm	Geometry	Tracer fill weight in g	Dosing screw speed in rpm	Tamping pin immersion depth in mm	Powder bed height in mm
CCF1	110	Reference	530	30	1-1-1-1-1	35
CCF2	50	Reference	530	20		
CCF3	110	1	600	30		
CCF4	50	1	600	20		20
CCF5	110	2	200	30		
CCF6	50	2	200	20		

### 3.3.1 Data Processing

The discontinuous powder movement, which is characteristic of a tamping pin system with its start-and-stop movement during tamping, necessitated a start-stop detection (stop of machine rotation while tamping) during the video processing. To determine the resting periods, the absolute difference between two adjacent video frames was calculated. In case of a small difference, below a selected threshold, the frames were tagged as resting. The first and last 2 frames of the resting period were discarded and the remaining frames were counted as one tamping event. The subsequent movement periods (transition from one segment to another) were neglected. This step is called “determine tamps” in Figure 22 and allows separating the movement periods from the tamping periods (where the segment is resting below the camera). The region of interest in each single capsule was selected manually and used to calculate an average red (R), green (G) and blue (B) value. These RGB values were then transformed into the luminosity (L), a and b color space, where a is assigned to red/green and b to yellow/blue. An averaged a-value was used calculate the concentration in one capsule with the help of the calibration curve (Eq. 1). Averaging all 5 capsules in one segment during a single tamp yielded one concentration value  $c(t)$ . A flowchart of data processing is given in Figure 22.

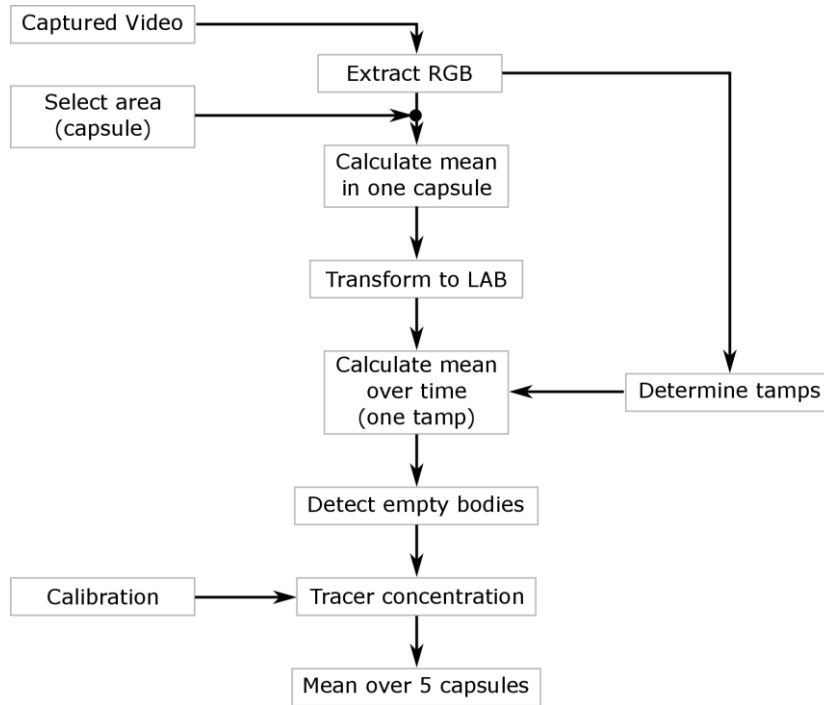


Figure 22: Flowchart of RTD data processing.

Normalization to an area under the curve equal to 1 leads to  $E(t)$ , the exit-age or RTD distribution [52,53]

$$E(t) = \frac{c(t)}{\int_0^{\infty} c(t) dt} \quad (3)$$

Based on the RTD the mean residence time can be computed:

$$\tau = \int_0^{\infty} t E(t) dt, \quad (4)$$

which corresponds to the first central moment of the exit-age-distribution (3). The second moment is the variance,

$$\sigma_{exp}^2 = \int_0^{\infty} (t - \tau)^2 E(t) dt. \quad (5)$$

The standard deviation can be calculated by

$$\sigma_{exp} = \sqrt{\sigma_{exp}^2} \quad (6)$$

Time  $t_x$ , which is the time until x% of tracer material has been washed out, is calculated as

$$\int_0^{t_x} E(t) dt = \frac{x}{100} \quad (7)$$

It was evaluated for x=50% and x=95% and compared for all three inserts.

## 3.4 Results and Discussion

This section is presenting the RTD measurements for a tamping capsule filling machine. It should be noted, that RTD is not the only important measure for suitability of this capsule filler for continuous production. Fill weight and fill weight variation, as well as content uniformity, are also critical quality attributes (CQAs). In this context, additional studies concerning filling performance was conducted and is presented in [54].

### 3.4.1 Material Characterization

PSD measurements for uncolored and colored Pharm-a-Spheres are presented in Figure 23. As can be seen, the  $x_{50}$  of the uncolored pellets was 122  $\mu\text{m}$  and was not changed significantly by the coloring procedure ( $x_{50}$  of the colored pellets: 126  $\mu\text{m}$ ). In addition, the coloring procedure did not significantly influence the shape of PSD. A detailed overview of various powder properties is provided in Table 9. A slight change in the CPL and FFC occurred, which can be attributed to the attachment of color pigments on the surface and a change in the surface roughness. The effect of the change in the CPL on the RTD measurements is negligible, since the immersion depth of the tamping pins was merely 1 mm and the powder was only slightly compressed. Although the ffc may influence the filling behavior of the dosing disc bores during the rotational movement and, as such, the fill weight and the fill weight variation, it does not significantly affect the RTD.

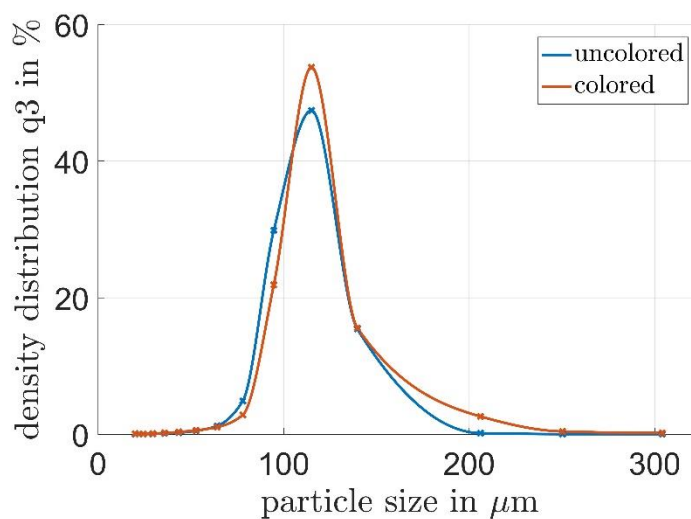


Figure 23: QICPIC measurements of the PSD of uncolored and colored pharm-a-spheres.

Table 9: Powder characterization results. Flowability and compression for uncolored and colored pellets.

Descriptor	Uncolored pellets	Colored pellets
------------	-------------------	-----------------

$x_{10}$ ( $\mu\text{m}$ )	97	99
$x_{50}$ ( $\mu\text{m}$ )	122	126
$x_{90}$ ( $\mu\text{m}$ )	152	157
BD (g/ml)	0.74	0.76
TD (g/ml)	0.76	0.77
CI (%)	2.2 (excellent flowability)	0.92 (excellent flowability)
AoR ( $^{\circ}$ )	28.95 (excellent flowability)	29.2 (excellent flowability)
C (kPa)	0.31	0.56
FFC	13.02 (free flowing)	8.23 (easily flowing)
AIF ( $^{\circ}$ )	16.9	15.3
CPL at 15kPa (%)	4.7	6.6

### 3.4.2 Experimental RTD

In this study, the RTD has been determined for one single material. In addition to a standard insert, two new inserts, one rotating and one stagnant, for reducing the volume of the powder bowl were developed in order to reduce the mean residence time  $\tau$  and  $t_{95}$ . All three inserts were compared to each other. When conducting experiments with the standard insert (cone-shaped), the powder pile-up in front of the transfer station was identified as a problem for continuous operation of the capsule filling machine. This pile-up region is leading to an uneven powder distribution inside the powder bowl, especially at the last tamping station resulting in an increased fill-weight variability caused by an inhomogeneous compression of the powder plug among the 5 tamping pins at station 5. The experiments also revealed, that in some critical areas, tracer material was still present after the experimental run, indicating a stagnant zone. One stagnant zone apparent for all inserts was identified on the horizontal surface (step) where the powder bowl diameter increased, indicated with “A” in Figure 24.

The new geometry 1 insert was developed to actively transport powder past the transfer station and was shaped like a turbine with paddles for that purpose. The experiments showed that the pile-up of material in front of the transfer station was reduced. However, stagnant zones near the paddles were still present (marked with “B” in Figure 24), as revealed during cleaning of the powder bowl after the RTD experiment.





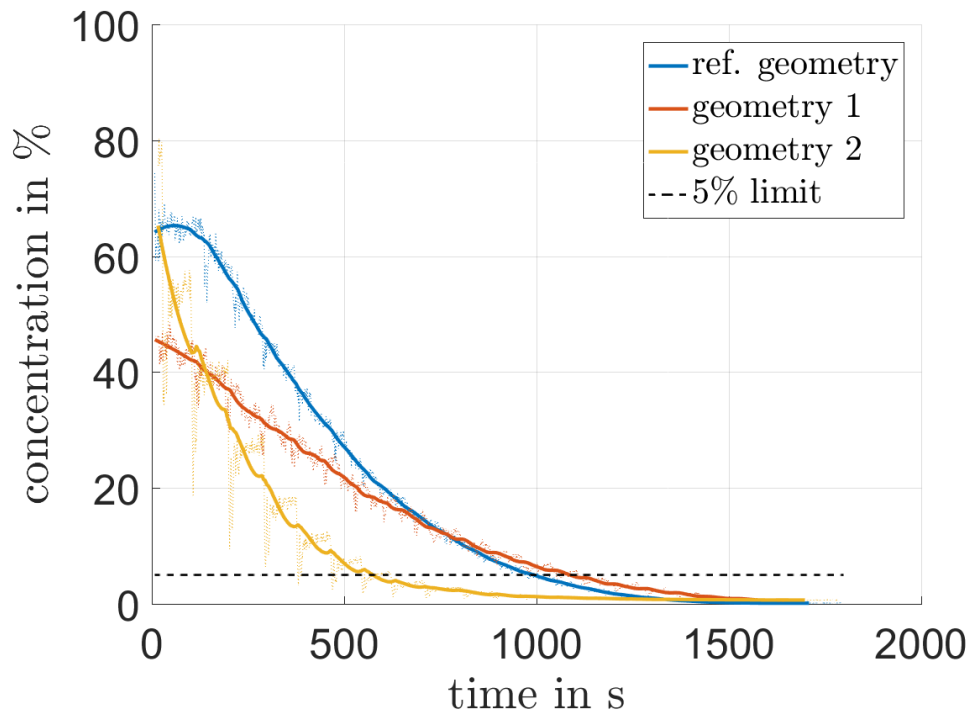
Figure 24: Stagnant zones revealed during cleaning (geometry 1, 110 tpm).

The second new geometry (geometry 2) was designed to reduce the volume of the powder bowl to a minimum. A special asymmetric geometry was created with a spare area at the transfer station to minimize the powder pile-up (see Figure 18). Due to the insert's form, the insert was fixed (i.e., not moving with the powder bowl), to reduce back mixing and reduce the  $t_{95}$  (i.e., resulting in a short) batch transition region. However, mixing is reduced, decreasing the damping capabilities of the system.

The results of RTD step response experiments are shown in Figure 25, where the red line denotes 5% concentration of tracer in the capsules. In a step response experiment the red material should be successively depleted by white material. Thus, in the first capsules only red material should be found. The reason for the fact that this is not the case (see Figure 25), is the excellent mixing of powder inside the powder bowl in combination with the sequential tamping process, pushing fresh white powder immediately into the die holes and the capsules. This leads to a 5-layer powder plug (5 tamping stations), with only the top surface being captured by the applied measurement technique. Therefore, some white material is immediately present in the top layer.

The dotted lines are the average concentration of 5 capsules in one segment, the solid line is smoothed using Savitzky-Golay filtering [55] with a window length of approximately two dosing intervals and a second-order polynomial to obtain sufficient smoothing of the concentration-plateaus apparent in the raw

data (see Figure 25). This is highlighted in Figure 26, where two feeding intervals are shown for geometry 2 at 50 tpm. It can be seen, that there is an immediate decrease in concentration after white powder has started to be feed into the powder bowl (indicated by arrows in Figure 26). The good mixing distributes the white powder inside the bowl, leading to an approximately constant level of tracer in the filled capsules (for about 70s) until new white powder is fed again. By monitoring the feeding indicator of the machine's human machine interface (HMI) and by manually measuring the time between the dosing intervals, we established that this phenomenon was due to intermittent feeding (there is not continuous feeding to the capsule filler in its current form). This is also in accordance with the powder bed height measurement by Wagner et al. [39].



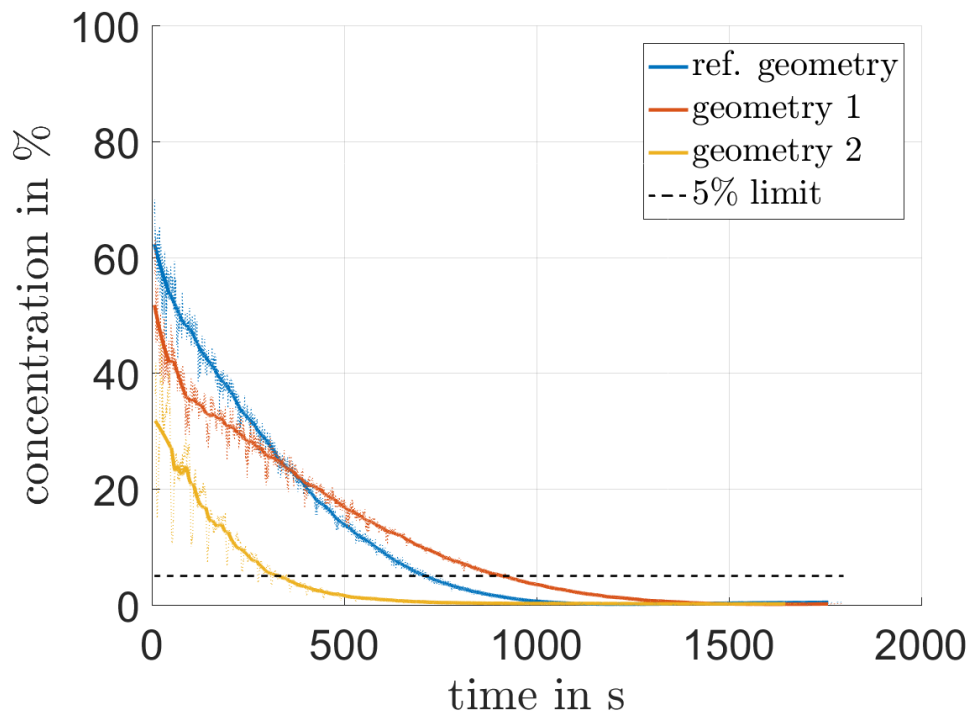


Figure 25: Concentration decay in step response experiments (top: 50 tpm, bottom: 110 tpm). The dotted lines are the average concentration of 5 capsules in one segment. The solid line is smoothed. The red line is the limit where the tracer concentration decreased to 5%.



Figure 26: Close up of two feeding intervals with stepwise decrease in concentration.

Table 10: Characteristic parameters of RTD.

Run number	t <sub>pm</sub> in 1/min	Geometry	PBH in mm	$\tau$ in s	$\sigma_{exp}$ in s	$\frac{\sigma_{exp}^2}{\tau^2}$ in [-]	$t_{50}$ in s	$t_{95}$ in s
CCF1	110	Ref.	35	304	231	0.58	256	770
CCF2	50	Ref.	35	500	288	0.32	434	1083
CCF3	110	1	35	381	342	0.83	303	1059
CCF4	50	1	35	548	362	0.45	482	1249
CCF5	110	2	20	190	157	0.70	147	487
CCF6	50	2	20	242	208	0.79	193	631

Table 10 summarizes the results of the RTD experiments.  $\tau$  is the mean residence time (first central moment) and  $\sigma_{exp}$  is the standard deviation (square root of second central moment).  $t_{50}$  and  $t_{95}$  are calculated according to Eq. 5. In addition to the mean residence time and the standard deviation, the relative variance  $\sigma_{exp}^2/\tau^2$  is provided as an indicator for mixing. A relative variance of 1 can be interpreted

as ideal continuous stirred tank reactor, whereas a relative variance of 0 is corresponding to ideal plug flow [56]. The normalization is allowing the comparison of mixing capabilities for all three inserts, which is not possible only by investigation of the standard deviation  $\sigma_{exp}$ , as the powder bed height is not the same for all inserts.

Geometry 1 and the reference geometry could be compared easily, as it was possible to run experiments at the same powder bed height. Therefore, the changes in RTD can be attributed to the insert. In case of geometry 2, a direct comparison with the other inserts is not that straightforward due to the lower powder bed height. Nevertheless, it has to be noted, that in terms of RTD, this geometry can be used for lower PBH. The reduction of mean residence time and standard deviation of the RTD cannot be attributed to the insert itself but rather to a reduced powder volume. Due to the lower PBH of 20 mm, the mean residence time  $\tau$  as well as  $t_{50}$  and  $t_{95}$  are the shortest.

When operating the capsule filler at 50 tpm, the mean residence time  $\tau$  as well as  $t_{50}$  and  $t_{95}$  are larger, compared to running the capsule filler at 110 tpm. As the tamping speed is directly related to the throughput, the increase of  $\tau$ ,  $t_{50}$  and  $t_{95}$  is expected. The relative variance  $\sigma_{exp}^2/\tau^2$  decreases at lower tamping speed, corresponding to less backmixing. Furthermore, it can be seen, that the difference in the relative variance between 50 tpm and 110 tpm is much higher for the reference geometry and geometry 1, compared to the results for geometry 2. This means, that the mixing behavior for the reference geometry and geometry 1 is sensitive to changes in tamping speed, whereas for geometry 2, the relative variance is roughly the same. This is leading us to the conclusion, that geometry 2 is highly beneficial for continuous manufacturing, as it allows to adjust the throughput of the capsule filling machine without changing the mixing behavior inside the powder bowl.

Comparison of the relative variance between the reference geometry and geometry 1 shows that powder is experiencing more mixing when using geometry 1, at both tamping speeds. For 110 tpm, the relative variance for geometry 2 is between reference geometry (less mixing) and geometry 1 (more mixing). The reduction of the tamping speed to 50 tpm does not reduce the relative variance for geometry 2, whereas it is reduced by approximately a factor of two for the reference geometry and geometry 1, leaving the highest relative variance for geometry 2.

The benefits of high backmixing (broad RTD) versus a short batch transition time (narrow RTD) have to be carefully weighed, as already stated in the introduction. For a broad RTD, geometry 1 is preferred, followed by the reference geometry. When a narrow RTD is desired, geometry 2 is the best choice, followed by the reference geometry.

The step response for all experiments appears to be of CSTR type, which, however, should start at a 100% tracer concentration. Thus, the development of an RTD model is not straight forward. Moreover, the

influence of feed fluctuations on model parameter identification has to be investigated. Modeling of a continuous capsule filling machine is highly interesting and will be addressed in future work.

### 3.5 Conclusion and Outlook

In our work we show a method for acquiring and analyzing the RTD of a tamping capsule-filling machine. Stagnant zones were identified and three different inserts, designed to reduce powder-bowl volume and powder pile-up, were compared in terms of mean residence time and mixing efficiency. It could be shown, that both size/volume and form of the inserts alter the RTD and the mixing in the bowl. In terms of back-mixing geometry 1 is superior over the reference geometry and geometry 2. If a narrow RTD is desired (to reduce mixing and batch transition time), geometry 2 is the best choice, followed by the reference geometry and geometry 1.

The intermittent feeding in the current configuration is not well suited for determination of the RTD of a continuous capsule filling machine. Therefore, further work will be performed to measure the RTD with a (PID-) controlled PBH and continuous feeding device to ensure continuous (and not intermittent) feeding, which is not possible with current tamping machines. This will also enable comparison of the three inserts at a PBH of 20 mm.

### 3.6 Acknowledgements

This work has been funded by the Austrian COMET Program under the auspices of the Austrian Federal Ministry of Transport, Innovation and Technology (bmvit), the Austrian Federal Ministry of Economy, Family and Youth (bmwfj) and by the State of Styria (Styrian Funding Agency SFG). COMET is managed by the Austrian Research Promotion Agency FFG.

The authors would like to thank BOSCH Packaging, for their financial and scientific support and CAPSUGEL for capsule supply. Furthermore, we want to thank Daniel Kaiser, Michael Piller and Thomas Wutscher for providing their technical support in the lab and pilot plant.

### 3.7 Literature

- [1] J.S. Srari, C. Badman, M. Krumme, M. Futran, C. Johnston, Future supply chains enabled by continuous processing-opportunities and challenges May 20-21, 2014 continuous manufacturing symposium, *J. Pharm. Sci.* 104 (2015) 840–849. doi:10.1002/jps.24343.
- [2] J. Rantanen, J. Khinast, The Future of Pharmaceutical Manufacturing Sciences, *J. Pharm. Sci.* 104 (2015) 3612–3638. doi:10.1002/jps.24594.

- [3] M. Ierapetritou, F. Muzzio, G. Reklaitis, Perspectives on the continuous manufacturing of powder-based pharmaceutical processes, *AIChE J.* 62 (2016) 1846–1862. doi:10.1002/aic.15210.
- [4] S. Chatterjee (FDA), FDA Perspective on Continuous Manufacturing, in: *IFPAC Annu. Meet.*, 2012.
- [5] Y. Gao, F.J. Muzzio, M.G. Ierapetritou, A review of the Residence Time Distribution (RTD) applications in solid unit operations, *Powder Technol.* 228 (2012) 416–423. doi:10.1016/j.powtec.2012.05.060.
- [6] P.M. Portillo, M.G. Ierapetritou, F.J. Muzzio, Effects of rotation rate, mixing angle, and cohesion in two continuous powder mixers—A statistical approach, *Powder Technol.* 194 (2009) 217–227. doi:10.1016/j.powtec.2009.04.010.
- [7] P.M. Portillo, M.G. Ierapetritou, F.J. Muzzio, Characterization of continuous convective powder mixing processes, *Powder Technol.* 182 (2008) 368–378. doi:10.1016/j.powtec.2007.06.024.
- [8] A.U. Vanarase, F.J. Muzzio, Effect of operating conditions and design parameters in a continuous powder mixer, *Powder Technol.* 208 (2011) 26–36. doi:10.1016/j.powtec.2010.11.038.
- [9] Y. Gao, A. Vanarase, F. Muzzio, M. Ierapetritou, Characterizing continuous powder mixing using residence time distribution, *Chem. Eng. Sci.* 66 (2011) 417–425. doi:10.1016/j.ces.2010.10.045.
- [10] J.C. Williams, M.A. Rahman, Prediction of the performance of continuous mixers for particulate solids using residence time distributions Part II, *Powder Technol.* 5 (1972) 87–92. doi:10.1016/0032-5910(72)80005-6.
- [11] J.C. Williams, M.A. Rahman, Prediction of the performance of continuous mixers for particulate solids using residence time distributions Part I. Theoretical, *Powder Technol.* 5 (1972) 87–92. doi:10.1016/0032-5910(72)80005-6.
- [12] J.G. Osorio, F.J. Muzzio, Effects of processing parameters and blade patterns on continuous pharmaceutical powder mixing, *Chem. Eng. Process. Process Intensif.* 109 (2016) 59–67. doi:10.1016/j.cep.2016.07.012.
- [13] L. Pernenkil, C.L. Cooney, A review on the continuous blending of powders, *Chem. Eng. Sci.* 61 (2006) 720–742. doi:10.1016/j.ces.2005.06.016.
- [14] H. Berthiaux, K. Marikh, C. Gatumel, Continuous mixing of powder mixtures with pharmaceutical process constraints, *Chem. Eng. Process. Process Intensif.* 47 (2008) 2315–2322. doi:10.1016/j.cep.2008.01.009.
- [15] A. Kumar, J. Vercruyssen, V. Vanhoorne, M. Toiviainen, P.-E.E. Panouillot, M. Juuti, C. Vervaet, J.P. Remon, K. V. Gernaey, T. De Beer, I. Nopens, Conceptual framework for model-based analysis of residence time distribution in twin-screw granulation, *Eur. J. Pharm. Sci.* 71 (2015) 25–34. doi:10.1016/j.ejps.2015.02.004.
- [16] A. Kumar, J. Vercruyssen, M. Toiviainen, P.-E. Panouillot, M. Juuti, V. Vanhoorne, C. Vervaet, J.P. Remon, K. V. Gernaey, T. De Beer, I. Nopens, Mixing and transport during pharmaceutical twin-screw wet granulation: experimental analysis via chemical imaging., *Eur. J. Pharm. Biopharm.* 87 (2014) 279–89. doi:10.1016/j.ejpb.2014.04.004.
- [17] A.S. El Hagrasy, J.R. Hennenkamp, M.D. Burke, J.J. Cartwright, J.D. Litster, Twin screw wet granulation: Influence of formulation parameters on granule properties and growth behavior,

- Powder Technol. 238 (2013) 108–115. doi:10.1016/j.powtec.2012.04.035.
- [18] A. Kumar, J. Vercruyse, S.T.F.C.F.C. Mortier, C. Vervaet, J.P. Remon, K. V Gernaey, T. De Beer, I. Nopens, Model-based analysis of a twin-screw wet granulation system for continuous solid dosage manufacturing, *Comput. Chem. Eng.* 89 (2016) 62–70. doi:10.1016/j.compchemeng.2016.03.007.
- [19] K.T. Lee, A. Ingram, N.A. Rowson, Twin screw wet granulation: the study of a continuous twin screw granulator using Positron Emission Particle Tracking (PEPT) technique., *Eur. J. Pharm. Biopharm.* 81 (2012) 666–673. doi:10.1016/j.ejpb.2012.04.011.
- [20] R.M. Dhenge, J.J. Cartwright, D.G. Doughty, M.J. Hounslow, A.D. Salman, Twin screw wet granulation: Effect of powder feed rate, *Adv. Powder Technol.* 22 (2011) 162–166. doi:10.1016/j.apt.2010.09.004.
- [21] J. Vercruyse, D. Córdoba Díaz, E. Peeters, M. Fonteyne, U. Delaet, I. Van Assche, T. De Beer, J.P. Remon, C. Vervaet, Continuous twin screw granulation: influence of process variables on granule and tablet quality., *Eur. J. Pharm. Biopharm.* 82 (2012) 205–11. doi:10.1016/j.ejpb.2012.05.010.
- [22] T.C. Seem, N. a. Rowson, A. Ingram, Z. Huang, S. Yu, M. de Matas, I. Gabbott, G.K. Reynolds, Twin Screw Granulation – A Literature Review, *Powder Technol.* 276 (2015) 89–102. doi:10.1016/j.powtec.2015.01.075.
- [23] J. Kruisz, J. Rehr, S. Sacher, I. Aigner, M. Horn, J.G. Khinast, RTD Modeling of a Continuous Dry Granulation Process for Process Control and Materials Diversion, *Int. J. Pharm.* 528 (2017) 334–344. doi:10.1016/j.ijpharm.2017.06.001.
- [24] W. Engisch, F. Muzzio, Using Residence Time Distributions (RTDs) to Address the Traceability of Raw Materials in Continuous Pharmaceutical Manufacturing, *J. Pharm. Innov.* 11 (2016) 64–81. doi:10.1007/s12247-015-9238-1.
- [25] S. García-Munoz, A. Butterbaugh, I. Leavesley, L.F. Manley, A flowsheet model for the development of a continuous process for pharmaceutical tablets – an industrial perspective, 0 (2017) 1–15. doi:10.1002/aic.
- [26] K. V. Gernaey, A.E. Cervera-Padrell, J.M. Woodley, A perspective on PSE in pharmaceutical process development and innovation, *Comput. Chem. Eng.* 42 (2012) 15–29. doi:10.1016/j.compchemeng.2012.02.022.
- [27] R. Ramachandran, J. Arjunan, A. Chaudhury, M.G. Ierapetritou, Model-Based Control-Loop Performance of a Continuous Direct Compaction Process, *J. Pharm. Innov.* 6 (2011) 249–263. doi:10.1007/s12247-011-9118-2.
- [28] R. Lakerveld, B. Benyahia, P.L. Heider, H. Zhang, A. Wolfe, C. Testa, S. Ogden, D.R. Hersey, S. Mascia, J. Evans, R.D. Braatz, P.I. Barton, The application of an automated control strategy for an integrated continuous pharmaceutical pilot plant, *Org. Process Res. Dev. Just Accept. Manuscr.* 19 (2014) 1088–1100. doi:10.1021/op500104d.
- [29] J. Rehr, J. Kruisz, S. Sacher, J. Khinast, M. Horn, Optimized continuous pharmaceutical manufacturing via model-predictive control, *Int. J. Pharm.* 510 (2016) 100–115. doi:10.1016/j.ijpharm.2016.06.024.
- [30] Stephen Byrn, M. Futran, H. Thomas, E. Jayjock, N. Maron, R.F. Meyer, A.S. Myerson, M.P. Thien, B.L. Trout, Achieving Continuous Manufacturing for Final Dosage Formation: Challenges and How



- to Meet Them, *Int. Symp. Contin. Manuf. Pharm.* (2014) White Paper 2. doi:10.1002/jps.24247.
- [31] R. Singh, A. Sahay, K.M. Karry, F. Muzzio, M. Ierapetritou, R. Ramachandran, Implementation of an advanced hybrid MPC-PID control system using PAT tools into a direct compaction continuous pharmaceutical tablet manufacturing pilot plant., *Int. J. Pharm.* 473 (2014) 38–54. doi:10.1016/j.ijpharm.2014.06.045.
- [32] R. Singh, M. Ierapetritou, R. Ramachandran, An engineering study on the enhanced control and operation of continuous manufacturing of pharmaceutical tablets via roller compaction., *Int. J. Pharm.* 438 (2012) 307–26. doi:10.1016/j.ijpharm.2012.09.009.
- [33] S.-P. Simonaho, J. Ketolainen, T. Ervasti, M. Toiviainen, O. Korhonen, Continuous manufacturing of tablets with PROMIS-line – Introduction and case studies from continuous feeding, blending and tableting, *Eur. J. Pharm. Sci.* (2016). doi:10.1016/j.ejps.2016.02.006.
- [34] A. Rogers, A. Hashemi, M. Ierapetritou, Modeling of Particulate Processes for the Continuous Manufacture of Solid-Based Pharmaceutical Dosage Forms, *Processes*. 1 (2013) 67–127. doi:10.3390/pr1020067.
- [35] F. Boukouvala, V. Niotis, R. Ramachandran, F.J. Muzzio, M.G. Ierapetritou, An integrated approach for dynamic flowsheet modeling and sensitivity analysis of a continuous tablet manufacturing process, *Comput. Chem. Eng.* 42 (2012) 30–47. doi:10.1016/j.compchemeng.2012.02.015.
- [36] T. Ervasti, S.-P. Simonaho, J. Ketolainen, P. Forsberg, M. Fransson, H. Wikström, S. Folestad, S. Lakio, P. Tajarobi, S. Abrahmsén-Alami, Continuous manufacturing of extended release tablets via powder mixing and direct compression., *Int. J. Pharm.* 495 (2015) 290–301. doi:10.1016/j.ijpharm.2015.08.077.
- [37] R. Singh, D. Barrasso, A. Chaudhury, M. Sen, M. Ierapetritou, R. Ramachandran, Closed-Loop Feedback Control of a Continuous Pharmaceutical Tablet Manufacturing Process via Wet Granulation, *J. Pharm. Innov.* 9 (2014) 16–37. doi:10.1007/s12247-014-9170-9.
- [38] Sven Stegemann, THE FUTURE OF THE CAPSULE MARKET: Fette Compacting, (n.d.). <http://www.fette-compacting.com/the-future-of-the-capsule-market/> (accessed December 2, 2016).
- [39] B. Wagner, T. Brinz, S. Otterbach, J. Khinast, Automation of a dosing-disc capsule filler from the perspective of reliability and safety, *Drug Dev. Ind. Pharm.* 44 (2018) 502–510. doi:10.1080/03639045.2017.1402920.
- [40] F. Podczec, B.E. Jones, Dry filling of hard capsules, *Pharm. Capsul.* (2004) 119–138. [www.pharmpress.com](http://www.pharmpress.com).
- [41] V. Moolchandani, L.L. Augsburger, A. Gupta, M.A. Khan, J. Langridge, S.W. Hoag, To investigate the influence of machine operating variables on formulations derived from lactose types in capsule filling: part 2, *Drug Dev. Ind. Pharm.* (2015) 1–12. doi:10.3109/03639045.2015.1062511.
- [42] F. Podczec, J.M. Newton, Powder filling into hard gelatine capsules on a tamp filling machine., *Int. J. Pharm.* 185 (1999) 237–254.
- [43] H. Li, M.R. Thompson, K.P. O'Donnell, Understanding wet granulation in the kneading block of twin screw extruders, *Chem. Eng. Sci.* 113 (2014) 11–21. doi:10.1016/j.ces.2014.03.007.

- [44] L. Pernenkil, Continuous Blending of Dry Pharmaceutical Powders, IIT Madras, 2003.
- [45] A.U. Vanarase, J.G. Osorio, F.J. Muzzio, Effects of powder flow properties and shear environment on the performance of continuous mixing of pharmaceutical powders, Powder Technol. 246 (2013) 63–72. doi:10.1016/j.powtec.2013.05.002.
- [46] B. Van Snick, J. Holman, C. Cunningham, A. Kumar, J. Vercruyssen, T. De Beer, J.P. Remon, C. Vervaet, Continuous direct compression as manufacturing platform for sustained release tablets, Elsevier B.V., 2017. doi:10.1016/j.ijpharm.2017.01.010.
- [47] USP, <616> Bulk Density and Tapped Density of Powders, (2012).
- [48] R.L. Carr, Evaluating flow properties of solids, Chem. Eng. 72 (1965) 69–72.
- [49] R. Freeman, Measuring the flow properties of consolidated, conditioned and aerated powders — A comparative study using a powder rheometer and a rotational shear cell, Powder Technol. 174 (2007) 25–33. doi:10.1016/j.powtec.2006.10.016.
- [50] USP, Powder Flow, (2012).
- [51] X. Wang, R. Hänsch, L. Ma, O. Hellwich, Comparison of different color spaces for image segmentation using graph-cut, Comput. Vis. Theory Appl. (VISAPP), 2014 Int. Conf. 1 (2014) 301–308.
- [52] E.B. Nauman, Residence Time Theory, Ind. Eng. Chem. Res. 47 (2008) 3752–3766. doi:10.1021/ie071635a.
- [53] P.V. Danckwerts, Continuous flow systems: Distribution of residence times, Chem. Eng. Sci. 2 (1953) 1–13.
- [54] B. Wagner, T. Brinz, S. Otterbach, J. Khinast, Rapid automated process development of a continuous capsule-filling process, Int. J. Pharm. 546 (2018) 154–165. doi:10.1016/J.IJPHARM.2018.05.009.
- [55] A. Savitzky, M.J.E. Golay, Smoothing and Differentiation of Data by Simplified Least Squares Procedures, Anal. Chem. 36 (1964) 1627–1639. doi:10.1021/ac60214a047.
- [56] E.L. Paul, Handbook of Industrial Mixing, John Wiley & Sons, Inc., Hoboken, NJ, USA, 2003. doi:10.1002/0471451452.

## 3.8 Appendix

### 3.8.1 Nomenclature

$a$	a-value (color value in LAB color scale)
$c$	concentration
$E$	exit-age-distribution
$k_{0\dots3}$	polynomial coefficients
$t_x$	time until cumulative tracer concentration reaches $x\%$ .

---

$\Delta a$	estimator for standard deviation of a-value
$\Delta c$	estimator for standard deviation of concentration
$\sigma_{exp}^2$	variance of exit-age-distribution
$\sigma_{exp}$	standard deviation of exit-age-distribution
$\tau$	mean residence time

### 3.8.2 Abbreviations

AIF	angle of internal friction
AoR	angle of repose
BD	bulk density
C	cohesion
CI	Carr index / compressibility index
CM	continuous manufacturing
cph	capsules per hour
CPL	compressibility
CQA	critical quality attribute
DS	design space
FFC	flow function coefficient
LIF	light induced fluorescence
PBH	powder bed height
PSD	particle size distribution
RTD	residence time distribution
TD	tapped density
tpm	tamps per min in 1/min
USP	United States Pharmacopeia

---

*A complex system that works is invariably found to have evolved from a simple system that works.*

John Gaule

## 4 Material tracking in a continuous direct capsule-filling process via residence time distribution measurements

Julia Krusz<sup>1</sup>, Jakob Rehl<sup>1</sup>, Eva Faulhammer<sup>1</sup>, Andreas Witschnigg<sup>1</sup>, Johannes G. Khinast<sup>1,2</sup>

<sup>1</sup>Research Center Pharmaceutical Engineering GmbH, Graz, Austria

<sup>2</sup>Institute for Process and Particle Engineering, Graz University of Technology, Graz, Austria

### 4.1 Abstract

Continuous production of pharmaceuticals requires traceability from the raw material to the final dosage form. With that regard, understanding the residence time distribution (RTD) of the whole process and its unit operations is crucial. This work describes a structured approach to characterizing and modelling of RTDs in a continuous blender and a tamping pin capsule filling machine, including insights into data processing. The parametrized RTD models were interconnected to model a continuous direct capsule-filling process, showing the batch transition as well as the propagation of a 2 min feed disturbance throughout the process. Various control strategies were investigated *in-silico*, aiding in the selection of optimal material diversion point to minimize the material waste. Additionally, the RTD models can facilitate process design and optimization. In this work, adaptations to the capsule filling machine were made and their influence on the RTD was examined to achieve an optimal machine setup.

Keywords: Continuous manufacturing, Blending, Capsule filling, Residence time distribution, Material tracking

## 4.2 Introduction

Continuous manufacturing (CM) is becoming increasingly important in the pharmaceutical industry. The transition from batch to continuous processing is driven by a shorter time to market of assets (both development and process transfer) due to the absence of scale-up, which is one of the main advantages of CM. Lab-scale equipment or small-scale industrial equipment can be used in industrial production since the amount of final product is determined by the production time. Moreover, smaller equipment reduces the footprint of the plant [1,2]. Sophisticated supply chain management can help to decrease in the storage capacity [3]. Increasing agility in manufacturing by effectively increasing flexibility of the supply chain is another major advantage.

The regulatory authority in the USA (FDA) endorsed continuous pharmaceutical manufacturing starting in 2004 with the analytical technology (PAT) initiative [4]. Ever since, new and revised guidelines introducing CM into the pharmaceutical industry have been published.

In terms of quality control for CM, traceability of material (material tracking) throughout the process is a key consideration [5]. The objective of this work is to achieve process understanding with regard to the residence time distribution (RTD). The basis for RTD modeling is given in various publications, either via axial dispersion models or by a cascaded CSTR (tanks-in-series) model [5]–[11]. This work focuses on RTD model development based on CSTR models. The CSTRs are represented in form of transfer functions, which allows to apply standard methods when using such models for model-based controller design [12]. Those RTD models in Laplace domain have been presented previously by Martinetz et al. [6] and Krusz et al. [7] for dry granulation processes. Furthermore, the developed RTD models enable *in-silico* material tracking with a specific focus on capsule filling where this process knowledge can facilitate batch definition by predicting transition regions between two raw material batches (Figure 15). The influence of process parameters on the filling performance, e.g., fill weight and fill weight variations were investigated by Wagner et al. [8,9].

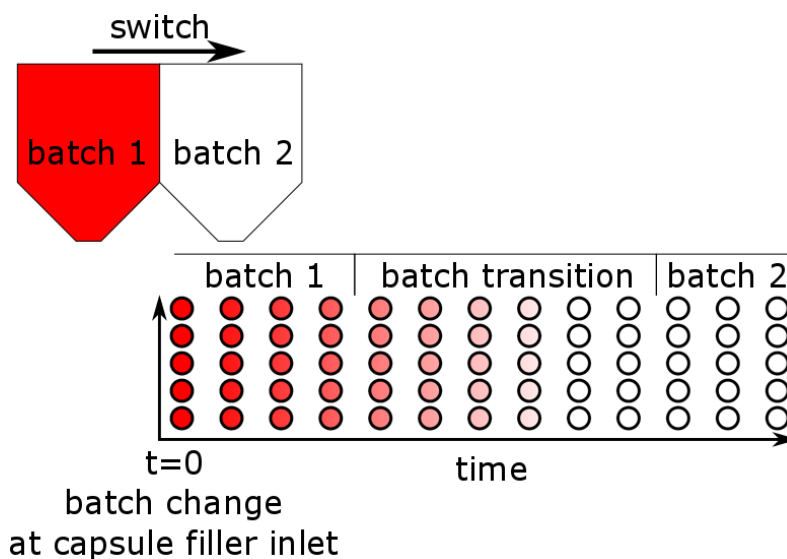


Figure 27: Batch definition: transition between raw material batches.

Material tracking concerns traceability of disturbances introduced into the process mainly by feeders [5], as well as the effects of feeding failures on the intermediate (blend) and final product. RTD models can be used to simulate raw-material batch changes and various process disruptions. Furthermore, the models can be used to identify the time periods at which the API concentration is out-of-spec (OOS) and therefore are a valuable tool for calculating the amount of rejected material. Usually, the concentration of an API is critical, which in this work is substituted by the tracer concentration. The paper at hand introduces a control concept for the API concentration as a main critical quality attribute (CQA) after blending and dosing into capsules which can be integrated into model predictive control (MPC) similar to Rehr et al. [10]. Selected disruption events were simulated for two throughput rates and two possible discharge points were compared in terms of estimated amount of waste material.

An important parameter of all unit operations is the mean residence time (MRT)  $\tau$  during which the material resides in the unit, which can be calculated as

$$\tau = \frac{V}{\dot{V}} \quad (8)$$

Clearly, for a constant density

$$\tau = \frac{m}{\dot{m}} \quad (9)$$

Here,  $V$  is the hold-up volume,  $\dot{V}$  is the volumetric flow rate,  $m$  is the mass and  $\dot{m}$  is the mass flow rate. For the same throughput a smaller amount of material (lower hold-up) in the process leads a shorter mean residence time. A low value of  $\tau$  indicates a reduction in the waste material during start-up and shut-down of the processing line. The RTD can be interpreted as the system's impulse response [11]. A narrow and short RTD leads to sharp batch transitions and shorter discharge times compared to a system with

significant back-mixing. Although a long MRT and a broad RTD can facilitate mixing and can dampen disturbances, it results in long batch transition times (see red boxes in Figure 15). The desired system dynamics, i.e., MRT and width of the RTD, have to be selected considering the actual process and disturbances. In this work, the benefits and drawbacks of broad and narrow RTDs are compared.

The goal of this work is the development of a RTD model for a direct capsule filling line, from which the batch transition time and material concentrations along the process can be calculated. To get an impression of the influence of process settings, the RTD of capsule filler was determined for three inserts (see Table 7) and for two throughputs. Regarding the blending step, the influence of the blender's rotational speed on its RTD was investigated at three throughput levels matching those in the capsule-filling process.

This paper is structured as follows: the Material and Methods section describes the bulk powder material, the coloring procedure for RTD measurement and the experimental setup in the blending and capsule-filling experiments. Furthermore, details on the data processing and the developed RTD models are provided, as well as the control concept with two possible discharge points. The Results and Discussion section focuses on the comparison of the three inserts. Lastly, the conclusion highlights the significant results and further applications.

## 4.3 Materials and Methods

The following section describes the materials used and methods applied to determine the RTD of the continuous capsule-filling process (Figure 28). The section is structured as follows. First, the processed materials are described, followed by the process line description, starting with the main component, the capsule filling machine, going upstream to blender and the feeders. The section continues with a detailed description of the experimental procedures as well as data acquisition method and data processing to determine the RTD of the blender and the capsule filling machine. The last part in this section deals with the derivation of RTD models for blender and capsule filling machine.

### 4.3.1 Material

All experiments were conducted with sugar pellets (Pharm-a-Spheres®, Hanns G. Werner GmbH + Co.KG, Tornesch, Germany), mainly due to their spherical shape and non-toxicity [12]. Moreover, we used this material in previous work to determine the RTD of the tamping pin capsule filling machine GKF 702 (Bosch Packaging, Waiblingen, Germany). For producing an inert (visible) tracer material a 4-step coloring procedure (mixing of bulk material and colorant, drying, de-agglomeration, sieving) is better-suited than laser-induced fluorescence (LIF) measurement. Sugar pellets colored via this 4-step coloring technique and used as a tracer material [13].

A continuous direct capsule-filling line test setup was considered in this study, consisting of a feeder, a continuous blender and a tamping pin capsule-filling machine. A schematic of this process is provided in Figure 28. Possible material discharge points are located after the blender and after the capsule filling machine.

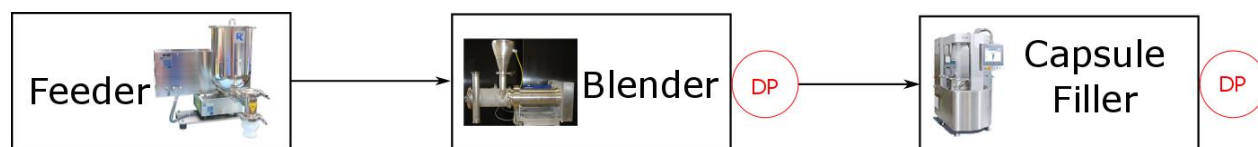


Figure 28: Schematic of continuous direct capsule filling line.

### 4.3.2 Capsule filling machine

The considered tamping pin capsule filling machine (GKF 702, Bosch Packaging, Waiblingen, Germany) has a powder bowl, 5 tamping stations and a transfer station. Each station has 5 tamping pins, allowing to fill 5 capsules simultaneously in one cycle. The powder is fed into the powder bowl, in which a constant powder bed height (PBH) is maintained. The PBH is considered a critical quality attribute (CQA) [14]. At the bottom of the powder bowl there is a dosing disc with dosing disc bores. The powder flows into the bores and is compressed by the downward movement of the tamping pins. After tamping, the dosing disc is rotated by 60 degrees, moving the powder plug to the next tamping station, where once again the powder flows into the bores and is compressed progressively. At the transfer station, the dosing disc bores are sealed by the so-called ship, which remove the excess powder on top of the bores. The downward movement of the tamping pins ejects the powder plug into an open capsule body beneath the dosing disc. A schematic of the process is provided in Figure 29.



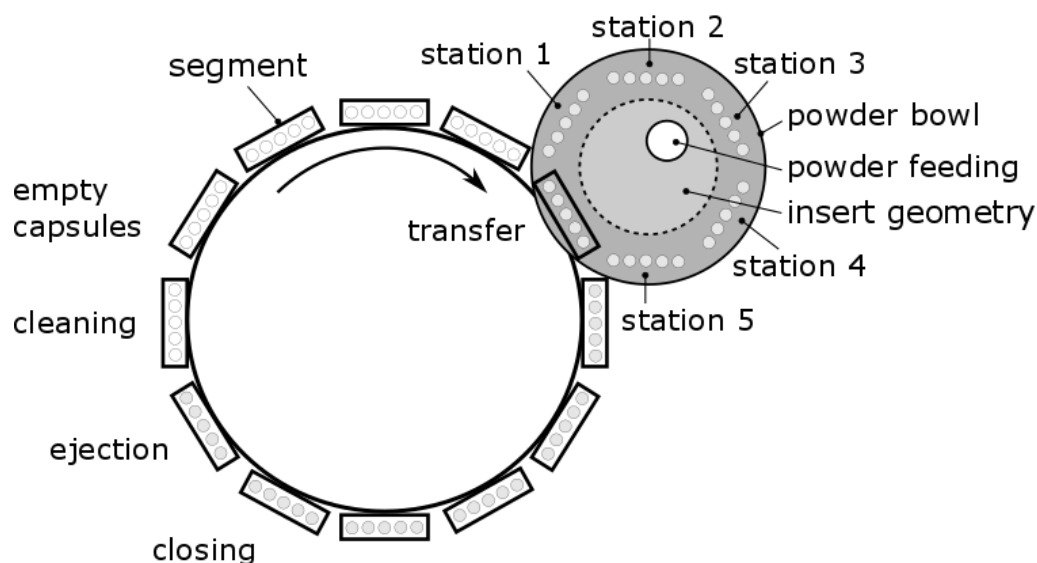


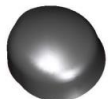


Figure 29: Sketch of the machine setup, depicting the empty capsule insertion, powder bowl with the insert geometry, tamping stations 1-5, transfer station, and closing and ejection steps with subsequent segment cleaning.

An insert was built into the powder bowl to reduce the amount of powder in the process and alter the mixing behavior, by reducing the volume in the bowl. The three investigated geometries and the associated powder volume for a PBH of 20 mm are described in Table 7.

Table 11: Overview of the inserts used in the RTD experiments. The bowl volume is the free volume of the bowl filled with powder to reach the desired powder bed height (PBH) of 20 mm.

tag	reference	geometry 1	geometry 2
shape			
bowl volume – 20 mm PBH	283 cm <sup>3</sup>	361 cm <sup>3</sup>	265 cm <sup>3</sup>

### 4.3.3 Blender

To determine the RTD of a continuous blender (Modulo Mix, Hosokawa Micron, Doetinchem, Netherlands), step response experiments were conducted. A schematic of the blender is given in Figure 30. I1, I2 and I3 are representing the three inlet ports. The outlet port is marked with O1. In this work, only inlet port 1 (I1) was used to feed the materials into the blender.

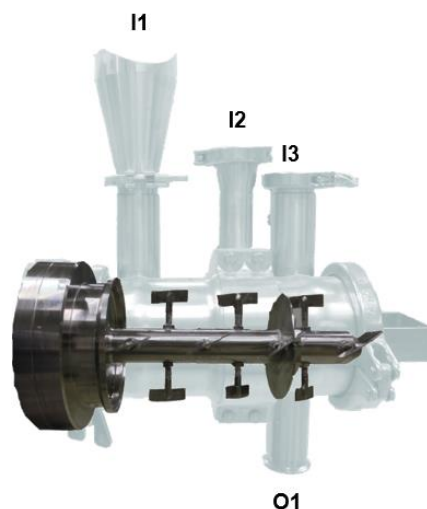


Figure 30: Schematic of the blender. I1, I2 and I3 are representing the three inlet ports whereas the outlet port is marked with O1.

#### 4.3.4 Feeders

Two equivalent gravimetric twin-screw feeders (KT20, Coperion K-Tron, NJ, USA) were positioned above the inlet of the blender. One feeder contained a white bulk material and the other one a red tracer.

#### 4.3.5 Experimental procedures

The blender reached steady state after 3 minutes and the feeders stabilized after about 30 s. To assure the steady state, the blender with red (tracer) material operated for 3 minutes. To obtain a stable feed rate of the white (bulk) material feeder, this feeder was started 30 s before a switch from red to white material was performed. The white material was manually collected and prevented from entering the blender. The collection bin was removed upon the shut-down of the red feeder, allowing only white material to flow into the blender. Simultaneously, the video acquisition was started. Three blender speeds were chosen to investigate the influence of this process parameter on the RTD. Experiments were conducted with two throughput rates matching the one of the capsule filler at a tamping speed of 50 tamps per minute (tpm), corresponding to 15,000 capsules per hour (cph) and 110 tpm (33,000 cph).

A different set-up was used in the step response experiment for the capsule filler. The red tracer was placed into the powder bowl to establish a powder bed height of 20 mm. The bulk powder feeder was placed on top of the GKF702. The material was continuously fed into the powder bowl. The powder feed rate that would match the throughput of the capsule filler was determined prior to the RTD experiments by averaging the capsule weight and calculating the throughput. The capsule-filling machine operated at 50 tpm and 110 tpm resulting in a throughput of 4.6 kg/h and 10.2 kg/h of sugar pellets, respectively. The tamping pin immersion depth was set to 1-1-1-1-1 mm.

### 4.3.6 Data acquisition and processing

The measurement data were acquired using a standard consumer camera Nikon 5200D. Videos with 50 frames/second and a resolution of 1920x1080 pixel were recorded. Data processing was performed using Matlab® (Mathworks, Natick, MA, USA). A detailed description of the applied algorithm can be found in Krusiz et al. [7]. The only difference in this case was that the RTD data were acquired via step response testing rather than impulse response experiments in [7].

Video analysis for establishing the blender's RTD was accomplished via frame-based evaluation of the color intensity in a rectangular region of the acquired video. A screenshot showing the region of interest (white) is provided in Figure 31 for the blender (left) and the capsule filling machine (right).

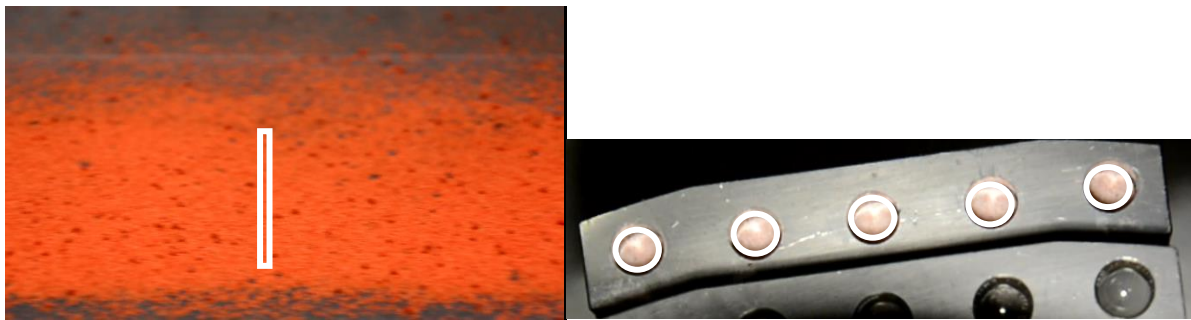


Figure 31: Screenshot of a video during the RTD measurement in the blender (left) and capsule filling machine (right). The color intensity is evaluated inside the white box or circle, respectively.

While each video frame for the blender contributes to the RTD data, the videos for evaluating the RTD in the capsule-filling machine require more complex data processing. Due to a discontinuous representation of the captured powder surface to the camera, not all frames are contributing to the RTD data. The segment with the open filled capsules moves between two tamping steps in front of the camera, resulting in non-representative data. Reliable RTD data can only be acquired during the tamping step, when the segment is stationary in front of the camera. As such, a start/stop detection within the video sequence is required. To obtain a concentration based on the recorded color intensity value, a calibration curve was established. To that end, predefined mixtures were manually filled into capsules and videos were acquired.

### 4.3.7 Modeling

RTD models of a continuous direct capsule filling line can predict concentrations after each unit operation of the processing line. The exit-age distribution is defined as

$$E(t) = \frac{c(t)}{\int_0^{\infty} c(t)dt} \quad (10)$$

where  $c(t)$  is the tracer concentration after the tracer impulse injection. The exit-age distribution is equal to the impulse response of the system. As described above, for practical reasons, step response

experiments were performed to obtain W-curve data (wash-out function  $W(t)$ ). The F-curve is related to the E-curve by Eq. 11 [15].

$$W(t) = 1 - F(t) = 1 - \int_0^{\infty} E(t)dt \quad (11)$$

Mean residence time  $\tau$  is calculated as

$$\tau = \int_0^{\infty} W(t) = \int_0^{\infty} t E(t) dt, \quad (12)$$

which corresponds to the first central moment of the exit-age-distribution (Eq. 3).

A continuously stirred tank reactor (CSTR) has an exponentially decreasing  $E(t) = \frac{1}{\tau} e^{-t/\tau}$ , allowing the computation of the outlet concentration for a given input concentrations. The outlet concentration can be modeled in the Laplace domain using the transfer function

$$P_{CSTR}(s) = \frac{C_{out,CSTR}(s)}{C_{in,CSTR}(s)} = \frac{1}{(1+sT_{1CSTR})} = \frac{1}{(1+s\tau_{CSTR})}. \quad (13)$$

A possible extension of this single CSTR model is a cascade of  $N$  CSTRs in series with different time constants for each reactor leading to a multiplication of the single transfer function, e.g.,

$$\frac{1}{(1+sT_{1CSTR})} \cdot \frac{1}{(1+sT_{2CSTR})} \cdots \frac{1}{(1+sT_{NCSTR})}. \quad (14)$$

In some cases, a delay (dead time)  $T_t$  is introduced to model the time delay from the tracer addition/switch from red to white to the first appearance of tracer at the outlet. This time delay can be interpreted as a plug flow reactor (PRF) in series with  $N$  CSTRs.

The blender's transfer function  $P_{bl}(s)$  is a combination of one CSTR and a time delay in the form of

$$P_{bl}(s) = \frac{C_{out,bl}(s)}{C_{in,bl}(s)} = \frac{1}{1+sT_{1bl}} \cdot e^{-sT_{tbl}}. \quad (15)$$

It was fitted to the acquired  $W_{bl}$ -curve by means of the Matlab® function `fmincon`.  $C_{out,bl}$  and  $C_{in,bl}$  are the output and input concentration of the blender, respectively. A step function was used to determine the wash-out function  $W_{bl}(t)$ .  $T_{1bl}$  of the CSTR model is a time constant, whereas  $T_{tbl}$  is the dead time or time delay.  $T_{1bl}$  and  $T_{tbl}$  are determined via a parameter estimation using the Matlab® function `fmincon`. They depend on the process parameters (blender speed, paddle angle) and the material properties.

The capsule filling process is different since 5 tamping steps are involved, with a 5-layer powder plug and only one concentration (on the surface of the uppermost layer) that can be recorded. Since the surface

layer already consists of a mixture of red and white powder at the start of the measurement, this system can be modeled via a bypass and an additional mixing block. The mixing block was modeled as a series of  $N$  CSTR. The structure is shown in Figure 32.

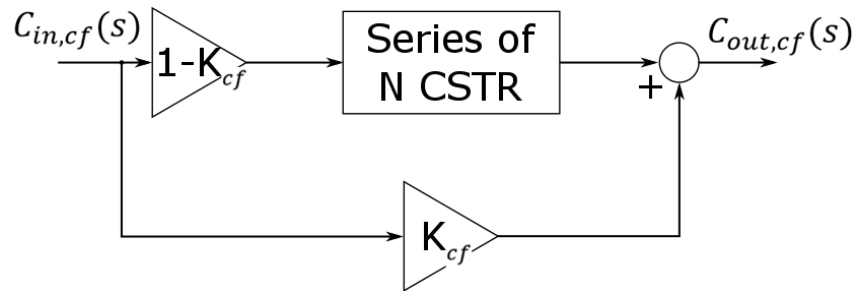


Figure 32: Structure of capsule filler model.

$P_{cf}(s)$  for 2 CSTR is provided in Eq. (16):

$$P_{cf}(s) = \frac{C_{out,cf}(s)}{C_{in,cf}(s)} = \frac{(1-K_{cf})}{(1+sT_{1cf})(1+sT_{2cf})(1+sT_{3cf})} + K_{cf} \quad (16)$$

where  $C_{out,cf}$  and  $C_{in,cf}$  are the output and input concentrations of capsule filler, respectively. The wash-out function  $W_{cf}(t)$  was determined by means of a step function.  $T_{1cf}$ ,  $T_{2cf}$  and  $T_{3cf}$  are time constants.  $T_{1cf}$ ,  $T_{2cf}$  and  $T_{3cf}$  are obtained using parameter estimation via the Matlab® function `fmincon`. These depend on the process parameters, geometry (powder volume inside powder bowl) and material properties. Factor  $K_{cf}$  corresponds to the weighing factor of the bypass path and must be between 0 and 1.  $K_{cf} = 0$  means that all material is mixed by  $N$  CSTR in series, where  $K_{cf} = 1$  corresponds to no mixing and hence a plug flow.

The transfer function  $P_{cf}(s)$  was fitted to the measurement data for all three inserts with which the machine operated at 50 tpm and 110 tpm. To show the repeatability of measurements, all experiments at 110 tpm were performed in duplicate.

Models describing the system's behaviour should always be as simple as possible but as complex as necessary [16]. Establishing the correct number of CSTR in a series prevents overfitting, which reduces the predictive power of the model [17]. The necessary number of CSTRs is determined based on the percentage of error reduction. Therefore, the model's error can be calculated as

$$error = \sum_{i=1}^{\infty} (W_{bl_{model}} - W_{bl_{experimental}})^2 \quad (17)$$

for various numbers of CSTRs. The percentage of error reduction is subsequently calculated for the increase in model order 1 (1 CSTR) to 2 (2 CSTR) as

$$error\ reduction\ \% = \frac{error(1\ CSTR) - error(2\ CSTR)}{error(1\ CSTR)} * 100. \quad (18)$$

Material tracking throughout the processing line can be accomplished via the RTD models for single unit operations. The RTD model of the continuous capsule-filling line can be computed by multiplying the transfer functions of the blender and capsule filler:

$$P_{plant}(s) = \frac{C_{out,cf}(s)}{C_{in,bl}(s)} = P_{bl}(s) \cdot P_{cf}(s) = \left( \frac{1}{1+sT_{1bl}} \right) \cdot \left( \frac{(1-K_{cf})}{\prod_N(1+sT_{n_{cf}})} + K_{cf} \right) \cdot e^{-s(T_{tbl}+T_{tcf})}. \quad (19)$$

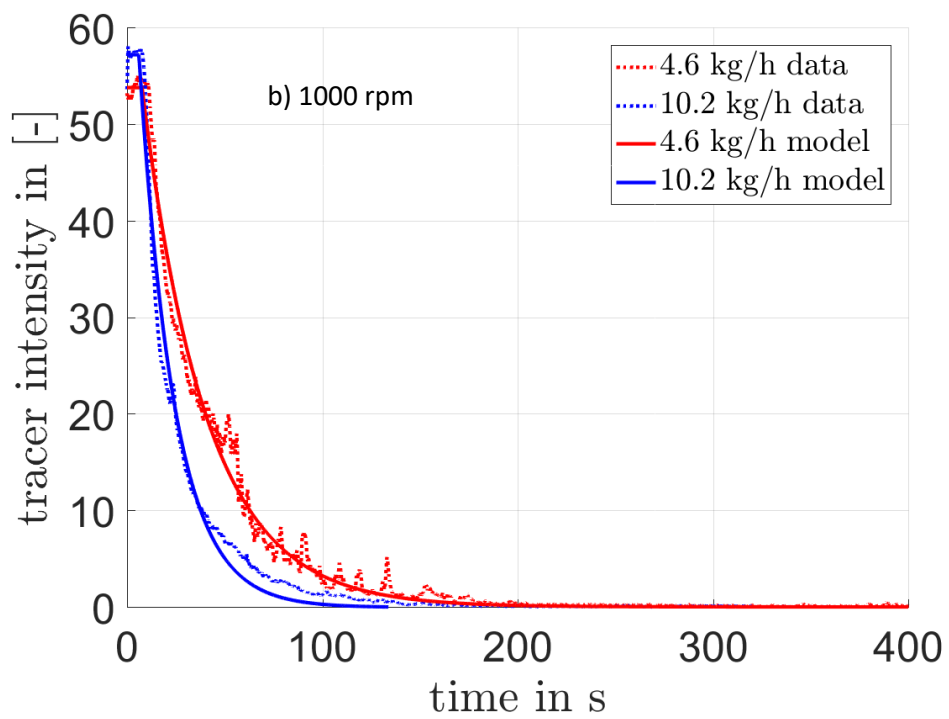
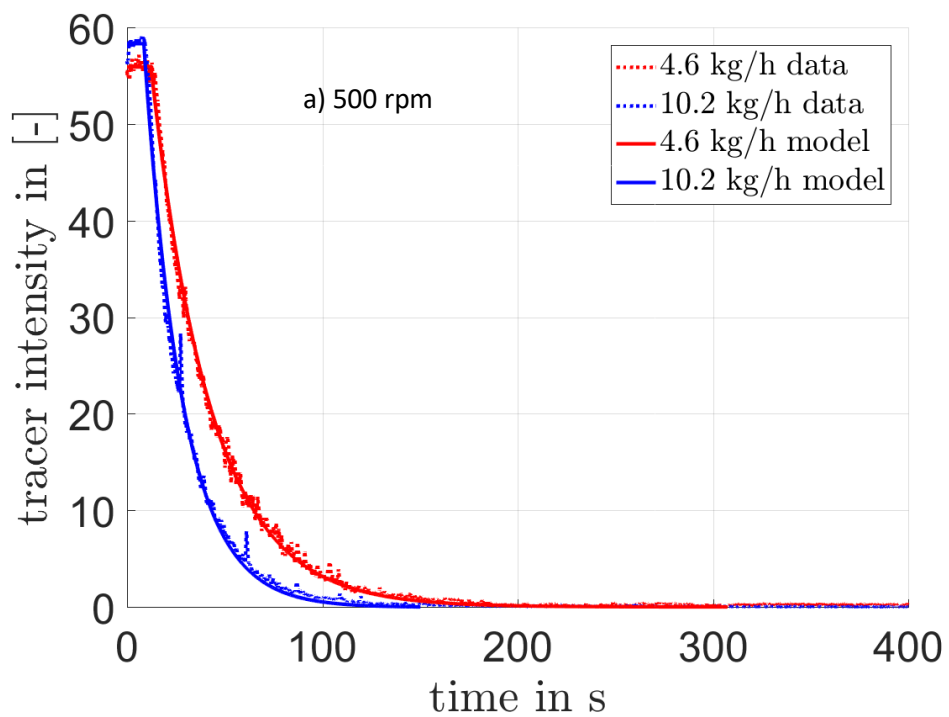
The concentration at the outlet of the capsule filler  $C_{out,cf}(s)$  can be calculated via multiplication with inlet concentration  $C_{in,bl}(s)$ . Selecting certain input functions allows a simulation of various feeding failure events, e.g., blockage of one feeder can be simulated by means of the plant transfer function. Using the RTD models, concentrations after each unit operation can be predicted. The damping characteristic of the blender can attenuate feed fluctuations to some extent, depending on the process parameters. If fluctuations are insufficiently attenuated, OOS material will be present after the blender. There are two ways of handling this material: it can be diverted either after the blender or after the capsule filler. A threshold between in-spec and OOS material can be defined and the diversion times for this threshold can be determined. Furthermore, if the material has to be diverted, precautions must be taken so that the subsequent unit operations do not run empty. To that end, buffers may be implemented, but they should be as small as possible. Simulations allow to calculate an optimum buffer size for particular processes.

## 4.4 Results and Discussion

The following three subsections describe the results obtained via the blender and the capsule filler RTD modelling and a simulation study of a direct continuous capsule-filling line. The latter addresses the effects of a batch transition and selected process upsets on the concentrations in the final product. All experiments were conducted with the same material to proof the applicability of the proposed methodology. In case also material dependency is of interest, their effect needs to be investigated separately.

#### 4.4.1 Blender

All experiments for determining  $W_{bl}(t)$  were conducted in duplicate. Parametrized model and data for wash-out experiments with the continuous blender are shown in Figure 33 at a blender speed of a) 500 rpm, b) 1000 rpm and c) 1500 rpm. The red dotted line indicates the measured wash-out function  $W_{bl}(t)$  for a throughput of 4.6 kg/h with the corresponding model shown in red with solid line. The blue dotted line represents the measurement data for a throughput of 10.2 kg/h with the corresponding model shown in blue solid line. Although the tracer intensity decays faster at a higher throughput, the shape of the curves remains the same, indicating that the model successfully describes the wash-out function. The measurement data at 1500 rpm with a throughput of 4.6 kg/h fluctuated more, which can be attributed to a smaller conveying belt coverage due to dusting. The higher the throughput and the lower the blender speed, the less dusting affects the measurement data. Mean residence time  $\tau_{bl}$ , time constant  $T_{1bl}$  and dead time  $T_{t_{bl}}$  are provided in Table 12 for all blender experiments.





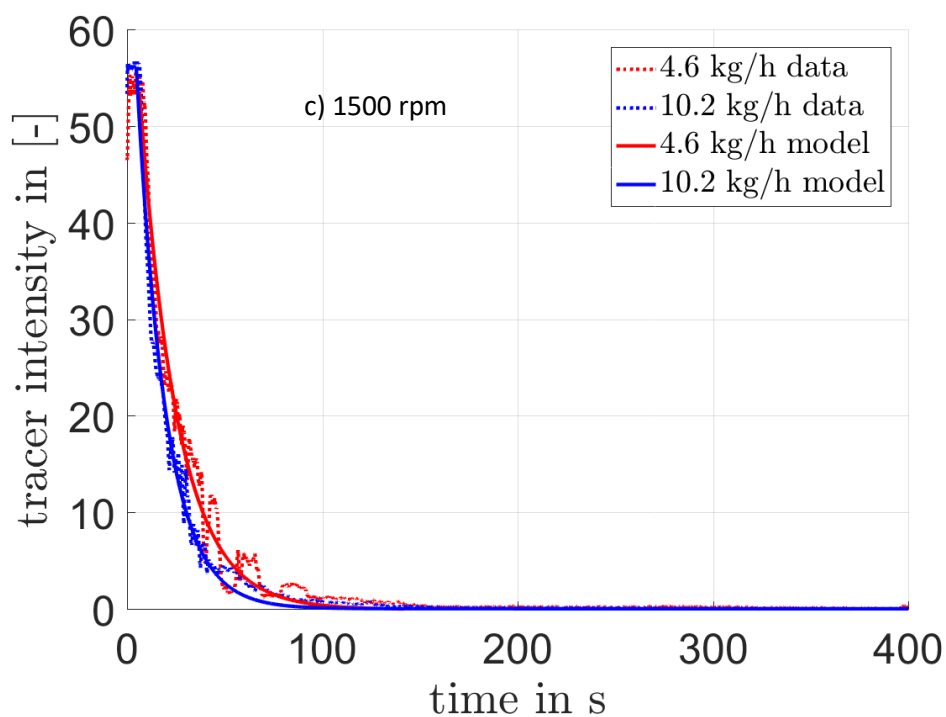


Figure 33: Wash-out functions (data and corresponding model) of blender at a) 500 rpm, b) 1000rpm and c) 1500 rpm at 4.6 kg/h and 10.2 kg/h.

Table 12: Overview of characteristic parameters of the RTD and the time constants obtained for the continuous blender. The excluded run is marked gray.

No.	Throughput in kg/h	Blender Speed in rpm	$\tau_{bl}$ in s	$T_{1_{bl}}$ in s	$T_{t_{bl}}$ in s
1*	4.6	500	42.9	30.6	12.3
2*	4.6	1000	40.5	32.8	7.7
3*	4.6	1500	25.8	19.4	6.4
4	4.6	500	43.4	35.7	7.7
5	4.6	1000	36.2	32.6	3.6
6	4.6	1500	22.1	16.2	5.9
7*	10.2	500	28.4	19.7	8.6
8*	10.2	1000	24.3	18.2	6.1
9*	10.2	1500	19.6	14.8	4.8
10	10.2	500	26.2	14.2	12.0
11	10.2	1000	26.2	18.5	7.7
12	10.2	1500	13.6	13.1	0.5

\* are shown in Figure 33.

Run No. 12 was excluded from further data evaluation and interpretation due to extremely low  $T_{t_{bl}}$  caused by an error in time alignment between adding the tracer and acquiring the data. Nevertheless, time constant  $T_{1_{bl}}$  of the rate of tracer decay is in good agreement with run No. 9 (14.8s vs. 13.1s).

To facilitate the interpretation of measurement results, graphical representations of mean residence time  $\tau_{bl}$  and  $T_{1_{bl}}$  are provided in Figure 34.

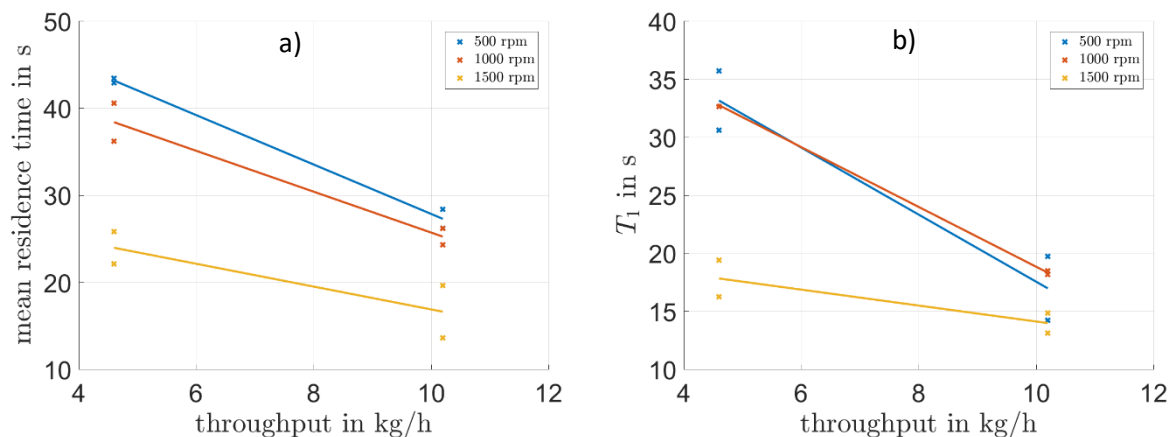


Figure 34: Graphical representation of  $\tau_{bl}$  (a) and  $T_{1_{bl}}$  depending on the process parameters and throughput in the continuous blending experiments. The lines can be used for guidance only, and the linearity cannot be proven at this stage.

As expected, mean residence time  $\tau_{bl}$  decreases with the increasing throughput and blender speed. The behavior of  $T_{1_{bl}}$  is similar in terms of decreasing with the throughput. As can be seen the blender speed between 500 and 1000 rpm has a minor influence on time constant  $T_{1_{bl}}$ . Interestingly, it is much lower when the blender operates at 1500 rpm, corresponding to a much faster decrease in the tracer intensity. A flow regime transition between 1000 rpm and 1500 rpm, leading to a faster powder transport through the blender may be responsible for this feature. The difference in mean residence time  $\tau_{bl}$  is also much larger for the increase from 1000 to 1500 rpm, than for the same increase from 500 to 1000 rpm, which supports this hypothesis.

#### 4.4.2 Capsule Filler

As mentioned in the modeling subsection, the error reduction in % was calculated and taken as measure to determine the number of CSTRs in series to model the RTD. Table 13 shows that the increase from 1 to 2 CSTR is beneficial in all experiments indicated by a high error reduction, except for run No. 8 which had an overall poor fitting performance. An error reduction from 2 to 3 CSTR is below 2 % for geometry 1 (0.9, 1.3 and 0.4 %), suggesting that model order 2 (i.e., with 2 CSTRs in series) is sufficient for this insert. The

error was further decreased by 2.8 - 14.9 % for the reference geometry and geometry 2, both of which were modeled using 3 CSTR in series. Due to experimental issues, CF5 had to be excluded.

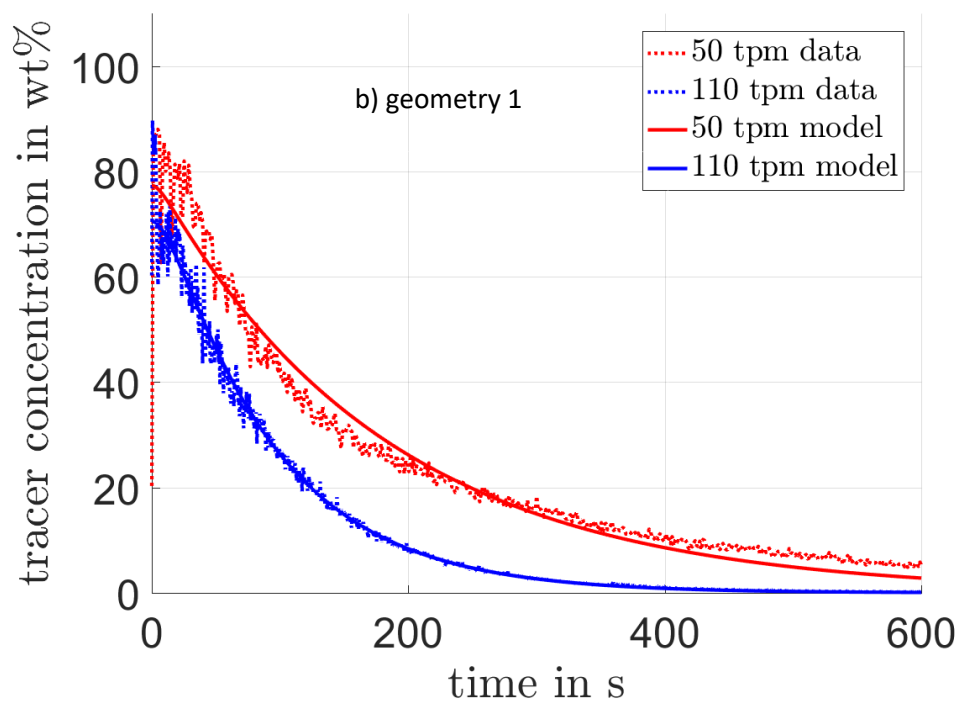
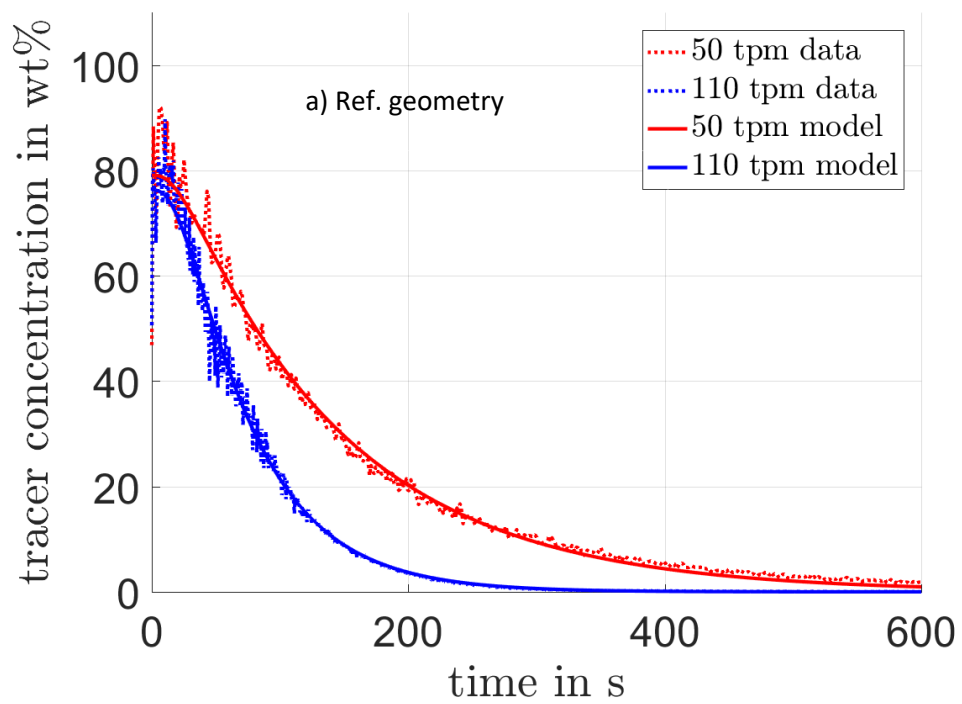
Table 13: Reducing model error by adding CSTR.

No.	Speed in tpm	Insert	error reduction in %		
			1-> 2 CSTR	2->3 CSTR	3-> 4 CSTR
CF1	110	Ref.	79.1	10.9	2.5
CF2	110	Ref.	70.4	11.5	5.3
CF3	110	1	12.8	0.9	0.0
CF4	110	1	46.3	1.3	0.0
CF5	110	2	62.7	7.5	0.8
CF6	110	2	75.6	14.9	2.2
CF7	50	Ref.	50.0	6.3	1.9
CF8	50	1	3.4	0.4	0.1
CF9	50	2	35.1	2.8	0.7

The large difference in error reduction between the repeatability experiments can be explained by slight changes in the RTD curve shape. The “plateau” at the beginning of the RTD experiment (see Figure 35) cannot be modeled by one single CSTR. In cases, where the data shows a distinct plateau, the error reduction from one to two CSTR is high. This variability in the data is introduced by slightly asynchronous (manual) start of the feeder and the capsule filling machine.

The RTD of capsule-filling machine is also shown in terms of wash-out function  $W_{cf}$ . Figure 35 depicts the measured wash-out function and the corresponding model for a) the reference geometry, b) geometry 1 and c) geometry 2. The red dotted line denotes the data measured at 50 tpm (4.6 kg/h), whereas the model is illustrated with a red solid line. At 110 tpm, the data and the associated model are depicted in blue, respectively.

While the shape of curves does not change at various throughputs, it is affected by the inserts since two rather than three CSTRs in series in the transfer function  $P_{cf}$  are required.



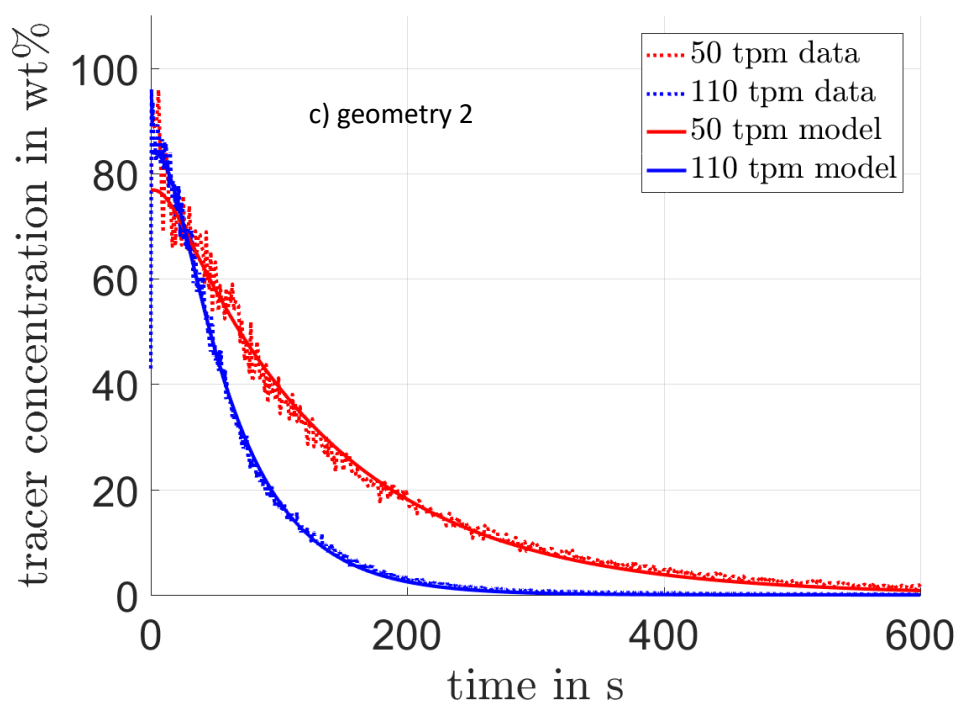


Figure 35: Wash-out functions (data and corresponding models) for the capsule-filling machine with all three inserts (a) reference geometry, b) geometry 1 and c) geometry 2 at two tamping speeds/throughputs.

Mean residence time  $\tau_{cf}$  and fitted time constants for all experiments are provided in Table 14. Run CF5 was excluded from further evaluation due to an unreasonably high  $K_{cf}$  of 0.77, indicating that more than  $\frac{3}{4}$  of the top layer of the first capsule is white bulk powder, i.e., the initial tracer concentration is only 23%. This can be attributed to starting the feeder too early in the experiments.

Table 14: Overview of characteristic parameters of RTD and time constants obtained for the capsule-filling machine. The excluded run is marked gray.

No.	Speed in tpm	Insert	$\tau_{cf}$ in s	$T_{1cf}$ in s	$T_{2cf}$ in s	$T_{3cf}$ in s	$K_{cf}$ in [-]
CF1*	110	Ref.	62.4	56.7	14.8	10.0	0.24
CF2	110	Ref.	55.0	64.8	8.1	8.1	0.32
CF3	110	1	59.4	78.5	3.6	-	0.28
CF4*	110	1	70.9	87.3	12.9	-	0.30
CF5	110	2	16.5	51.1	10.3	10.3	0.77
CF6*	110	2	58.8	51.0	9.4	9.4	0.16
CF7	50	Ref.	120.2	131.0	10.2	10.2	0.21
CF8	50	1	143.4	179.2	5.9	-	0.23
CF9	50	2	109.9	128.7	6.9	6.8	0.23

\* are shown in Figure 35.

Figure 36 shows mean residence time  $\tau_{cf}$  over the tamping speed (throughput) for all three insert geometries. As expected,  $\tau_{cf}$  decreases at higher tamping speed. Geometry 1 has the highest and geometry 2 has the lowest mean residence times  $\tau_{cf}$ .

At 50 tpm, the difference between the maximum and minimum  $\tau_{cf}$  is 33.5 s. This is 50% higher than 15.9 s obtained at 110 tpm, which can be attributed to significant powder mixing due to the acceleration forces in the powder bowl resulting from a faster start/stop movement of the machine at 110 tpm, thus decreasing the effect of the insert on the mean residence time  $\tau$ .

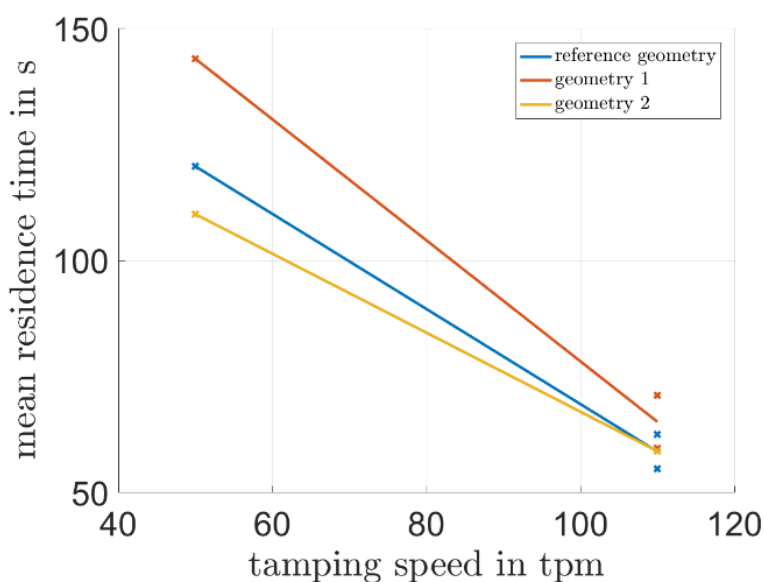


Figure 36: Mean residence time of material in the capsule filling machine for all three inserts. The lines can be used for guidance only, and the linearity cannot be proven at this stage.

#### 4.4.3 Direct Continuous Capsule-Filling Line

The blender and capsule filler RTD models were combined to yield a model of a full direct capsule filling line (plant transfer function  $P_{plant}(s)$ ). This allows simulating a batch change and various process disruptions, e.g., total feed failure, short-time disturbances and propagation of impurities throughout the process. Two scenarios were investigated: 1) a batch change, with the batch transition time determined, and 2) short-time (up to 2 minutes) shut-downs of the API feeder. They were simulated for various process settings (blender speeds and inserts). A threshold of 5% of the nominal API concentration was defined as the OOS threshold. The batch transition time (Figure 37) was defined as the time interval between the time when the concentration in batch 1 is below 95 % and the time when the concentration in batch 1 reaches 5 % (i.e., batch 2 concentration reaches 95 %).

The simulations from which batch transition times and discharge times were obtained are based on the results of parameter estimation for the transfer functions in blender runs No. 1-3 and 7-9 and capsule filling machine runs No. 1, 4 and 6-9.

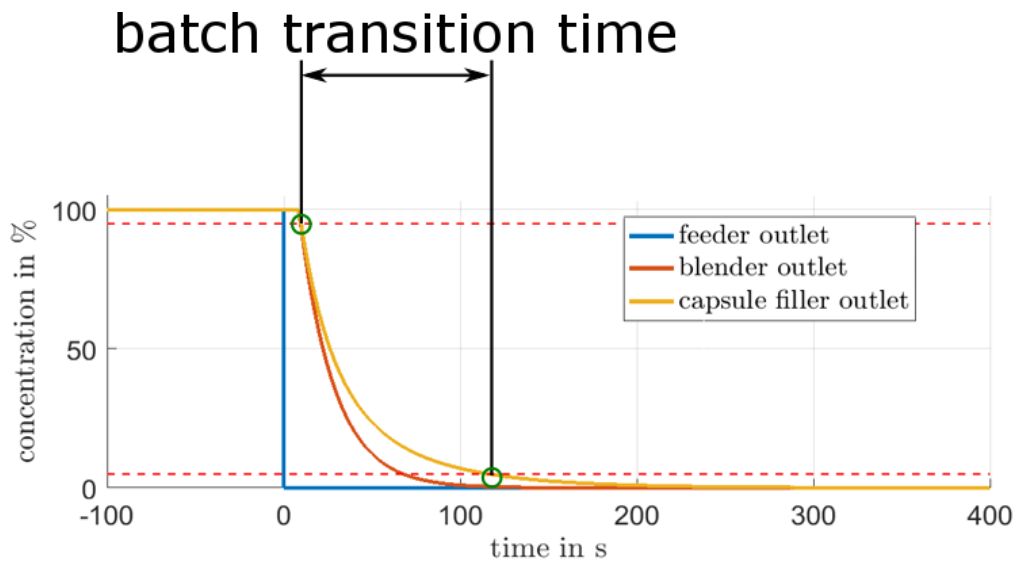


Figure 37: Sketch of how the batch transition time was determined. The red horizontal lines denote 95% and 5% limits of the remaining material in batch 1, respectively.

Chapter 4

1  
2

Table 15: Batch transition time at three investigated blender speeds with the three inserts at two throughput mass flow rates. Positive and negative values indicate an increase and a decrease compared to the reference geometry, respectively.

throughput in kg/h	blender speed in rpm	insert	batch transition time in s	difference in batch transition time compared to Ref. in s	batch transition material in g	difference in batch transition material compared to Ref. in g	change in batch transition time/material compared to Ref. in %
4.6	500	Ref.	242.1	-	309.4	-	-
		1	308.4	66.3	394.1	84.7	27.4
		2	244.6	2.5	312.5	3.2	1.0
	1000	Ref.	245.3	-	313.4	-	-
		1	311.1	65.8	397.5	84.1	26.8
		2	247.7	2.4	316.5	3.1	1.0
	1500	Ref.	228.5	-	292.0	-	-
		1	296.1	67.6	378.4	86.4	29.6
		2	230.9	2.4	295.0	3.1	1.1
10.2	500	Ref.	139.3	-	386.9	-	-
		1	190.0	50.7	527.8	140.8	36.4
		2	106.1	-33.2	294.7	-92.2	-23.8
	1000	Ref.	137.0	-	380.6	-	-
		1	188.0	51.0	522.2	141.7	37.2
		2	103.1	-33.9	286.4	-94.2	-24.7
	1500	Ref.	132.6	-	368.3	-	-
		1	184.2	51.6	511.7	143.3	38.9
		2	97.4	-35.2	270.6	-97.8	-26.5

3



Table 15 summarizes the batch transition time and the amount of material in the mixed raw material batches at two throughput mass flow rates, at three blender speeds and for three inserts. Positive and negative values correspond to an increase and a decrease in the batch transition time compared to the reference geometry, respectively.

The batch transition time depends on the throughput, as expected and shown by Eq. 9. When short batch transition times are desired, the continuous capsule-filling line should operate at the highest possible throughput. In terms of process settings, a high blender speed of 1500 rpm and geometry 2 at a throughput of 10.2 kg/h (110 tpm) result in the shortest batch transition time of 97.4 s. Decreasing the blender speed to 1000 rpm slightly increases the batch transition time to 103.1 s. The lowest blender speed of 500 rpm leads to the highest batch transition time of 106.1 s for geometry 2. The inserts influence the batch transition time much more than the blender speed does. The batch transition time at a throughput of 10.2 kg/h at 500 rpm can be reduced from 190 s (geometry 1) to 106.1 s (geometry 2). By changing the reference geometry to geometry 2, the batch transition time can be reduced by approximately 25%, whereas geometry 1 increases the batch transition time by 37%.

At a lower throughput of 4.6 kg/h (50 tpm), the blender speed affects the batch transition time less than the inserts do. The difference in batch transition time between the reference geometry and geometry 2 is no more than 3 s. Geometry 1 results in 25% longer batch transition times than the reference geometry. Increasing the blender speed from 1000 rpm to 1500 rpm reduces the batch transition time for the reference geometry from 245.3 s to 228.5 s (difference of 16.8 s or 6.8 %).

The amount of material in the mixed raw material batches at low throughputs is between 292 g and 397.5 g (difference of 105.5 g). However, at a throughput of 10.2 kg/h it is between 270.6g and 527.8g (difference of 257.2g). At the same blender speed, compared to the reference geometry there is approximately 100g less batch transition material when using geometry 2. For geometry 1, the amount of material in the mixed material batches is nearly doubled (511 g – 528 g) compared to the reference geometry. As such, geometry 2 is preferable since the amount of material lost during the batch transition is below 300 g. Geometry 2 is beneficial if a high throughput is desired, especially for small batch sizes. Since a small batch size requires more frequent batch transitions, shorter batch transition times are more efficient. At larger batch sizes, a better disturbance attenuation is favored since the likelihood of batch failure decreases (although at the expense of longer batch transition times).

The second scenario investigated in this work is the effect of a short-time (2 minutes) API feed failure at the outlets of the blender and the capsule filler. The material discharge times after the blender and after the capsule filling machine were calculated for a material with API concentrations between 4.75% and 5.25% as OOS ( $\pm 5\%$  of nominal concentration). This calculation can estimate the amount of waste material at each discharge point. An example of how the discharge times are determined is provided in Figure 38.

The discharge times at the three blender speeds and with three inserts at two throughput levels are shown in Table 16.

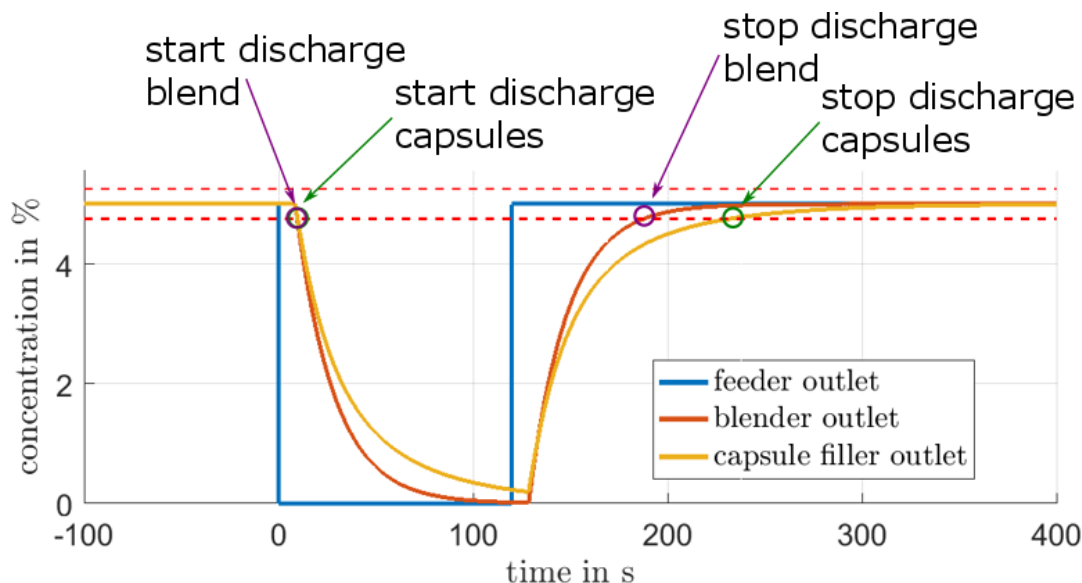


Figure 38: Concentrations after the blender (orange) and after the capsule filler (yellow). The red lines denote the 5% limit for the nominal concentration. The throughput is 10.2 kg/h at 500 rpm. Geometry 2 is used.

Table 16: Discharge times at two discharge points (after the blender and after the capsule filler) in the case of a 2-minute API feed failure at three investigated blender speeds with three inserts at two throughput levels.

throughput in kg/h	blender speed in rpm	insert	discharge time after blender in s	discharged material after blender in g	discharge time after CF in s	discharged material after CF in g
4.6	500	Ref.	209.7	268.0	299.3	382.4
		1	209.7	268.0	305.5	390.4
		2	209.7	268.0	303.7	388.1
	1000	Ref.	216.1	276.1	303.6	387.9
		1	216.1	276.1	310.0	396.1
		2	216.1	276.1	307.8	393.3
	1500	Ref.	177.3	226.5	282.1	360.5
		1	177.3	226.5	288.2	368.3
		2	177.3	226.5	287.0	366.7
10.2	500	Ref.	178.2	495.0	252.1	700.3

		1	178.2	495.0	284.8	791.1
		2	178.2	495.0	221.7	615.8
	1000	Ref.	173.6	482.2	249.8	693.9
		1	173.6	482.2	282.8	785.6
		2	173.6	482.2	218.7	607.5
	1500	Ref.	163.9	455.3	245.3	681.4
		1	163.9	455.3	278.9	774.7
		2	163.9	455.3	212.7	590.8

Material discharge times depend on the time constants of the CSTRs: the higher the time constant, the slower the system's response. The same applies to the batch transition time. In general, the higher the throughput, the shorter the discharge time and the higher throughput, resulting in more discharged material. The discharge times after the blender at 1000 rpm at throughputs of 10.2 kg/h and 4.6 kg/h are 173.6 s and 216.1 s, respectively. In contrast to a higher throughput level with OOS material of 482.2 g, at 4.6 kg/h there were only 276.1 g of OOS material. A reduction of 43% in the OOS material at 1000 rpm can be achieved by decreasing the throughput to 4.6 kg/h (although the discharge time is 25% longer). At 500 rpm, the material loss can be reduced by more than 45 % when operating the capsule filling line at a lower throughput of 4.6 kg/h. A full summary of the effect of decreased throughput (from 10.2 kg/h to 4.6 kg/h) on the OOS time in [s] and in % and on the amount of OOS material in [g] and in % is provided in the Appendix (Table A1).

In general, the discharge times after the blender are shorter than those after the capsule filler since the RTD in the latter increases the OOS time but decreases the amplitude. There is 20 %- 41 % less OOS material discharged after the blender than after the capsule filler in the case of a 2-minute feed disruption of the API feeder. The discharge point after the capsule filling machine can be beneficial in terms of OOS material if there is a disturbance in OOS material after the blender that can be attenuated by dampening of the capsule-filling machine. In this case, there is no waste material after the capsule filling machine despite the OOS material present after the blender. A full summary of the difference in the OOS time and amount of OOS material after the blender and the capsule filling machine is provided in the Appendix (Table A2). Discharging the material after the blender is not always preferable.

A shorter discharge time after the blender does not necessarily mean that it is beneficial to discharge the OOS material after the blender since a continuous powder flow into the capsule filler should be ensured to prevent emptying the powder bowl. It is reported in the literature that the PBH is a CQA that greatly affects the fill weight variation of the capsules [18]. As such, the PBH has to be considered when designing a control concept. The continuous powder flow can be established either via a buffer and some feeding

device, ideally coupled with a PBH sensor and adjustable feed rate, or by stopping the capsule-filling machine synchronously with the material discharge. In the latter case, additional feasibility studies will be required to assess the quality of the final product.

Discharging after the capsule filling machine is fairly easy since the capsules produced during the discharge time can simply be disposed of (together with the capsule shells). Knowing the RTD, the discharge times and the expected amount of waste material under certain failure scenarios can facilitate the selection of optimal storage/buffer capacity for known disruption times. However, integrating a buffer may introduce additional challenges into the process, such as varying bulk density due to compaction that depends on the buffer fill level, and may lead to fill weight variations in the capsules. Moreover, the buffer should not run empty, meaning that a control concept for an OOS event should make it possible to run the feeder and blender unit at a higher throughput to refill the buffer so that a second OOS event could be bridged.

## 4.5 Conclusion and Outlook

The presented method is representing a proof of concept study enabling material tracking throughout a continuous direct capsule-filling process. The proposed RTD models serve as a basis for simulating failure scenarios and determining the discharge times appropriate for a certain quality threshold, which can be defined according the quality target product profile (QTPP). Furthermore, it makes possible process optimization, such as establishing the optimal blender speed for a given throughput and insert geometry upon certain feed disruptions. The robustness of the processing line in terms of feed disruptions can also be assessed. The amount of waste material (OOS material) after unit operations can be determined and compared. Based on this information, *in-silico* process optimization can be performed. In future work, the RTD models will be used to develop and test various control strategies, e.g., the line's reaction to the material discharge.

## 4.6 Acknowledgement

This work has been funded by the Austrian COMET Program under the auspices of the Austrian Federal Ministry of Transport, Innovation and Technology (bmvit), the Austrian Federal Ministry of Economy, Family and Youth (bmwfj) and by the State of Styria (Styrian Funding Agency SFG). COMET is managed by the Austrian Research Promotion Agency FFG.

The authors would like to thank BOSCH Packaging, for their financial and scientific support and CAPSUGEL for capsule supply. Furthermore, we want to thank Daniel Kaiser and Vanessa Herndler for providing their technical support in the lab and pilot plant.

## 4.7 References

- [1] J. Rantanen, J. Khinast, The Future of Pharmaceutical Manufacturing Sciences, *J. Pharm. Sci.* 104 (2015) 3612–3638. doi:10.1002/jps.24594.
- [2] M. Ierapetritou, F. Muzzio, G. Reklaitis, Perspectives on the continuous manufacturing of powder-based pharmaceutical processes, *AIChE J.* 62 (2016) 1846–1862. doi:10.1002/aic.15210.
- [3] J.S. Srari, C. Badman, M. Krumme, M. Futran, C. Johnston, Future supply chains enabled by continuous processing-opportunities and challenges May 20-21, 2014 continuous manufacturing symposium, *J. Pharm. Sci.* 104 (2015) 840–849. doi:10.1002/jps.24343.
- [4] FDA, Guidance for Industry Guidance for Industry PAT — A Framework for Innovative Pharmaceutical, (2004) 19.
- [5] W. Engisch, F. Muzzio, Using Residence Time Distributions (RTDs) to Address the Traceability of Raw Materials in Continuous Pharmaceutical Manufacturing, *J. Pharm. Innov.* 11 (2016) 64–81. doi:10.1007/s12247-015-9238-1.
- [6] M.C. Martinetz, A.-P. Karttunen, S. Sacher, P. Wahl, J. Ketolainen, J.G. Khinast, O. Korhonen, RTD-based Material Tracking in a Fully-Continuous Dry Granulation Tableting Line, *Int. J. Pharm.* 547 (2018) 469–479. doi:10.1016/J.IJPHARM.2018.06.011.
- [7] J. Kruisz, J. Rehr, S. Sacher, I. Aigner, M. Horn, J.G. Khinast, RTD Modeling of a Continuous Dry Granulation Process for Process Control and Materials Diversion, *Int. J. Pharm.* 528 (2017) 334–344. doi:10.1016/j.ijpharm.2017.06.001.
- [8] B. Wagner, T. Brinz, S. Otterbach, J. Khinast, Automation of a dosing-disc capsule filler from the perspective of reliability and safety, *Drug Dev. Ind. Pharm.* 44 (2018) 502–510. doi:10.1080/03639045.2017.1402920.
- [9] B. Wagner, T. Brinz, S. Otterbach, J. Khinast, Rapid automated process development of a continuous capsule-filling process, *Int. J. Pharm.* 546 (2018) 154–165. doi:10.1016/J.IJPHARM.2018.05.009.
- [10] J. Rehr, J. Kruisz, S. Sacher, J. Khinast, M. Horn, Optimized continuous pharmaceutical manufacturing via model-predictive control, *Int. J. Pharm.* 510 (2016) 100–115. doi:10.1016/j.ijpharm.2016.06.024.
- [11] C.-T. Chen, *Signals and Systems*, 3rd ed., 2004.
- [12] sugar spheres - Pharm-a-spheres - sugar spheres as carrier for your sustained-release formulation and globuli sacchari as basis for your homoeopathic medicine, (n.d.). <http://www.pharm-a-spheres.com/index.php/sugar-spheres.html> (accessed July 31, 2018).
- [13] O. Scheibelhofer, J. Kruisz, S. Manz, J. Rehr, T. Wutscher, E. Faulhammer, A. Witschnigg, J.G. Khinast, LIF or dye: Comparison of different tracing methods for granular solids, 2018.
- [14] F. Podczeczek, J.M. Newton, Powder filling into hard gelatine capsules on a tamp filling machine., *Int. J. Pharm.* 185 (1999) 237–254.
- [15] E.L. Paul, *Handbook of Industrial Mixing*, John Wiley & Sons, Inc., Hoboken, NJ, USA, 2003. doi:10.1002/0471451452.
- [16] A.C. Cullen, H.C. Frey, *Probabilistic Techniques in Exposure Assessment*, Springer, 1999.

- [17] D.M. Hawkins, The Problem of Overfitting, J. Chem. Inf. Comput. Sci. 44 (2004) 1–12. doi:10.1021/ci0342472.
- [18] F. Podczec, S. Blackwell, M. Gold, J.M. Newton, The filling of granules into hard gelatine capsules, Int. J. Pharm. 188 (1999) 59–69. doi:10.1016/S0378-5173(99)00208-2.

## 4.8 Appendix

### 4.8.1 Nomenclature

$E$	exit-age-distribution
$P(s)$	transfer function
$t_x$	time until cumulative tracer concentration/intensity reaches $x\%$ .
$W$	wash-out function
$\sigma_{exp}^2$	variance of exit-age-distribution
$\sigma_{exp}$	standard deviation of exit-age-distribution
$\tau$	mean residence time

### 4.8.2 Abbreviations

CM	continuous manufacturing
cph	capsules per hour
CQA	critical quality attribute
CSTR	continuously stirred tank reactor
LIF	light induced fluorescence
PBH	powder bed height
PFR	plug flow reactor
PSD	particle size distribution
QTPP	quality target product profile
RTD	residence time distribution

tpm            tamps per min in 1/min

### 4.8.3 Subscripts

*bl*            blender

*cf*            capsule filler

*CSTR*        continuous stirred tank reactor

*exp*          experimental

*plant*        plant (direct capsule filling line)

## 4.8.4 Tables

Table A1: OOS time and material a throughput of 4.6kg/h and 10 kg/h. 10 kg/h are a reference, and a negative difference corresponds to a reduction in the OOS time or material.

Comparison of OOS time & material between 4.6 kg/h & 10 kg/h									
process parameters		after blender				after capsule filling machine			
		OOS time difference		OOS material difference		OOS time difference		OOS material difference	
blender speed in rpm	insert	in s	in %	in g	in %	in s	in %	in g	in %
500	Ref.	-31.5	-17.7	227.0	45.9	-47.2	-18.7	317.8	45.4
	1	-31.5	-17.7	227.0	45.9	-20.7	-7.3	400.8	50.7
	2	-31.5	-17.7	227.0	45.9	-82.0	-37.0	227.8	37.0
1000	Ref.	-42.5	-24.5	206.1	42.7	-53.8	-21.5	306.0	44.1
	1	-42.5	-24.5	206.1	42.7	-27.2	-9.6	389.4	49.6
	2	-42.5	-24.5	206.1	42.7	-89.1	-40.7	214.2	35.3
1500	Ref.	-13.4	-8.2	228.7	50.2	-36.8	-15.0	320.9	47.1
	1	-13.4	-8.2	228.7	50.2	-9.3	-3.3	406.5	52.5
	2	-13.4	-8.2	228.7	50.2	-74.3	-34.9	224.1	37.9

Table A2: OOS time and material after the blender and after the capsule-filling machine. The blender is a reference, and a positive value corresponds to an increase in the discharge time or material.

Difference between OOS time & material after blender and after capsule filling machine						
throughput in kg/h	blender speed in rpm	insert	OOS time difference		OOS material difference	
			in s	in %	in g	in %
4.6	500	Ref.	89.60	42.73	114.49	29.94
		1	95.80	45.68	122.41	31.36
		2	94.00	44.83	120.11	30.95
	1000	Ref.	87.50	40.49	111.81	28.82
		1	93.90	43.45	119.98	30.29
		2	91.70	42.43	117.17	29.79
	1500	Ref.	104.80	59.11	133.91	37.15
		1	110.90	62.55	141.71	38.48
		2	109.70	61.87	140.17	38.22
10	500	Ref.	73.90	41.47	205.28	29.31
		1	106.60	59.82	296.11	37.43
		2	43.50	24.41	120.83	19.62
	1000	Ref.	76.20	43.89	211.67	30.50
		1	109.20	62.90	303.33	38.61
		2	45.10	25.98	125.28	20.62
	1500	Ref.	81.40	49.66	226.11	33.18
		1	115.00	70.16	319.44	41.23
		2	48.80	29.77	135.56	22.94



---

*...when you have eliminated the impossible, whatever remains,  
however improbable, must be the truth.*

Sir Arthur Conan Doyle

## 5 Summary and Conclusion

Within this work, various unit operations for continuous pharmaceutical production have been investigated regarding their residence time distribution. Methods for manufacturing of a suitable tracer material were established and data processing procedures were developed.

In chapter 1, an introduction is given and the reasons for this work are elaborated, followed by a brief description of the characterized unit operations, including feeding. The RTD of the feeders was not assessed, as there are so many influential factors and in this work, the feeders were treated as material source. This is in agreement with all the software tools, where feeders are basically first-in-first-out material sources, where a certain outflow (volumetric or gravimetric) can be chosen. Additionally, an introduction to residence time theory, the RTD measurements as well as modeling approaches is given in this chapter.

Chapter 2 is dealing with the RTD of a continuous dry granulation line consisting of two feeders, a continuous blender and a roller compactor. The tablet press was not considered in this work due to the already known wide RTD of our tablet press in combination with a large in-process material volume, thus, a discharge point after the tablet press was found infeasible. The connection of blender and a discharge point after the blender with the roller compactor including a discharge point afterwards was found sufficient. For blender and roller compactor were transfer function models developed and fitted to the experimental data. The single models were combined to perform simulations evaluating the effect of selected feed disruption on the process. The quantification of severity of these disruption was based on the amount of waste material at both possible discharge points. Based on the amount of waste material, the selection of an appropriate discharge point and design of eventually needed buffers was shown.

The following chapter 3 is focusing on the development of a RTD measurement method for a (continuous) capsule filling machine. The capsule filling machine has a large powder volume in the powder bowl and a difficult accessible inlet, rendering impulse response tests impossible as the excellent mixing in the powder bowl is diluting the tracer extremely well, resulting in very low (not detectable) tracer concentration at the outlet, inside the capsules. As discussed in the introduction, an inert tracer needed to be found, to perform step response experiments in order not to influence the flow behavior and obtain wrong measurement data. In a side-study, comparison of light induced fluorescence (LIF) and food dye, a visible tracer, was conducted. After selection of food dye as coloring agent and the development of a suitable coloring procedure, the next challenge was, to measure the tracer intensity inside the capsules. A consumer camera was used to capture a video from the

machine's capsule segment conveying the filled capsule bodies from filling to the closing step. Furthermore, a sophisticated video/image analysis algorithm was developed where the moving periods of the segment and the time spans, where the segment was at rest (during the tamping step) was determined and color intensity was evaluated only during the resting period for the regions of interest.

The evaluation of the RTD measurements provided in chapter 3, a stepwise decrease in tracer intensity were observed. The hypothesis, that these steps are arising from an intermittent powder feeding into the powder bowl could be proven in chapter 4. The measurement method was refined in a way, where the machine's internal powder bed height sensor and control was bypassed and powder was continuously supplied to the capsule filling machine. The data processing, as described in chapter 3 was applied to the data acquired with this continuous feeding approach. Furthermore, these datasets were used to develop a RTD model of a continuous capsule filling line, consisting of feeders, a blender and a capsule filling machine. Similar to the approach proposed in chapter 2, the RTD transfer function models were combined and selected feed disruptions were simulated. Again, their effect on concentration after the blender and after the capsule filler have been compared in terms of OOS-time and OOS-material.

Residence time distributions for blender, roller compactor and capsule filling machine were successfully measured and transfer function models were established and parametrized for these three unit operations.

---

*Science may set limits to knowledge,  
but should not set limits to imagination.*

Bertrand Russell

## 6 Outlook

The transition from pharmaceutical batch production to continuous production is still ongoing. Currently, only a few drug products are approved for continuous manufacturing but the trend is clearly visible. This transition from batch to continuous started nearly 15 years ago, it is still a long way to go to achieve fully continuous pharmaceutical production.

One crucial aspect for regulatory approval of continuous pharmaceutical manufacturing is the traceability of final product with documented process conditions, back to the raw materials and storage conditions. Knowledge about the RTD enables exactly this traceability of materials through the process. Additionally, sophisticated process monitoring systems can be utilized to collect all process data combined with environmental conditions to provide full documentation.

The currently available tools, especially gProms from PSE (Process Systems Enterprise Limited, London, UK) are providing large libraries containing phenomenological powder models, such as breakage or agglomeration but do not yet include RTD models. This thesis provides model structures, which can be included into such simulation tools. The parametrization need to be done for each material/formulation. Future work will apply this concept to various materials, aiming to close the gap between material attributes and RTD. This means, that by measuring material attributes, a parametrization of RTD models should be enabled, allowing in-silico process optimization. Simulations of feed failure events additionally aid in the selection of appropriate discharge points with optimization of buffer sizes. Refilling strategies of the feeders can be included, assessing the effect of the refilling step on feeder performance and furthermore simulate the effect of such disturbances on the final product. When discharging material, the buffers included may run empty or at least will have a decreased fill level. Further studies on a controlled higher throughput and the effect on the final product will allow variation in throughput to fill buffers or keep the hopper fill level in a certain range. Current work is dealing with the application of the herein developed RTD models for model predictive control to keep the hopper fill level of a tablet press within a certain range. The controller predicts, based on feeder information, how the disturbance will propagate through the blender and when it will require discharge, the throughput of the tablet press is decreased in order to fill the hopper slightly higher. When the material is discharged, the hopper level does not decrease to that extent as was compensated upfront.

This thesis can serve as basis for various applications, such as process development, design, optimization and control to bring pharmaceutical manufacturing one step ahead on its way to becoming continuous.

## 7 Appendix

### 7.1 Curriculum Vitae

**Name** Julia Krusz

**Date of Birth** 11/11/1986

**Nationality** Austrian

#### Education

**Oct. 2014** PhD Process Engineering (Chemical and Pharmaceutical Engineering), Graz University of Technology

**Oct. 2006 – Aug. 2016** Bachelor Biomedical Engineering at Graz University of Technology

**Oct. 2005 – Apr. 2013** Diploma of Electrical Engineering with focus on Biomedical Engineering at Graz University of Technology

**Sep. 2001 – Jun. 2005** Gymnasium Jennersdorf with focus on Informatics

#### Practical Experience

**01/07/2014** Scientist (Area III - Process and Manufacturing Science), Research Center Pharmaceutical Engineering

**01/09/2011 – 30/09/2012** Research Assistant at Medical University Graz, Clinical Research Center

**01/04/2008 – 26/07/2010** Research Assistant at Joanneum Research, Institute of Medical Technologies and Health Management

**Aug. 2007 – Dec. 2007** Research Assistant at Joanneum Research, Institute of Medical Technologies and Health Management

## 7.2 Publications

### 7.2.1 Poster

QbD based model development for continuous pharmaceutical manufacturing (Minisymposium VT 14.und 15.April, Wien)

Development of a Model-Based Control Concept for a Direct Compaction Process (Partec April 2016, Nürnberg)

### 7.2.2 Presentation

Kruisz J., Rehl J., Gruber A., Sacher S., Khinast J.G., Flowsheet Modeling as a Tool for Plant-wide Control Strategy Development for Continuous Processes (EuPAT 18. und 19. Mai 2015, Graz)

J. Kruisz, J. Rehl, I. Aigner, S. Sacher, M. Horn, J. G. Khinast, RTD modeling of a continuous dry granulation process enabling an advanced control concept for out-of-spec handling (ICPE 14<sup>th</sup>-15<sup>th</sup> September 2016, Graz)

J. Kruisz, J. Rehl, O. Scheibelhofer, E. Faulhammer, A. Witschnigg, J. G. Khinast, Challenges for Continuous Capsule Filling (PSSRC Meeting 28<sup>th</sup> – 30<sup>th</sup> June 2017, Graz)

### 7.2.3 Research Articles

J. Kruisz, J. Rehl, S. Sacher, I. Aigner, M. Horn, J.G. Khinast, RTD Modeling of a Continuous Dry Granulation Process for Process Control and Materials Diversion, *Int. J. Pharm.* 528 (2017) 334–344. doi:10.1016/j.ijpharm.2017.06.001.

J. Kruisz, E. Faulhammer, J. Rehl, O. Scheibelhofer, A. Witschnigg, J.G. Khinast, Residence Time Distribution of a Continuously-operated Capsule Filling Machine: Development of a Measurement Technique and Comparison of Three Volume-Reducing Inserts, *Int. J. Pharm.* (2018). doi:10.1016/J.IJPHARM.2018.08.017.

J. Kruisz, J. Rehl, E. Faulhammer, A. Witschnigg, J.G. Khinast, Material tracking in a continuous direct capsule-filling process via residence time distribution measurements, *Int. J. Pharm.* 550 (2018) 347–358. doi:10.1016/J.IJPHARM.2018.08.056.

J. Rehl, J. Kruisz, S. Sacher, J. Khinast, M. Horn, Optimized continuous pharmaceutical manufacturing via model-predictive control, *Int. J. Pharm.* 510 (2016) 100–115. doi:10.1016/j.ijpharm.2016.06.024.

O. Scheibelhofer, J. Kruisz, S. Manz, J. Rehl, T. Wutscher, E. Faulhammer, A. Witschnigg, J.G. Khinast, LIF or dye: Comparison of different tracing methods for granular solids, 2018.

## 7.2.4 Summer School

Hybrid Modeling (07.bis 09.September 2015, Magdeburg)

Hybrid Modeling (05.bis 07.Juli 2017, Wien)